MOLECULAR BIOLOGY AND ECOLOGY OF BACTERIAL-FUNGAL SYMBIOSES

A Dissertation

Presented to the Faculty of the Graduate School

of Cornell University

In Partial Fulfillment of the Requirements for the Degree of

Doctor of Philosophy

by

Olga Lastovetsky

May, 2017

MOLECULAR BIOLOGY AND ECOLOGY OF BACTERIAL-FUNGAL SYMBIOSES

Olga Lastovetsky, Ph. D.

Cornell University 2017

Interactions between fungi and bacteria are gaining attention for their role in human health, agriculture, food production and ecosystem functioning. They are prominent examples of cross-kingdom associations and range from mutualistic to antagonistic. Little is known about how fungi and bacteria interact at the molecular level. I utilized the association between the fungus *Rhizopus microsporus* and its beta-proteobacteria endosymbiont *Burkholderia* as a model for understanding mechanisms of fungal-bacterial interactions. I uncovered a mechanism governing symbiosis establishment, which centered on specific alterations in fungal lipid metabolism and showed that these metabolic changes were due, at least in part, to the activity of a previously uncharacterized class of diacylglycerol kinase enzymes. I explored the interaction of endobacteria with the sexual cycle of *R. microsporus*, showing that, unlike bacterial control over fungal asexual reproduction, control over sexuality is incomplete. This incomplete control was exerted through bacterial manipulation of expression of fungal *ras2* which encodes a small GTPase potein. Moreover, endobacteria buffered the negative effects of exogenous cyclic AMP on fungal mating. Furthermore, I reconstructed the molecular dialogues between *R. microsporus* and *Burkholderia* in different types of symbioses, antagonism versus mutualism. Fungal cell wall modifications and changes in reactive oxygen species metabolism were central to both types of interactions, whereas bacteria engaged a common set of genes during antagonism as well as mutualism with fungi revealing novel symbiosis factors. Lastly, I conducted an ecological study of arbuscular mycorrhizal fungi (AMF) and their bacterial endosymbionts,

‘*Candidatus* Glomeribacter gigasporarum’ (*Ca*Gg, beta-proteobacteria) and ‘*Candidatus* Moeniiplasma glomeromycotorum’ (*Ca*Mg, Mollicutes) in a natural dune ecosystem. I discovered that soil calcium levels correlated with distribution of both types of endobacteria in dune AMF, which was likely linked to the effects of calcium on the host plant. Population structure analyses confirmed the existence of highly diverse *Ca*Mg within AMF isolates, uncovered a new clade of *Ca*Gg and lead to the discovery of a previously undescribed group of *Burkholderia*-related endosymbionts in AMF. Overall, I uncovered mechanisms of how fungi and bacteria interact at the molecular level, as well as provided insights into the distribution of bacterial endosymbionts of fungi in the environment.

BIOGRAPHICAL SKETCH

Olga Lastovetsky was born in Baikonur, Kazakhstan in 1988, home to the world's first space launch facility. She lived in Russia until the age of 11 when she moved to County Wicklow, Ireland with her family. She received a Bachelor of Science in Environmental Biology from University College Dublin (UCD), Ireland in 2011, graduating with First Class Honors. For her undergraduate research thesis, she worked under the guidance of Dr. Nicolas Clipson and Dr. Evelyn Doyle on the bacterial community structure of soils polluted with polycyclic aromatic hydrocarbons. She was the recipient of a number of awards and scholarships at UCD including the Entrance Exhibition Award, B.Sc. Biology Stage 2 Scholarship, and the Environmental Biology Medal. In August 2011 she began her graduate career in the Department of Microbiology at Cornell University with Teresa Pawlowska. She was married to her husband, Marc, in August 2013, had her beautiful baby daughter Milana on January 7, 2017 and received her PhD in May 2017.

ACKNOWLEDGMENTS

I am enormously grateful to my thesis advisor Teresa Pawlowska for her guidance in all aspects of life and science during my graduate career at Cornell. Teresa has been a wonderful mentor and role model, always knowing how to motivate, advise, support and comfort when needed. I am also grateful to my committee members Gillian Turgeon and Magdalen Lindeberg for their expert guidance and advice throughout my graduate career. I would like to thank all the people that helped me with different aspects of research throughout the years including Stephen Mondo, Ezekiel Ahn, Colin Barber, Nikki Schwardt, Adam Bogdanove, Sara Carpenter, Aolin Zhang, Qi Sun, M. Laura Gaspar and Wojtek Pawlowski. I would like to thank Stephen Parry, Lynn Johnson and Francoise Vermeylen at the Cornell Statistical Consulting Unit for their help with statistical analysis. Thank you to my cohort members: Chantal Koechli, Dave Sannino and Eugenia Nazarova and fellow Microbiology Graduate students for their friendship, comradery and commiseration. I am grateful to my parents Alexey and Gulnara, my sister Oksana and my loving husband Marc for their unconditional support and motivation that got me through the rough patches. Lastly, I am thankful to and for my lovely daughter Milana.

TABLE OF CONTENTS

Lipid metabolic changes in an early divergent fungus govern the establishment of a mutualistic symbiosis with endobacteria

Olga A. Lastovetsky[a], Maria L. Gaspar[b], Stephen J. Mondo[c], Kurt M. LaButti[c], Laura Sandor[c], Igor V. Grigoriev[c], Susan A. Henry[b], and Teresa E. Pawlowska[d,1]

[a]Graduate Field of Microbiology, Cornell University, Ithaca, NY 14853; [b]Department of Molecular Biology and Genetics, Cornell University, Ithaca, NY 14853; [c]US Department of Energy Joint Genome Institute, Walnut Creek, CA 94598; and [d]School of Integrative Plant Science, Plant Pathology and Plant-Microbe Biology, Cornell University, Ithaca, NY 14853

Edited by Nancy A. Moran, University of Texas at Austin, Austin, TX, and approved October 25, 2016 (received for review September 16, 2016)

The recent accumulation of newly discovered fungal–bacterial mutualisms challenges the paradigm that fungi and bacteria are natural antagonists. To understand the mechanisms that govern the establishment and maintenance over evolutionary time of mutualisms between fungi and bacteria, we studied a symbiosis of the fungus *Rhizopus microsporus* (Mucoromycotina) and its *Burkholderia* endobacteria. We found that nonhost *R. microsporus*, as well as other mucoralean fungi, interact antagonistically with endobacteria derived from the host and are not invaded by them. Comparison of gene expression profiles of host and nonhost fungi during interaction with endobacteria revealed dramatic changes in expression of lipid metabolic genes in the host. Analysis of the host lipidome confirmed that symbiosis establishment was accompanied by specific changes in the fungal lipid profile. Diacylglycerol kinase (DGK) activity was important for these lipid metabolic changes, as its inhibition altered the fungal lipid profile and caused a shift in the host–bacterial interaction into an antagonism. We conclude that adjustments in host lipid metabolism during symbiosis establishment, mediated by DGKs, are required for the mutualistic outcome of the *Rhizopus–Burkholderia* symbiosis. In addition, the neutral and phospholipid profiles of *R. microsporus* provide important insights into lipid metabolism in an understudied group of oleaginous Mucoromycotina. Lastly, our study revealed that the DGKs involved in the symbiosis form a previously uncharacterized clade of DGK domain proteins.

mutualism evolution | antagonism | Mucoromycotina | oleaginous fungi | *Rhizopus–Burkholderia* symbiosis

The ubiquity of antagonistic interactions between fungi and bacteria in nature is widely appreciated due to medically important antimicrobials that mediate these relationships. In contrast, mutually beneficial associations of fungi with bacteria are only beginning to gain recognition for their abundance and role in human health, agriculture, food production, and general ecosystem functioning (1). Among these alliances, the mutualisms formed with various endobacteria by early divergent Mucoromycotina (2) and Glomeromycota (3), stand out as examples of a high level of coadaptation between the partners. However, little is known about the molecular mechanisms underlying establishment and maintenance of fungal–bacterial associations over evolutionary time, as the difficulties in cultivation and experimental manipulation of the symbiotic partners present a big impediment for elucidation of their biology. In this respect, the symbiosis of an early divergent fungus *Rhizopus microsporus* (Mucoromycotina) and its bacterial endosymbiont *Burkholderia* (β-proteobacteria) is emerging as a model for the study of fungal–bacterial mutualisms because both partners are easy to manipulate under laboratory conditions (4). *R. microsporus* is a soil saprotroph responsible for food spoilage and pathogenesis of plants and immune-compromised humans (2). Plant pathogenesis is facilitated by *Burkholderia*-mediated synthesis of a potent toxin, rhizoxin (2). The endobacteria, in turn, benefit from energy provision by the host (5). Several factors are known to contribute to the ability of *Burkholderia* endobacteria to form a stable association with the *R. microsporus* host (6–8). It remains an enigma, however, as to what fungal factors contribute to symbiosis formation.

In this study, we used the existence of closely related isolates of *R. microsporus* that differ in their interaction with *Burkholderia* endobacteria for the identification of the molecular underpinnings underlying fungal–bacterial symbiosis establishment. We discovered that unlike the symbiont-containing host isolates of *R. microsporus*, closely related but naturally symbiont-free nonhost isolates are antagonized by *Burkholderia* endobacteria and do not form symbioses with them. We compared fungal transcriptional responses during initial physical contact with *Burkholderia* endobacteria and found that host and nonhost fungi engaged different sets of genes in the reactions to endobacteria. In the host, the most striking response involved changes in the expression of lipid metabolic genes, whereas such changes were absent in the nonhost. Analysis of the host fungal lipidome revealed that symbiosis establishment was accompanied by an increase in the pools of triacylglycerol (TAG) and phosphatidylethanolamine (PE). When we altered the TAG:PE ratio with pharmacological inhibitors, the host–*Burkholderia* interaction

Significance

Mutually beneficial interactions of fungi with bacteria are increasingly recognized as ubiquitous and economically important. However, little is known about their establishment and maintenance. Utilizing the association between the fungus *Rhizopus microsporus* and its endosymbiont *Burkholderia* as a model, we provide first insights into fungal molecular mechanisms governing symbiosis establishment with bacteria. We show that specific changes in fungal lipid metabolism, mediated by diacylglycerol kinase enzymes, are required to maintain a mutualistic outcome of interaction with bacteria, a pattern consistent with the addiction model of mutualism evolution. We also offer insights into genetics and biochemistry of lipid metabolism in an understudied group of oleaginous fungi, which are a promising source of oils for biodiesel production.

Author contributions: O.A.L., M.L.G., I.V.G., S.A.H., and T.E.P. designed research; O.A.L., M.L.G., S.J.M., K.M.L., and L.S. performed research; O.A.L., S.J.M., K.M.L., L.S., and T.E.P. analyzed data; and O.A.L., M.L.G., and T.E.P. wrote the paper.

The authors declare no conflict of interest.

This article is a PNAS Direct Submission.

Freely available online through the PNAS open access option.

Data deposition: The Whole Genome Shotgun projects are deposited at GenBank under accession MCGZ00000000 (*R. microsporus* ATCC 52814) and MCOJ00000000 (*R. microsporus* ATCC 11559). The transcriptome data reported in this paper have been deposited in the Gene Expression Omnibus (GEO) database, www.ncbi.nlm.nih.gov/geo (accession no. GSE89305).

[1]To whom correspondence should be addressed. Email: tep8@cornell.edu.

This article contains supporting information online at www.pnas.org/lookup/suppl/doi:10.1073/pnas.1615148113/-/DCSupplemental.

shifted toward an antagonism, indicating that specific adjustments in lipid metabolism are required for the mutualistic outcome of this symbiosis. Collectively, we identified fungal genes important for symbiosis establishment with bacteria and a metabolic landscape favoring a mutualism. In addition, we provide genetic and biochemical insights into lipid metabolism in an understudied group of fungi, the Mucoromycotina.

Results

Host and Nonhost Fungi Differ in How They Interact with *Burkholderia* Endobacteria. To explore the relationship between host and nonhost isolates of *R. microsporus*, we examined whether they meet the phylogenetic species recognition criterion (9). Using a partition homogeneity test (10), we compared genealogies of three genes (11) sampled across host and nonhost isolates, designated in culture collections as representatives of the *R. microsporus* species. We found evidence of a history of gene flow across these isolates ($P = 0.002$; *SI Appendix*, Fig. S1), supporting their placement within a single interbreeding species. Moreover, comparison of genomes of host [*R. microsporus* American Type Culture Collection (ATCC) 52813] and nonhost (*R. microsporus* ATCC 11559), sequenced for this study and summarized in *SI Appendix*, Table S1, revealed that they share a 92% whole-genome average nucleotide identity, ANI (*SI Appendix*, Fig. S2), which offers an important insight into the intraspecific levels of ANI in fungi.

Nonhost isolates differ from host isolates in being naturally endosymbiont-free and in control of their asexual reproduction, which in the host isolates is dependent on endobacteria. As host isolates of *R. microsporus* are capable of establishing symbioses with nonnative *Burkholderia* isolated from other host *R. microsporus* (12), we tested whether nonhosts had the ability to form associations with *Burkholderia* endobacteria. Cocultivation of cured host fungi with endobacteria reestablishes a functional symbiosis whereby bacteria populate fungal hyphae and spores (*SI Appendix*, Fig. S3*A*). When we cocultivated nonhost *R. microsporus* ATCC 11559 and ATCC 52807 with endobacteria isolated from host *R. microsporus* ATCC 52813 and ATCC 52814, we found that nonhost isolates did not take up the bacteria into their hyphae (*SI Appendix*, Fig. S3*C*). Moreover, we noticed that nonhost fungi were antagonized by bacteria and changed their growth pattern by reducing hyphal extension around the site of bacterial inoculation, creating a "zone of inhibition" (*SI Appendix*, Fig. S3*D*). Similar growth changes were observed in other nonhost Mucoromycotina [*Rhizopus oryzae* ATCC 11423 and ATCC 13440 as well as *Mucor circinelloides* Centraalbureau voor Schimmelcultures (CBS) 277.49] during cocultivation with endosymbionts of host *R. microsporus* (*SI Appendix*, Fig. S4). Such phenotypic alterations were never observed in the host during interaction with endobacteria (*SI Appendix*, Fig. S3 *B*).

We conclude that two types of interactions are possible between mucoralean fungi and *Burkholderia* endobacteria: a mutualistic interaction arising as a consequence of symbiosis establishment in which bacteria populate fungal hyphae, and an antagonistic interaction in which bacteria do not populate fungal hyphae and cause phenotypic alterations in fungal growth. This finding prompted us to analyze the genetic underpinnings governing the interactions of the closely related host and nonhost isolates of *R. microsporus* with endobacteria with the aim of identifying molecular determinants of symbiosis establishment.

Different Sets of Genes Are Engaged by Host and Nonhost Fungi in the Interaction with Endobacteria. Using RNA sequencing (RNA-seq), we analyzed global gene expression changes in host and nonhost *R. microsporus* during cocultivation with *Burkholderia* endobacteria at a time point when the fungal colony has just come into physical contact with bacteria. This time point was expected to represent symbiosis establishment. Differentially expressed (DE) genes were identified by comparing: (*i*) cured host *R. microsporus* ATCC 52813 growing with its native *Burkholderia* endobacteria to (*ii*) cured host ATCC 52813 growing alone, as well as (*iii*) nonhost *R. microsporus* ATCC 11559 growing with endobacteria isolated from the host to (*iv*) nonhost ATCC 11559 growing alone. We reasoned that a portion of DE genes would exhibit similar expression patterns in host and nonhost, representing a nonspecific response to bacteria. Genes involved in this nonspecific response could then be subtracted from the pool of DE genes in the host, and the remainder would represent genes specifically involved in symbiosis establishment.

Using a threshold false discovery rate of 0.01, we found 508 DE genes in the host in response to interaction with its native endobacteria (representing fungal response during symbiosis establishment), and 183 DE genes in the nonhost in response to interaction with the same endobacteria. To directly compare host and nonhost gene expression changes, we identified orthologs by clustering all protein-coding genes from the host and nonhost. To discover genes involved in the nonspecific response to bacteria, we focused on genes that were commonly DE in both fungi. Contrary to our expectations, only 10 common DE genes exhibited the same expression patters (either up- or down-regulated), indicating a very limited nonspecific response (*SI Appendix*, Table S2). Clearly, establishment of symbiosis was governed by a very specific set of genes. The minimal overlap in host and nonhost transcriptomic responses was not due to expression of genes exclusively present in either of the two fungi. In fact, 97% of the DE host genes were also present in the nonhost genome, and vice versa, 95% of the DE genes in the nonhost were present in the host genome. The remaining 3% of the genes without homologs in the nonhost were also absent from another host *R. microsporus* ATCC 52814, and therefore could not represent symbiosis-specific genes. As the majority of DE host genes were unique to symbiosis establishment, we focused on these genes in our analysis of the genetic underpinnings of symbiosis.

Up-Regulation of Genes Responsible for the HOG Pathway and Lipid Metabolism During Symbiosis Establishment. Of the 508 host genes DE during symbiosis establishment, 298 were up- and 210 were down-regulated. To gain insight into the function of these genes, we conducted orthologous clustering across seven fungal genomes, including *Saccharomyces cerevisiae* (yeast), *Aspergillus nidulans*, and members of Mucoromycotina, followed by gene ontology (GO) enrichment analyses. Consistent with enrichment of the signal transduction category (*SI Appendix*, Fig. S5), we observed overexpression of many protein kinase genes (19 up, 8 down). Two of these protein kinase genes, encoding proteins with identification nos. 300418 and 286014, are homologous to the yeast gene encoding Hog1 MAPK (Fig. 1). The yeast Hog1 controls responses to a wide range of environmental stimuli, and signaling through Hog1 MAPK activates accumulation of glycerol, which counterbalances water molecule outflow from the cell under hypertonic conditions (13). Known upstream regulators of the Hog1 MAPK include the two-component histidine kinase phosphorelay system, involving Ssk1 (13). In *R. microsporus*, we identified an up-regulated two-component response regulator (201417) homologous to the *A. nidulans* AN3101, closest match to *SSK1* in yeast, that could have acted upstream of this MAPK. The yeast Hog1 activates glycerol synthesis by controlling the expression of a NAD-dependent glycerol-3-phosphate dehydrogenase, Gpd1 (13). In our RNA-seq experiment, a homolog of *GPD1* and another gene with the same function (222441) were up-regulated, together with homologs of genes *STL1*, encoding a glycerol symporter, *SKO1*, encoding a transcription factor, and *GUT1*, encoding a glycerol kinase. In yeast, *GDP1*, *STL1*, and *SKO1* are known to be regulated by Hog1 (13). The glycerol symporter functions to transport glycerol into the cell, whereas glycerol kinase and NAD-dependent glycerol-3-phosphate dehydrogenases convert different precursors into glycerol-3-phosphate (Gro-3-P). Gro-3-P can be further converted to glycerol via a glycerol-3-phosphatase. However, we did not detect differential expression of genes with this function. Therefore, based on

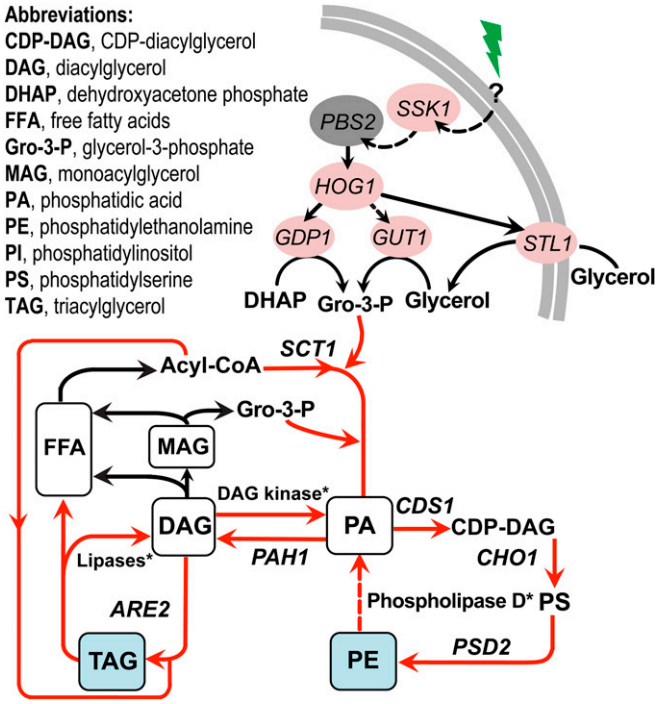

Fig. 1. Hypothetical representation of the link between the Hog1 MAPK and the lipid metabolic pathways activated in *R. microsporus* during symbiosis establishment. Genes are named according to *S. cerevisiae* nomenclature. Red circles and arrows represent genes up-regulated during symbiosis establishment; gray circles and black arrows depict genes not DE; dashed arrows represent unknown links, or uncertainty of precursor. In the metabolic pathway, names of the up-regulated genes are written adjacent to the metabolic conversions in which they are involved. Asterisks denote *R. microsporus* ATCC 52813 predicted protein annotations: DAG kinases (protein ID 315343 and 249146), phospholipases D (protein ID 277488 and 209457), and lipases (protein ID 249672, 281243, and 250139). The well-characterized yeast lipid metabolic pathway was used in the construction of this figure (14, 16, 18).

gene expression patterns in *R. microsporus*, which we mapped to known signaling networks in yeast, we hypothesize that the HOG pathway was activated in the host during symbiosis establishment, and in turn, likely activated synthesis and accumulation of Gro-3-P, but not that of glycerol.

In yeast, Gro-3-P serves as a precursor for the synthesis of glycerolipids (14) by becoming converted into phosphatidic acid (PA) via a Gro-3-P acyltransferase, Sct1 (15), whose homolog was also up-regulated in our RNA-seq experiment (Fig. 1). Therefore, based on these gene expression patterns, we hypothesized that establishment of symbiosis was mediated by signaling through the *R. microsporus* homologs of yeast Hog1 MAPK, which ultimately activated Gro-3-P synthesis. Gro-3-P was then likely channeled into glycerolipid synthesis by becoming acylated via a homolog of the yeast Sct1. Consistent with this hypothesis, the lipid metabolism GO category was enriched among the DE host genes during symbiosis establishment (*SI Appendix*, Fig. S5). To elucidate what pathways in lipid metabolism were important, we annotated the lipid-related genes in the *R. microsporus* genomes based on homology to functionally characterized lipid metabolic genes in *S. cerevisiae* (16). Of the 92 yeast genes, 77 had homologs in *R. microsporus*, of which 14 were DE. Additionally, we identified another 26 DE genes that had no homologs in yeast lipid metabolism but were annotated as being part of the "lipid metabolism" GO category (*SI Appendix*, Table S3). By mapping all of these DE lipid-related genes onto known pathways of lipid metabolism (16), we inferred that de novo biosynthesis of PE and turnover of TAG were likely initiated during symbiosis establishment (Fig. 1). Central intermediates of this pathway are diacylglycerol (DAG) and PA, which, besides being precursors for the biosynthesis of lipids, have important signaling function in eukaryotes (17, 18). They are interconvertible, i.e., PA can be dephosphorylated by a PA phosphatase to produce DAG (19), and DAG can be phosphorylated by DAG kinase (DGK) to yield PA (20). Interestingly, two DGKs were among the top most up-regulated genes due to bacteria (*SI Appendix*, Table S3), indicating their importance in symbiosis establishment. Additionally, two genes encoding phospholipase D (PLD), which are not homologs of the yeast *PLD1*, were upregulated; PLD makes PA through the breakdown of phospholipids (21, 22). Finally, a homolog of yeast *SCT1*, a gene encoding an acyltransferase that synthesizes PA de novo was also up-regulated. Based on these patterns, we hypothesized that the activities of PA-producing enzymes, DGK, PLD, and Gro-3-P acyltransferase, govern the lipid metabolic changes during symbiosis establishment.

Pharmacological Inhibition of DGK Activity, but Not PLD Activity, Shifts the Host–Endosymbiont Interaction into Antagonism. To determine whether the activities of fungal PA-producing enzymes were important during symbiosis establishment, we set up interactions of host and nonhost fungi with *Burkholderia* endobacteria in the presence of chemical inhibitors of PLD and DGK; there are no commercially available Gro-3-P acyltransferase inhibitors. We chose to work with chemical inhibitors because, at present, no genetic transformation technology is available for *R. microsporus*. Fungi were inoculated into liquid media and allowed to grow for 24 h before bacteria were added. Following a 24-h incubation with bacteria, fungal colony diameter was measured. DGK and PLD inhibitors were not expected to affect endobacteria, as their genome does not encode either a DGK or a PLD gene (5), although it is possible that inhibitors had undetected effects on bacterial physiology.

In the absence of bacteria, the inhibitors did not affect the growth of either cured host or nonhost fungi (*SI Appendix*, Fig. S6). In contrast, in the presence of bacteria, the growth of nonhost fungi was significantly reduced relative to growth without bacteria ($P < 0.001$), and this growth reduction occurred regardless of the presence or absence of chemical inhibitors (Fig. 2*A*). This was expected, considering that we observed a reduction in nonhost growth during interaction with the same bacteria on solid media (*SI Appendix*, Fig. S1*D*). Growth of cured host fungi was unaffected by bacteria in the absence of inhibitors and in the presence of the PLD inhibitor (Fig. 2*B*). However, when cured host fungi were grown with bacteria in the presence of DGK inhibitors, their growth was significantly reduced relative to growth without bacteria in the presence of DGK inhibitors ($P < 0.001$) in a way that resembled the reduction in nonhost growth during interaction with bacteria (Fig. 2*B*). Lastly, growth of host fungi that were not cured of endobacteria was also significantly reduced in the presence of DGK inhibitors ($P < 0.0001$), but was unaffected by inhibition of PLD (*SI Appendix*, Fig. S7).

Together, these results indicate that the activity of DGKs is important for the outcome of the interaction between host *R. microsporus* and *Burkholderia* symbionts, whereas PLD activity is dispensable. Inhibition of DGK appeared to shift the interaction toward an antagonism with a reduced fitness outcome in the fungus. Consistent with our transcriptomic observations that the expression of DGK and PLD remained unchanged in the nonhost during interaction with endobacteria, DGK and PLD inhibitors had no affect on the interaction between nonhost and endobacteria, which remained antagonistic. Lastly, the negative effect of DGK inhibition on the host fungus in an already fully established symbiosis indicates that DGK activity may be important not just for symbiosis establishment but also for the continued maintenance of the mutualism between the host and endobacteria (*SI Appendix*, Fig. S7).

Changes in the Host Lipid Profile Accompany the Shift to an Antagonistic Interaction with Endobacteria During Symbiosis Establishment. Pharmacological inhibition of DGK activity was expected to affect fungal lipid metabolism. In particular, we hypothesized that changes in

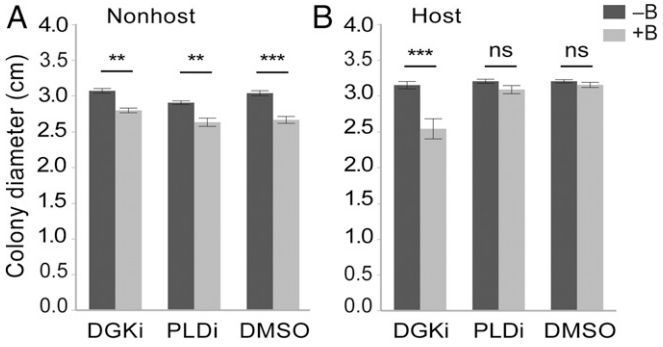

Fig. 2. Pharmacological inhibition of DGK and PLD activity. Effect of bacteria on growth of (*A*) nonhost and (*B*) host in the presence and absence of inhibitors. +B, with bacteria; –B, without bacteria; DGKi, diacylglycerol kinase inhibitors; PLDi, phospholipase D inhibitor; and DMSO indicates no inhibitor control. ***$P < 0.0001$, **$P < 0.001$, n.s., not significant, from post hoc Student's *t* test, corrected for multiple comparisons. Error bars represent 1 SEM.

lipid metabolism might account for the shift in the host–symbiont interaction into antagonism. Furthermore, gene expression analysis of host fungi during symbiosis establishment pointed to specific changes in lipid metabolism, namely activation of de novo synthesis of PE and turnover of TAG (Fig. 1). Therefore, we analyzed the lipid profiles of cured host *R. microsporus* during symbiosis establishment in the absence and in the presence of DGK inhibitors. Growth conditions and timing of bacterial addition were the same as during the pharmacological inhibition experiment described in the previous section. Total lipids were extracted and separated by one-dimensional TLC, followed by quantification of individual phospholipids and neutral lipids.

In the absence of DGK inhibitors, we found a significant increase in the pools of TAG and PE in the host fungi during symbiosis establishment (Fig. 3 *C* and *D*). This increase was consistent with our interpretation of the RNA-seq data whereby genes involved in de novo synthesis of PE and turnover of TAG were overexpressed (Fig. 1). The DGK inhibitors alone also caused alterations to the fungal lipid profile. With inhibitors, we observed a significant increase in TAG and a significant decrease in monoacylglycerol (MAG) and free fatty acid (FFA) (*SI Appendix*, Fig. S8). Such changes are consistent with inhibition of DGK activity, which would cause an accumulation of DAG. In yeast, DAG is normally present in small amounts (23). Consequently, we hypothesize that in *R. microsporus*, to maintain physiological levels of DAG, it was channeled into biosynthesis of TAG, a storage molecule. A similar pattern of TAG accumulation was observed in the yeast DGK deletion mutant *Δdgk1* (24). Accumulation of TAG would explain the observed decrease in levels of FFA, as they become used up in the biosynthesis of TAG from DAG. Finally, inhibition of DGK activity was expected to decrease the pool of PA; however, we detected no such decrease (*SI Appendix*, Fig. S8 *A* and *B*). This could be explained by the existence of alternative pathways of PA synthesis, such as de novo biosynthesis of PA from the breakdown products of MAG, i.e., FFA and Gro-3-P, consistent with the observed decrease in the MAG pool.

Addition of bacteria to cured host fungi grown in the presence of inhibitors, which had a significant effect on fungal growth, did not induce any further alterations to the fungal lipid profile relative to fungi grown with inhibitors but without bacteria (Fig. 3 *A* and *B*). In other words, an increase in TAG and a decrease in MAG and FFA during interaction with endobacteria in the presence of DGK inhibitors (*SI Appendix*, Fig. S8) was the effect of the inhibitors alone. Finally, comparison of lipid profiles of host fungi grown with bacteria in the presence and absence of inhibitors revealed a significantly larger pool of TAG in the presence of inhibitors (*SI Appendix*, Fig. S8 *C* and *D*).

Together, these results indicate that during symbiosis establishment, fungi accumulated TAG and PE. During the interaction with an antagonistic outcome, suggested by fungal growth decline brought about by inhibition of DGK activity, fungi accumulated additional TAG, but maintained the same levels of PE. These patterns suggest that a specific TAG:PE ratio may be important for the interaction. We calculated these ratios for all conditions tested in our experiment and found that, in the absence of DGK inhibitors, TAG:PE ratio was 1.1, whereas in the presence of DGK inhibitors, this ratio increased significantly to 1.7 ($P < 0.0001$; *SI Appendix*, Fig. S9 and Table S4). Based on these results, we propose that a TAG:PE ratio close to 1 in *R. microsporus* during symbiosis establishment with *Burkholderia* endobacteria is important for the mutualistic outcome of the interaction, and a higher TAG:PE ratio shifts the interaction toward an antagonism, marked by a fitness cost to the fungus.

Phylogenetic Analysis of DGKs Implicated in the Interaction with Endosymbionts. The two DGK genes overexpressed in host *R. microsporus* during symbiosis establishment were not homologs of the yeast gene encoding diacylglycerol kinase, *DGK1*. A homolog of *DGK1* is present in *R. microsporus* but it was not DE during symbiosis establishment. The two genes overexpressed due to bacteria were, instead, homologs of each other. Annotation of the protein domains of these genes revealed the presence of a DGK catalytic domain (PF00781, IPR001206) and a DGK accessory domain (PF00609, IPR000756), both absent from the yeast *DGK1* gene. Phylogenetic analyses of representative DGK domain proteins indicated that the two DGKs encoded by genes DE during symbiosis establishment belong to a cluster that is unique to some members of early divergent fungi (Fig. 4 and *SI Appendix*, Fig. S10). Overall, fungal DGKs separate into two main clusters: All Fungi and Early Divergent Fungi, with a single chytrid sequence grouping with the animal DGKs as part of the Animal/Chytrid cluster. The All Fungi cluster contains DGKs from a diverse group of fungi, including Ascomycota, Basidiomycota,

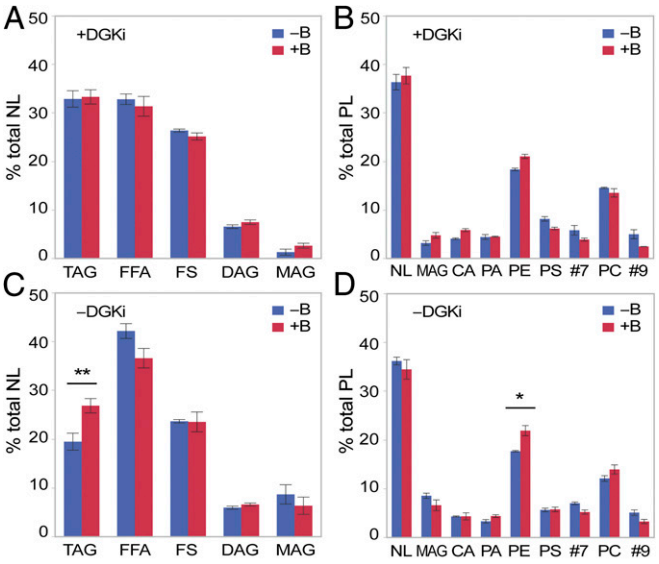

Fig. 3. Effects of DGKi on relative abundance of phospholipid (PL) and neutral lipid (NL) species in cured host *R. microsporus* ATCC 52813 grown with (+B) and without (–B) endobacteria. (*A*) Percent of total NLs in the presence of DGKi. (*B*) Percent of total PLs in the presence of DGKi. (*C*) Percent of total NLs in the absence of DGKi. (*D*) Percent of total PLs in the absence of DGKi. **$P < 0.001$, *$P < 0.01$, from post hoc Student's *t* test, corrected for multiple comparisons. FFA, free fatty acids; MAG, monoacylglycerol; DAG, 1,2- diacylglycerol; PA, phosphatidic acid; PS, phosphatidylserine; PE, phosphatidylethanolamine; PC, phosphatidylcholine; TAG, triacylglycerol; CA, cardiolipin; #7 and #9, unknown. Error bars represent 1 SEM.

MICROBIOLOGY

Glomeromycota, and Mucoromycotina. The Early Divergent Fungi cluster, which harbors the symbiosis-activated DGKs, forms a sister group to the All Fungi cluster and harbors only representatives of the early divergent Mucoromycotina, Kickxellomycotina, and Chytridiomycota. Genomes of Mucoromycotina, including *R. microsporus*, encode DGKs that belong to both fungal DGK clusters, whereas genomes of Dikarya and Glomeromycota encode only representatives of the All Fungi cluster. Remarkably, with the exception of one DGK from chytrids, fungal DGKs are more closely related to DGKs in alveolates than to those in animals, even though, based on the organismal phylogeny (25), fungi and animals are part of the Opistokont supergroup. Collectively, we conclude that the two DGK genes overexpressed during symbiosis establishment represent a previously uncharacterized group of DGK genes.

Discussion

Antagonism–Mutualism Shift in the Course of Evolution of the *Rhizopus–Burkholderia* Symbiosis. The existence of *R. microsporus* host isolates that harbor *Burkholderia* and nonhost isolates that are endobacteria-free presents a unique opportunity to understand evolution of mutualisms in fungi. In particular, the *Rhizopus–Burkholderia* symbiosis was proposed to exemplify the addiction model of mutualism evolution (26), based on the obligate dependence of host fungi on endobacteria for asexual reproduction (4). However, the specific mechanism that keeps fungi cured of endobacteria from sporulation is unknown. The addiction model postulates that, after developing mechanisms to compensate for negative effects of an antagonistic symbiont, a host population may become dependent on, or addicted to the symbiont's continued presence (27). In the present study, we demonstrate that the nonhosts, including mucoralean fungi other than *R. microsporus*, exhibit growth inhibition when confronted by endobacteria derived from host fungi. These antagonistic outcomes suggest that endosymbiont-free nonhosts represent a preaddiction stage of the fungus. Whereas we did not identify specific compensatory mechanisms responsible for *Burkholderia* control of *Rhizopus* sporulation, we show that symbiosis establishment is governed by a set of fungal genes expressed uniquely by the host, with lipid metabolic genes playing a central role in this process (*SI Appendix*, Fig. S11). Specifically, analysis of fungal lipid profiles revealed that symbiosis establishment was accompanied by the accumulation of two lipid molecules, TAG and PE at a ratio of ~1. Perturbation of this ratio caused a shift in the fungal–bacterial interaction during symbiosis establishment from mutualism to antagonism. From this pattern, we propose that accumulation of TAG and PE at a specific ratio is part of the fungal addiction syndrome to endobacteria.

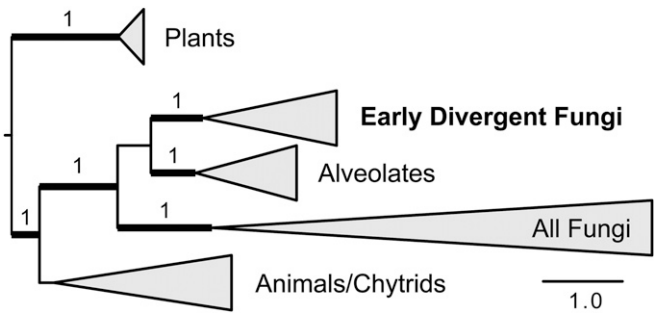

Fig. 4. Cartoon representation of the DGK phylogeny. DGKs encoded by genes DE during symbiosis are in the Early Divergent Fungi cluster. Bayesian posterior probability values >0.8 are displayed above branches; branches with maximum likelihood bootstrap support over 70% are thickened. The complete phylogeny is displayed in *SI Appendix*, Fig. S10, with strain and sequence IDs listed in *SI Appendix*, Table S5, and sequence alignment in *SI Appendix*, Dataset S1.

HOG-Mediated Activation of Lipid Metabolism During Symbiosis Establishment Leads to Accumulation of TAG and PE. The HOG signaling pathway has not been studied in early divergent fungi such as the Mucoromycotina. Based on gene expression analysis, we showed that in *R. microsporus* the HOG pathway was involved in mediating symbiosis establishment with bacteria and likely activated Gro-3-P accumulation. We further linked Gro-3-P accumulation to the observed activation of lipid metabolism. Analysis of lipid metabolic genes that were DE during symbiosis establishment revealed the likely activation of de novo biosynthesis of PE and the turnover of TAG. Examination of the fungal lipidome confirmed that symbiosis establishment was accompanied by a significant accumulation of PE and TAG.

PE is a ubiquitous component of eukaryotic membranes and is essential for growth of *S. cerevisiae* (28). However, accumulation of PE during interaction with bacteria cannot be explained by the need to synthesize new fungal membranes, because *Burkholderia* endosymbionts of *R. microsporus* are not housed within fungus-derived vesicles nor does host *R. microsporus* undergo increased rates of hyphal growth that would require biogenesis of new membranes. PE is also directly involved in the autophagic process (29) and has been implicated in affecting membrane curvature, fluidity, and polarized organization of actin (30). It is, therefore, more conceivable that increased PE levels might play a role in altering the biophysical properties of the membrane (31), although how that might be important for symbiosis establishment remains to be elucidated.

TAG is an important storage molecule that is typically localized to lipid droplets. It is likely that TAG serves as an energy reservoir for endobacteria, which, once inside the hyphae, must rely on fungus-derived carbon. Indeed, the genome of endobacteria revealed their ability to use glycerol, a breakdown product of TAG, as a sole carbon source (5). It is unclear, however, why fungi would accumulate TAG during symbiosis establishment, when a more plausible progression would be to break down TAG to release the energy source for bacteria. An alternative explanation is that the accumulation of TAG and PE during symbiosis establishment could be a result of transient accumulation of their precursor PA. PA is known to have signaling roles in eukaryotes (18) and it is possible that an accumulation of PA, undetected in this study, serves a signaling function in the coordination of symbiosis establishment. Accumulation of TAG and PE could thus be the end result of transient accumulation of PA, which, upon serving its signaling function, could become converted into PE through the cytidine diphosphate (CDP)–DAG pathway and channeled into biosynthesis of TAG by first becoming converted into DAG via a PA phosphatase. This hypothesis is supported by the up-regulation of PA-producing genes during symbiosis establishment.

Lipid Metabolism in Early Divergent Fungi. In addition to unraveling the mechanisms of mutualism establishment, we provide insights into the lipid metabolism in an understudied group of oleaginous fungi, the Mucoromycotina, which are a promising source of microbial oils for biodiesel production. We found that the genomes of *R. microsporus* encode homologs of well-characterized lipid metabolic genes from *S. cerevisiae*, which is the best-studied fungus in terms of lipid metabolism (16). Moreover, we analyzed the neutral lipid and phospholipid composition of *R. microsporus* and found that pharmacological DGK inhibitors affect its lipid profile in a way that is consistent with inhibition of DGK activity. This serves as evidence for the conservation of DGK enzyme activity between fungi and mammals, for which the inhibitors were developed (32).

We showed that fungal DGKs separate into two major groups, with one cluster unique to some members of early divergent fungi and a sister cluster containing representatives of all fungi. Such expansion of the DGK gene family in the Mucoromycotina genomes appears to mirror the enlargement of gene families involved in signal transduction in *M. circinelloides* and *Phycomyces blakesleeanus*, where it was attributed to a whole genome duplication

event predating the diversification of the Mucoromycotina (33). Moreover, with the exception of a DGK from chytrids, fungal and alveolate DGKs cluster together to the exclusion of animal DGKs, which is inconsistent with the organismal phylogeny uniting fungi and animals in the Opistokont supergroup (25). This pattern could be interpreted as a result of an ancient horizontal gene transfer event, although it is hard to speculate about the directionality and conditions that would favor such transfer, given how little is known about the function of DGKs in alveolates and early divergent fungi.

Conclusion

Overall, we identified a mechanism governing the transition from an antagonistic to mutualistic interaction between fungi and bacteria. We showed that symbiosis establishment is accompanied by specific changes in the lipid metabolic landscape of the fungus and perturbations of this landscape shift the interaction toward an antagonism during symbiosis establishment. Additionally, we provide first insights into the pathways and genetic basis of lipid metabolism in an understudied group of early divergent fungi, the Mucoromycotina.

Materials and Methods

Detailed descriptions of materials and methods are provided in *SI Appendix*. In brief, fungi were cultivated, cured, and endobacteria were isolated and visualized as previously described (2) with slight modifications. Infection success was confirmed by reestablishment of asexual sporulation in the host (4), PCR with *Burkholderia*-specific primers (3), and microscopy. A partition homogeneity test (10) with markers described in ref. 11 was performed to resolve the *R. microsporus* host and nonhost isolate relationship. Sequencing, assembly, and annotation of host and nonhost genomes was conducted at the Joint Genome Institute. In the RNA-seq experiment, mycelia were harvested from the interaction zone during initial physical contact with bacteria. RNA was extracted and rRNA was removed using commercial kits, followed by sequencing on the Illumina platform. Reads were mapped to the draft assemblies of host (JOSV00000000) and nonhost genomes. DE analysis was performed using standard tools. DGK inhibitor I (8 μM) and II (1 μM) (EnzoLife), and PLD inhibitor 5-fluoro-2-indolyl des-chlorohalopemide (1 mM) (Sigma) were used. Total lipids were extracted with chloroform:methanol (2:1 vol/vol). Phospholipids were visualized as in ref. 34. Neutral lipids were separated in hexane:diethyl ether: formic acid (80:20:2, vol/vol) solvent system. Phylogenetic analyses of amino acid sequences at DGK loci were conducted using Bayesian and maximum likelihood methods.

ACKNOWLEDGMENTS. We thank N. Schwardt for assistance with cocultivation of *M. circinelloides* with bacteria; Q. Sun for advice on RNA-seq analyses; F. Vermeylen for help with statistical analyses; A. Collmer and J. Worley for the gift of the pBS46:YFP plasmid; and A. Griganskyi and T. James for permission to analyze unpublished genomes of *Backusella circina* Jena Microbial Resource Collection (FSU) 941, *Lichtheimia hyalospora* FSU 10163, *Linderina pennispora* ATCC 12442, and *Martensiomyces pterosporus* CBS 209.56. This work was supported by National Science Foundation Grant IOS-1261004 (to T.E.P.) and NIH Grant GM19629 (to S.A.H.). Genomes of *R. microsporus* ATCC 52814 and ATCC 11559 were sequenced within the framework of the US Department of Energy (DOE) Joint Genome Institute (JGI) Community Sequencing Project Proposal ID 1450. The work conducted by the DOE JGI was supported by the Office of Science of the DOE under Contract DE-AC02-05CH11231.

1. Olsson S, Bonfante P, Pawlowska TE (2017) Ecology and evolution of fungal-bacterial interactions. *The Fungal Community: Its Organization and Role in the Ecosystem*, eds Dighton J, White JF (Taylor & Francis, Abingdon, UK), 4th Ed, pp 563–583.
2. Partida-Martinez LP, Hertweck C (2005) Pathogenic fungus harbours endosymbiotic bacteria for toxin production. *Nature* 437(7060):884–888.
3. Mondo SJ, Toomer KH, Morton JB, Lekberg Y, Pawlowska TE (2012) Evolutionary stability in a 400-million-year-old heritable facultative mutualism. *Evolution* 66(8): 2564–2576.
4. Partida-Martinez LP, Monajembashi S, Greulich KO, Hertweck C (2007) Endosymbiont-dependent host reproduction maintains bacterial-fungal mutualism. *Curr Biol* 17(9): 773–777.
5. Lackner G, Moebius N, Partida-Martinez L, Hertweck C (2011) Complete genome sequence of *Burkholderia rhizoxinica*, an Endosymbiont of *Rhizopus microsporus*. *J Bacteriol* 193(3):783–784.
6. Moebius N, Üzüm Z, Dijksterhuis J, Lackner G, Hertweck C (2014) Active invasion of bacteria into living fungal cells. *eLife* 3:e03007.
7. Leone MR, et al. (2010) An unusual galactofuranose lipopolysaccharide that ensures the intracellular survival of toxin-producing bacteria in their fungal host. *Angew Chem Int Ed Engl* 49(41):7476–7480.
8. Lackner G, Moebius N, Hertweck C (2011) Endofungal bacterium controls its host by an *hrp* type III secretion system. *ISME J* 5(2):252–261.
9. Taylor JW, et al. (2000) Phylogenetic species recognition and species concepts in fungi. *Fungal Genet Biol* 31(1):21–32.
10. Farris JS, Källersjö M, Kluge AG, Bult C (1995) Testing significance of incongruence. *Cladistics* 10(3):315–319.
11. Abe A, Asano K, Sone T (2010) A molecular phylogeny-based taxonomy of the genus *Rhizopus*. *Biosci Biotechnol Biochem* 74(7):1325–1331.
12. Mondo SJ (2013) Evolutionary stability of fungal-bacterial endosymbioses. PhD dissertation (Cornell University, Ithaca, NY).
13. Brewster JL, Gustin MC (2014) Hog1: 20 years of discovery and impact. *Sci Signal* 7(343):re7.
14. Nevoigt E, Stahl U (1997) Osmoregulation and glycerol metabolism in the yeast *Saccharomyces cerevisiae*. *FEMS Microbiol Rev* 21(3):231–241.
15. Zheng Z, Zou J (2001) The initial step of the glycerolipid pathway: Identification of glycerol 3-phosphate/dihydroxyacetone phosphate dual substrate acyltransferases in *Saccharomyces cerevisiae*. *J Biol Chem* 276(45):41710–41716.
16. Henry SA, Kohlwein SD, Carman GM (2012) Metabolism and regulation of glycerolipids in the yeast *Saccharomyces cerevisiae*. *Genetics* 190(2):317–349.
17. Topham MK, Prescott SM (2001) Diacylglycerol kinase zeta regulates Ras activation by a novel mechanism. *J Cell Biol* 152(6):1135–1143.
18. Henry SA, Gaspar ML, Jesch SA (2014) The response to inositol: Regulation of glycerolipid metabolism and stress response signaling in yeast. *Chem Phys Lipids* 180:23–43.
19. Pascual F, Carman GM (2013) Phosphatidate phosphatase, a key regulator of lipid homeostasis. *Biochim Biophys Acta* 1831(3):514–522.
20. Han G-S, O'Hara L, Carman GM, Siniossoglou S (2008) An unconventional diacylglycerol kinase that regulates phospholipid synthesis and nuclear membrane growth. *J Biol Chem* 283(29):20433–20442.
21. Mayr JA, Kohlwein SD, Paltauf F (1996) Identification of a novel, $Ca^{(2+)}$-dependent phospholipase D with preference for phosphatidylserine and phosphatidylethanolamine in *Saccharomyces cerevisiae*. *FEBS Lett* 393(2–3):236–240.
22. Rose K, Rudge SA, Frohman MA, Morris AJ, Engebrecht J (1995) Phospholipase D signaling is essential for meiosis. *Proc Natl Acad Sci USA* 92(26):12151–12155.
23. Gaspar ML, Aregullin MA, Jesch SA, Henry SA (2006) Inositol induces a profound alteration in the pattern and rate of synthesis and turnover of membrane lipids in *Saccharomyces cerevisiae*. *J Biol Chem* 281(32):22773–22785.
24. Fakas S, Konstantinou C, Carman GM (2011) DGK1-encoded diacylglycerol kinase activity is required for phospholipid synthesis during growth resumption from stationary phase in *Saccharomyces cerevisiae*. *J Biol Chem* 286(2):1464–1474.
25. Baldauf SL, Roger AJ, Wenk-Siefert I, Doolittle WF (2000) A kingdom-level phylogeny of eukaryotes based on combined protein data. *Science* 290(5493):972–977.
26. Aanen DK, Hoekstra RF (2007) The evolution of obligate mutualism: If you can't beat 'em, join 'em. *Trends Ecol Evol* 22(10):506–509.
27. Pannebakker BA, Loppin B, Elemans CP, Humblot L, Vavre F (2007) Parasitic inhibition of cell death facilitates symbiosis. *Proc Natl Acad Sci USA* 104(1):213–215.
28. Storey MK, et al. (2001) Phosphatidylethanolamine has an essential role in *Saccharomyces cerevisiae* that is independent of its ability to form hexagonal phase structures. *J Biol Chem* 276(51):48539–48548.
29. Ichimura Y, et al. (2000) A ubiquitin-like system mediates protein lipidation. *Nature* 408(6811):488–492.
30. Iwamoto K, et al. (2004) Local exposure of phosphatidylethanolamine on the yeast plasma membrane is implicated in cell polarity. *Genes Cells* 9(10):891–903.
31. Dawaliby R, et al. (2016) Phosphatidylethanolamine is a key regulator of membrane fluidity in eukaryotic cells. *J Biol Chem* 291(7):3658–3667.
32. de Chaffoy de Courcelles DC, Roevens P, Van Belle H (1985) R 59 022, a diacylglycerol kinase inhibitor. Its effect on diacylglycerol and thrombin-induced C kinase activation in the intact platelet. *J Biol Chem* 260(29):15762–15770.
33. Corrochano LM, et al. (2016) Expansion of signal transduction pathways in fungi by extensive genome duplication. *Curr Biol* 26(12):1577–1584.
34. Vaden DL, Gohil VM, Gu Z, Greenberg ML (2005) Separation of yeast phospholipids using one-dimensional thin-layer chromatography. *Anal Biochem* 338(1):162–164.

1.9 SUPPORTING INFORMATION

Materials & Methods

Fungal strains, culture conditions, removal and extraction of *Burkholderia* endosymbionts. *R. microsporus* host strains ATCC 52813 and ATCC 52814 as well as nonhost strains ATCC 11559 and ATCC 52807 were cultivated and cured of endobacteria as previously described (1). To isolate bacteria from the host strains, 3-day old mycelium was ground in 800 µL of Luria-Bertani (LB) broth using a plastic mortar and centrifuged at 4000×g for 2 min. The supernatant was passed twice through a 2 µm Whatman filter, plated onto LB agar plates supplemented with 1% glycerol, and incubated at 30^{o}C. For visualization, they were transformed with a YFP-expressing and gentamicin resistance-conferring plasmid pBS46.

Infection of host and nonhost fungi with *Burkholderia* endosymbionts. To test whether host and nonhost *R. microsporus* as well as *R. oryzae* ATCC 11423, *R. oryzae* ATCC 13440 and *Mucor circinelloides* CBS 277.49 can be infected with endosymbionts, fungi and bacteria were inoculated on opposite sides of a potato dextrose agar (PDA) plate supplemented with an LB agar plug. Specifically, an agar plug was removed from one side of a PDA plate using the reverse end of a 1000 µL pipet tip and filled with LB+1% glycerol agar medium. Bacteria were inoculated onto this LB plug and a ~0.5 cm^2 mycelial mat was placed on the other side of the plate. After the fungal mycelium grew over the bacteria, and filled the plate, a tuft of aerial hyphae was subcultured onto a fresh PDA plate. Successful infections of the cured host *R. microsporus* were monitored by: **(1)** visual inspection of re-establishment of asexual sporulation (2), **(2)** 23S rRNA gene PCR with *Burkholderia*-specific primers (3), and **(3)** microscopy to detect YFP-expressing *Burkholderia* endobacteria inside fungal hypahe. Infection success of the nonhost was monitored by PCR and microscopy, as the bacteria-free nonhost strains display intact sporulation. Genomic DNA for PCR was extracted from 3-day old mycelium using the Qiagen DNeasy Plant Mini Kit (QIAGEN).

Relationship between *R. microsporus* host and nonhost isolates. Using a partition homogeneity test (4) with 1,000 replicates, as implemented in PAUP* (5), we tested the null hypothesis of phylogenetic congruity among genealogies of three genes encoding actin, translation elongation factor 1α, and the rRNA internal transcribed spacer ITS (6), sampled from a collection of host and nonhost isolates of *R. microsporus,* including the genomes of ATCC 52813 and ATCC 11559. Rejection of the null hypothesis indicates incongruity among the marker genealogies, suggesting a history of gene flow across the isolates, a pattern characteristic for an interbreeding species.

***R. microsporus* ATCC 11559 and ATCC 52814 genome sequencing, assembly and annotation.** The genomes of *R. microsporus* ATCC 11559 and ATCC 52814 were sequencing using the Illumina platform. 100 ng of DNA was sheared to 300 bp using the covaris LE220 (Covaris) and size selected using SPRI

beads (Beckman Coulter). The fragments were treated with end-repair, A-tailing, and ligation of Illumina compatible adapters (IDT, Inc) using the KAPA-Illumina library creation kit (KAPA Biosystems). The prepared library was quantified using KAPA Biosystem's next-generation sequencing library qPCR kit and run on a Roche LightCycler 480 real-time PCR instrument. The quantified library was prepared for sequencing on the Illumina HiSeq sequencing platform utilizing a TruSeq Paired-End Cluster Kit v4, and Illumina's cBot instrument to generate a clustered flowcell for sequencing. Sequencing of the flowcell was performed on the Illumina HiSeq2500 sequencer using HiSeq TruSeq SBS Sequencing Kits v4, following a 2x150 indexed run recipe. Illumina reads were trimmed for quality, filtered for contamination, and initially assembled using Velvet (7). The resulting assembly was used to create *in silico* long mate-pair library with 3 Kbp inserts, which was then assembled together with the initial dataset using AllPathsLG release version R49403 (8). The genome was annotated using the JGI Annotation pipeline and made available via JGI fungal genome portal MycoCosm (jgi.doe.gov/fungi) and (9).

RNA-seq experiment and data analysis. Four conditions were examined: (1) cured host *R. microsporus* (ATCC 52813) cultured alone, (2) cured host *R. microsporus* (ATCC 52813) cultured with its native endobacteria, (3) nonhost *R. microsporus* (ATCC 11559) cultured alone, (4) nonhost *R. microsporus* (ATCC 11559) cultured with endobacteria extracted from the host. For each condition bacteria were inoculated on an LB+1% glycerol agar plug on one side of a half-strength PDA plate and a ~0.5 cm^2 mat of fungal mycelium placed on the other side. Plates were incubated at 30^{o}C. Fungal mycelium was harvested from the interaction zone just as the hyphae have come into physical contact with the bacterial plug. Each condition had three biological replicates, each consisting of three culture plates pooled prior to RNA extraction. Total RNA was extracted with the Ambion ToTALLY Total RNA Isolation Kit (Life Technologies) and rRNA was removed with RiboZero Magnetic Gold Kit (Epicentre). RNA sequencing libraries were prepared using the NEBNext® mRNA Library Prep Reagent Set for Illumina® and sequenced at the Cornell University Biotechnology Resource Center using the Illumina Hi-Seq2500 100 bp paired-end platform. Illumina data were quality controlled using the FASTX-Toolkit (10) and the reads were mapped onto either host *R. microsporus* (ATCC 52813) or nonhost (ATCC 11559) genomes using TopHat (11). Transcript abundances were quantified with CuffDiff (11) and differential gene expression analysis was performed with EdgeR (12). The false discovery rate (FDR) value of 0.01 was used as a cutoff for the identification of differentially expressed genes.

Identification of orthologs in the host and nonhost *R. microsporus* genomes and annotation of host lipid-related and signaling genes. We collected amino acid sequences for all protein-coding genes from *Rhizopus microsporus* ATCC 52813 (JOSV00000000), *Rhizopus microsporus* ATCC 52814 (this study), *Rhizopus microsporus* ATCC 11559 (this study), *Mucor circinelloides* CBS 277.49 (13), *Aspergillus nidulans* FGSC A4 (14) and *Saccharomyces cerevisiae* S288C (15) and conducted an All-vs-All BLASTp (16) search with parameters: E-value cutoff = 1×10^{-3} and maximum matches = 500.

OrthoMCL (17) was used to identify orthologs with parameters: mode = 3, pi_cutoff = 0, pv_cutoff = 1×10^{-3}, and inflation = 0.

GO category functional enrichment analysis. GO annotation for all the genes from the *R. microsporus* ATCC 52813 (host) genome were obtained from JGI Mycocosm (9), imported into BLAST2GO (18) software and a functional enrichment analysis was performed using a Fisher's Exact Test with a *P* value cutoff of 0.01 on all the up-regulated genes in response to interaction with bacteria.

Interaction between fungi and bacteria in the presence of chemical inhibitors. *R. microsporus* ATCC5 52813 (host) and *R. microsporus* ATCC 11559 (nonhost) were co-cultured with endobacteria isolated from *R. microsporus* ATCC 52813 in LB broth medium. The medium was supplemented with either: (1) inhibitors of diacylglycerol kinase, DGK inhibitors I (8 μM) and II (1 μM) (EnzoLife) dissolved in DMSO, (2) inhibitor of phospholipase D, 5-fluoro-2-indolyl des-chlorohalopemide, FIPI (1 mM) (Sigma), dissolved in DMSO, or (3) equivalent volumes of DMSO. Fungi were cultured with and without endobacteria in the following configurations: (i) host cured of its endobacteria cultured alone, (ii) host cured of its endobacteria cultured with endobacteria, (iii) nonhost cultured alone, (iv) nonhost cultured with the endobacteria extracted form the host, (v) host not cured of its endobacteria cultured alone. Each condition was replicated with DGK inhibitors (DGKi), and with PLD inhibitor (PLDi). The experiment was carried out in 6-well plates, each well serving as a replicate of that condition and the entire experiment was repeated twice to account for variability among plates. Wells were inoculated with a 0.5 cm^2 mycelial mat of the fungus and incubated at 30^{o}C, 50 rpm for 24 h. After 24 h the fungal colony diameter was measured and 80 μl of a 3-day old bacterial liquid culture was added to conditions (ii) and (iv). Fungal colony diameter was again measured after 48 h of growth, 24 h after bacteria added to conditions (ii) and (iv). Differences in fungal growth were assessed with ANOVA and post-hoc Student's t-test corrected for multiple comparisons.

Lipid extraction and TLC analysis. Cured host *R. microsporus* ATCC 52813 was grown with and without bacteria in the presence of chemical inhibitors of DGK as described above. Mycelial mats were harvested after 48 h from each well and 2 wells were pooled to make up a replicate, with a total of 3 replicates per condition. Samples were lyophilized, ground under liquid nitrogen, weighed, transferred to glass tubes and kept at -80^{o}C until extraction. To extract total lipids, the ground mycelium was re-suspended in 4 ml chloroform:methanol (2:1 v/v) and sonicated for 1 h. 800 μl NaCl (0.6%) was added to the samples and layers were separated by centrifugation. The chloroformic phase was transferred to a new pre-weighed vial and dried under liquid N_2. Total extracted lipids were quantified by weight and re-suspended in chloroform:methanol (2:1 v/v). Phospholipids were visualized by one-dimensional thin-layer chromatography as described by Vaden et al. (19). Briefly, Sigma-Aldrich silicagel on TLC plates with concentration zone were wetted with 1.8% boric acid prepared with 100% ethanol, dried for 5 min and the

concentration zone was divided into several lanes. 300 µg of lipids (10 µl) were applied to each lane and the plate placed in a chromatography tank equilibrated with solvent chloroform:ethanol:water:triethylamine (30:35:7:35, v/v). Neutral lipids were loaded onto silica gel plates in the same way and run in hexane:diethyl ether:formic acid (80:20:2, v/v) solvent system. Chromatograms were developed by spraying the plates with a solution of 10% cupric sulphate (w/v) and 8% phosphoric acid (v/v). Plates were incubated at 140^{o}C overnight. Neutral lipid and phospholipid identity was based on the mobility of known standards.

Image processing and statistical analysis. ImageJ Fiji 2.0.0-rc-34/1.50a (20) was used to compare the sizes and intensities of different lipid spots on the TLC plates among the conditions. Using the gel plugin in Fiji, we obtained integrated density plots for each lane on the TLC plate, whereby each lipid spot corresponded to a peak on the plot. We measured the area of each peak by extrapolating its Gaussian shape to the baseline. The sum of all peaks in a lane corresponded to total lipids in that sample, and each different lipid spot was represented as a percentage of total lipids in that lane. Differences in lipid profiles among conditions were analyzed with ANOVA.

Phylogenetic analyses of DGK amino acid sequences. Annotation of the protein domains of DGK genes DE during symbiosis establishment was performed with InterPro Scan and HMMER (21). Amino acid sequences for phylogenetic analyses were obtained as described in Table S5. Sequence alignment was performed with MUSCLE (22) and manually edited. Bayesian phylogeny was reconstructed under the WAG amino acid substitution model (23) estimated during the run under the amino acid substitution model mixed+I+Γ to identify substitution models that best fit the data, using MrBayes 3.2.5 (24) run for 1,500,000 generations with 25% burn-in, with the average standard deviation of split frequencies used as a convergence diagnostic. Maximum likelihood (ML) phylogeny was reconstructed with 1,000 bootstrap replicates using RAxML (25).

References

1. Partida-Martinez LP & Hertweck C (2005) Pathogenic fungus harbours endosymbiotic bacteria for toxin production. *Nature* 437(7060):884-888.
2. Partida-Martinez LP, Monajembashi S, Greulich KO, & Hertweck C (2007) Endosymbiont-dependent host reproduction maintains bacterial-fungal mutualism. *Curr. Biol.* 17(9):773-777.
3. Mondo SJ, Toomer KH, Morton JB, Lekberg Y, & Pawlowska TE (2012) Evolutionary stability in a 400-million-year-old heritable facultative mutualism. *Evolution* 66(8):2564-2576.
4. Farris JS, Källersjö M, Kluge AG, & Bult C (1995) Testing significance of incongruence. *Cladistics* (10):315-319.
5. Swofford DL (2003) *PAUP*. Phylogenetic Analysis Using Using Parsimony (*and Other Methods). Version 4.* (Sinauer Associates, Sunderland, MA).

6. Abe A, Asano K, & Sone T (2010) A molecular phylogeny-based taxonomy of the genus *Rhizopus*. *Biosci. Biotech. Biochem.* 74(7):1325-1331.
7. Zerbino DR & Birney E (2008) Velvet: Algorithms for *de novo* short read assembly using de Bruijn graphs. *Genome Res.* 18(5):821-829.
8. Gnerre S*, et al.* (2011) High-quality draft assemblies of mammalian genomes from massively parallel sequence data. *P. Natl. Acad. Sci. USA* 108(4):1513-1518.
9. Grigoriev IV*, et al.* (2014) MycoCosm portal: gearing up for 1000 fungal genomes. *Nucleic Acids Res.* 42(D1):D699-D704.
10. Gordon A & Hannon GJ (2010) FASTX-Toolkit. http://hannonlab.cshl.edu/fastx_toolkit.
11. Trapnell C*, et al.* (2012) Differential gene and transcript expression analysis of RNA-seq experiments with TopHat and Cufflinks. *Nat. Protoc.* 7(3):562-578.
12. Robinson MD, McCarthy DJ, & Smyth GK (2010) edgeR: a Bioconductor package for differential expression analysis of digital gene expression data. *Bioinformatics* 26(1):139-140.
13. Corrochano LM*, et al.* (2016) Expansion of signal transduction pathways in fungi by extensive genome duplication. *Curr. Biol.* 26(12):1577-1584.
14. Galagan JE*, et al.* (2005) Sequencing of *Aspergillus nidulans* and comparative analysis with *A. fumigatus* and *A. oryzae*. *Nature* 438(7071):1105-1115.
15. Goffeau A*, et al.* (1996) Life with 6000 genes. *Science* 274(5287):546-567.
16. Altschul SF, Gish W, Miller W, Myers EW, & Lipman DJ (1990) Basic local alignment search tool. *J. Mol. Biol.* 215(3):403-410.
17. Doerks T, Copley RR, Schultz J, Ponting CP, & Bork P (2002) Systematic identification of novel protein domain families associated with nuclear functions. *Genome Res.* 12(1):47-56.
18. Conesa A*, et al.* (2005) Blast2GO: a universal tool for annotation, visualization and analysis in functional genomics research. *Bioinformatics* 21(18):3674-3676.
19. Vaden DL, Gohil VM, Gu Z, & Greenberg ML (2005) Separation of yeast phospholipids using one-dimensional thin-layer chromatography. *Anal. Biochem.* 338(1):162-164.
20. Schindelin J, Rueden CT, Hiner MC, & Eliceiri KW (2015) The ImageJ ecosystem: An open platform for biomedical image analysis. *Mol. Reprod. Dev.* 82(7-8):518-529.
21. Finn RD*, et al.* (2015) HMMER web server: 2015 update. *Nucleic Acids Res.* 43(W1):W30-38.
22. Edgar RC (2004) MUSCLE: multiple sequence alignment with high accuracy and high throughput. *Nucleic Acids Res.* 32(5):1792-1797.
23. Whelan S & Goldman N (2001) A general empirical model of protein evolution derived from multiple protein families using a maximum-likelihood approach. *Mol. Biol. Evol.* 18(5):691-699.
24. Ronquist F*, et al.* (2012) MrBayes 3.2: efficient Bayesian phylogenetic inference and model choice across a large model space. *Syst. Biol.* 61(3):539-542.
25. Stamatakis A (2014) RAxML version 8: a tool for phylogenetic analysis and post-analysis of large phylogenies. *Bioinformatics* 30(9):1312-1313.

26. Cerqueira GC*, et al.* (2014) The *Aspergillus* Genome Database: multispecies curation and incorporation of RNA-Seq data to improve structural gene annotations. *Nucleic Acids Res.* 42(D1):D705-D710.
27. Chang Y*, et al.* (2015) Phylogenomic analyses indicate that early fungi evolved digesting cell walls of algal ancestors of land plants. *Genome Biol. Evol.* 7(6):1590-1601.
28. Attrill H*, et al.* (2015) FlyBase: establishing a Gene Group resource for *Drosophila melanogaster*. *Nucleic Acids Res.* 10.1093/nar/gkv1046.
29. Schwartze VU*, et al.* (2014) Gene Expansion Shapes Genome Architecture in the Human Pathogen Lichtheimia corymbifera: An Evolutionary Genomics Analysis in the Ancient Terrestrial Mucorales (Mucoromycotina). *PLoS Genetics* 10(8):1-16.
30. Takeda I*, et al.* (2014) Draft genome sequence of an oleaginous Mucoromycotina fungus *Mucor ambiguus* NBRC6742. *EMBL/GenBank/DDBJ databases*.
31. Baker SE*, et al.* (2015) Draft genome sequence of *Neurospora crassa* strain FGSC 73. *Genome Announc.* 3(2):e00074-00015.
32. Tisserant E*, et al.* (2013) Genome of an arbuscular mycorrhizal fungus provides insight into the oldest plant symbiosis. *Proc Natl Acad Sci U S A* 110(50):20117-20122.
33. Wang D, Wu R, Xu Y, & Li M (2013) Draft genome sequence of *Rhizopus chinensis* CCTCCM201021, used for brewing traditional Chinese alcoholic beverages. *Genome Announc.* 1(2):e00195-00112.
34. Ma LJ*, et al.* (2009) Genomic analysis of the basal lineage fungus *Rhizopus oryzae* reveals a whole-genome duplication. *PLoS Genet.* 5(7):e1000549.
35. Engel SR*, et al.* (2014) The reference genome sequence of *Saccharomyces cerevisiae*: Then and now. *G3* 4(3):389-398.
36. Kämper J*, et al.* (2006) Insights from the genome of the biotrophic fungal plant pathogen *Ustilago maydis*. *Nature* 444(7115):97-101.

Table S1. Genome assembly statistics for *R. microsporus* ATCC 11559 and ATCC 52814 as well as previously-sequenced *R. microsporus* ATCC 52813 (JOSV00000000) included for comparison.

	***Rhizopus microsporus* ATCC 11559**	***Rhizopus microsporus* ATCC 52814**	***Rhizopus microsporus* ATCC 52813**
Assembly length, bp	24,077,254	24,950,816	25,972,395
Number of scaffolds	595	560	131
Scaffold N50	87	8	8
Scaffold L50, bp	84,607	105,542	1,118,338
Number of contigs	653	649	823
Contig N50	96	84	111
Contig L50, bp	73,149	92,626	69,382
% GC	37.25	37.42	37.48

Table S2. Differentially expressed genes in response to bacteria exhibiting the same expression patterns in host and nonhost *R. microsporus.* Rows in red denote genes that were upregulated, in green, downregulated.

Host ATCC 52813 protein ID	Nonhost ATCC 11559 protein ID	Annotation
202842	204754	Chitin synthase, glycoside hydrolase family 2
11368	186000	Ras GTPase-activating protein
235493	265146	SPX, N-terminal - involved in G-protein associated signal transduction
212705	294600	NRPS-like AMP-dependent synthetase and ligase, Phosphopantetheine-binding
195307	21877	Thiamine biosynthesis Thi4 protein
291973	294475	Immunoglobulin E-set
221818	224748	Cytchrome b5, Fatty acid desaturase, type 1, N-terminal
284015	224748	Cytchrome b5, Fatty acid desaturase, type 1, N-terminal
239054	74686	Thiamine biosynthesis protein, homolog to Thi11/12/13/15 in *S. cerevisiae*
239553	89755	Cytochrome P450, E-class, group I

Table S3. Host *R. microsporus* DE genes with lipid-related function. *R. microsporus* ATCC 52813 protein IDs corresponding to DE genes are given in the first column, protein homologs in *S. cerevisiae* (Sc) and *A. nidulans* (An) are given in the second column as gene names; genes marked with an asterisk have been functionally characterized in the *S. cerevisiae* lipid metabolism pathway. Rows in red denote genes that were upregulated, in green, downregulated.

Protein ID in *R. microsporus*	**Homolog in *S. cerevisiae*/*A. nidulans***	**Annotation**
315343		Diacylglycerol kinase
249145		Diacylglycerol kinase, catalytic region
247363		Ca2+-dependent lipid-binding protein CLB1/vesicle protein vp115/Granuphilin A, contains C2 domain
205576	*PMP3*^{Sc}	Small plasma membrane protein; confers resistance to amphotericin B
253854		Cellular retinaldehyde-binding/triple function, C-terminal
250672		Methyltransferase type 11
236634	*ARE1*^{Sc}, *ARE2*^{Sc}*	Acyl-CoA sterol acyltransferase
39178	*GDP1*^{Sc}*	Homolog that synthesizes glycerol-3-phosphate
316518	*POX1*^{Sc}	Fatty-acyl coenzyme A oxidase
277488		Phospholipase D/Transphosphatidylase
222497	*dnfB*^{An}, *dnfA*^{An}	Phospholipid-translocating P-type ATPase, flippase
229679	*plaA*^{An}	Lysophospholipase/Phospholipase B
228323	*SLT1*^{Sc}*	Glycerol symporter
312984	*ITR1*^{Sc}, *ITR2*^{Sc}*	Inositol transporter
100147	*aoxA*^{An}, *aoxB*^{An}	Acyl-CoA oxidase/dehydrogenase, type 1
294209	*CHO1*^{Sc}*	PS synthase
242323	AN8743^{An}	Lipase, class 3
209457	*pldA*^{An}	Phospholipase D/Transphosphatidylase
202982	*MSS4*^{Sc}*	PI 4-P 5-kinase
256795	*PAH1*^{Sc}*	PA phosphatase
249672		Lipase, class 3
255094	*CYP539B2*^{An}	Cytochrome P450
291594		AMP-dependent synthetase and ligase
285170		Glycosyl transferase, family 15
204827	*SCT1*^{Sc}*	Glycerol-3-P /dihydroxyacetone-P acyltransferase
281243		Lipase, class 3
9421	*GUT1*^{Sc}*	Glycerol kinase
201222	AN5484^{An}	Sterol-binding
264309	*PSD2*^{Sc}*	PS decarboxylase

250139		Lipase, GDXG, active site
222441		NAD-dependent glycerol-3-phosphate dehydrogenase, C-terminal
284927	*MSS4*^{Sc*}	PI 4-P 5-kinase
221818	*OLE1*^{Sc*}	Delta9 Fatty acid desaturase
200197	*URA7*^{Sc}, *URA8*^{Sc*}	CTP synthetase
273299		Lipase, GDXG, active site
313597	*PIK1*^{Sc*}	PI 4-kinase
284015	*OLE1*^{Sc*}	Delta9 Fatty acid desaturase
290001		Metallophosphoesterase
266765		AMP-dependent synthetase and ligase
295175	*FAA1*^{Sc}, *FAA3*^{Sc}, *FAA4*^{Sc*}	Fatty acyl CoA synthetase

Table S4. Results of a two-way ANOVA of the effect of inhibitor and bacteria on the TAG:PE ratio.

Source	Nparm	DF	Sum of Squares	F Ratio	Prob > F
Bacteria	1	1	0.0051	0.2686	0.6183
Inhibitor	1	1	0.97556	51.2186	**<0.0001**
Bacteria × Inhibitor	1	1	0.06565	3.4469	0.1005

Table S5. Sources and full sequence IDs of amino acid sequences used in phylogeny reconstructions of DGK domain proteins displayed in Fig. 4 and Fig. S10.

Organism	Strain	Sequence ID	Source	Citation
Aspergillus nidulans	FGSC A4	AN1404	http://www.aspergillusgenome.org	(26)
Backusella circina	FSU 941	244085 333936	JGI Mycocosm	NA
Caenorhabditis elegans		DGK-1 DGK-2 DGK-3	http://www.wormbase.org	http://www.wormbase.org/db/get?name=WBGene00000958;class=gene http://www.wormbase.org/db/get?name=WBGene00000959;class=gene http://www.wormbase.org/db/get?name=WBGene00000960;class=gene
Coemansia reversa	NRRL 1564	24808	JGI Mycocosm	(27)
Drosophila melanogaster		rdgA-PI DGK-PI	http://flybase.org/	(28)
Homo sapiens		DGKA DGKE DGKI DGKZ DGKD DGKH DGKB DGKG DGKQ	UniProt	http://www.uniprot.org/uniprot/P23743 http://www.uniprot.org/uniprot/P52429 http://www.uniprot.org/uniprot/O75912 http://www.uniprot.org/uniprot/Q13574 http://www.uniprot.org/uniprot/Q16760 http://www.uniprot.org/uniprot/Q86XP1 http://www.uniprot.org/uniprot/Q9Y6T7 http://www.uniprot.org/uniprot/P49619 http://www.uniprot.org/uniprot/P52824
Linderina pennispora	ATCC 12442	221248	JGI Mycocosm	NA
Lichtheimia hyalospora	FSU 10163	180828	JGI Mycocosm	NA
Lichtheimia corymbifera	FSU:9682	1085	JGI Mycocosm	(29)
Martensiomyces pterosporus	CBS 209.56	255062	JGI Mycocosm	NA
Mucor ambiguus	NBRC6742	MAM1_0120d05820 MAM1_0040c02849	UniProt	(30)
Mucor circinelloides	CBS 277.49	77537 108146 76354	JGI Mycocosm	(13)
Neurospora crassa	FGC 73	5918 5474	JGI Mycocosm	(31)
Perkinsus marinus	ATCC 50983	PMAR006522 PMAR023096	UniProt	NZ_AAXJ00000000.1

Phycomyces blakesleeanus	NRRL1555	188773 155448 175731 77550	JGI Mycocosm	(13)
Rhizophagus irregularis	DAOM 181602	19888 342772	JGI Mycocosm	(32)
Rhizopus microsporus	ATCC 52813	244500 283554 249145 315343	JGI Mycocosm	NA
Rhizopus microsporus	ATCC 52814	250008 73907 252673 257218	JGI Mycocosm	This study
Rhizopus microsporus	ATCC 11559	255942 203539 224971 223686	JGI Mycocosm	This study
Rhizopus microsporus	CCTCC M201021	2034 15011	JGI Mycocosm	(33)
Rhizopus oryzae	99-880	RO3G_16093 RO3G_1433 RO3G_1764	JGI Mycocosm	(34)
Saccharomyces cerevisiae	S288C	LCB4	http://www.yeastgenome.org	(35)
Ustilago maydis		6021	JGI Mycocosm	(36)
Vitrella brassicaformis		Vbra_3729	Uniprot	http://www.uniprot.org/uniprot/A0A0G4EF06

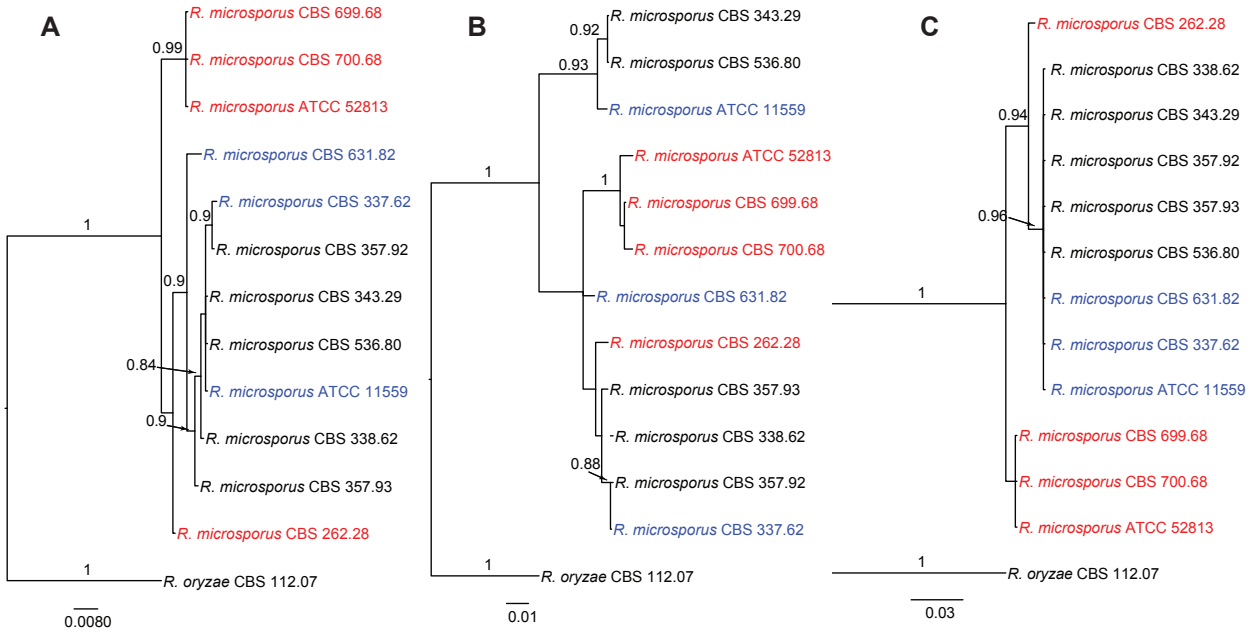

Figure S1. Bayesian genealogies of nucleotide sequences sampled from host and nonhost isolates of *R. microsporus* at three loci. (A) Actin, *act1.* (B) Translation elongation factor 1α, *tef1.* (C) rRNA ITS. Values above branches represent posterior probability values, values above 0.8 are shown. Red, host isolates; blue, nonhost isolates; back, unknown.

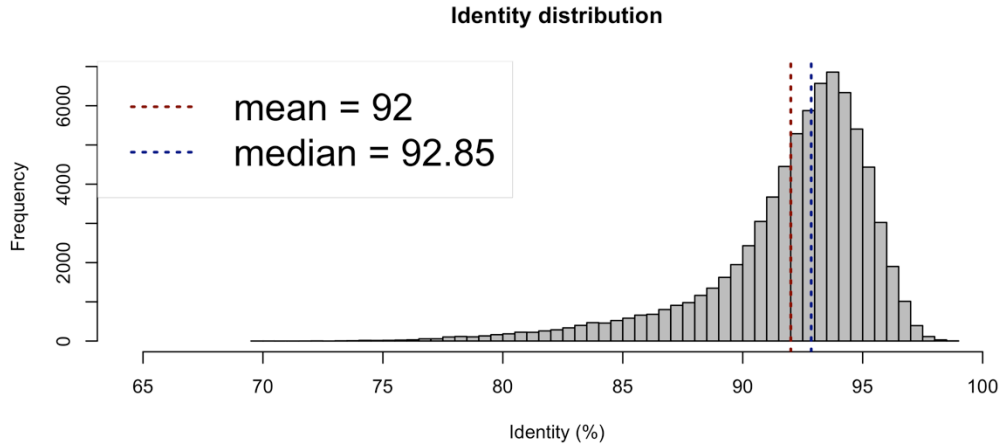

Figure S2. Average nucleotide identity (ANI) calculated between genomes of host (ATCC 52813) and nonhost (ATCC 11559) *R. microsporus* using the ANI calculator online tool (http://enve-omics.ce.gatech.edu/ani/index). The tool splits the genomes into 1000 bp fragments and compares nucleotide identity between them. Histogram shows frequency distribution of genome fragments sorted by percent nucleotide identity between the two genomes.

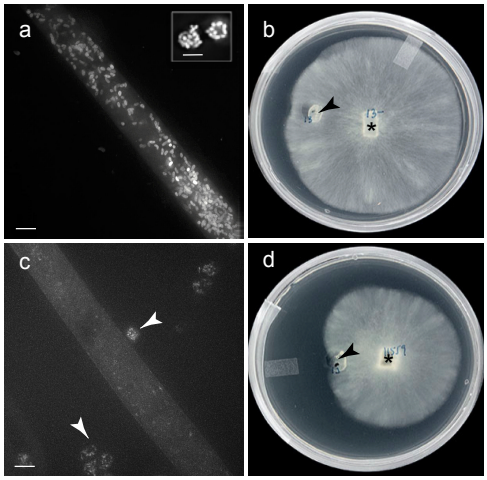

Figure S3. Interactions of host and nonhost *R. microsporus* with *Burkholderia* isolated from the host. (**a**) Host (ATCC 52814) hypha and spores (inset) populated with yellow fluorescent protein (YFP)-expressing *Burkholderia* endosymbionts. (**b**) Host colony during symbiosis formation with *Burkholderia* endobacteria. (**c**) Nonhost (ATCC 11559) hypha and spores (indicated by arrowheads) free of endobacteria. (**d**) Nonhost colony displaying an antagonistic response to endobacteria of the host. Scale bars in **a** and **c** represent 5 µm. In **b** and **d,** arrowheads indicate site of bacterial inoculation, asterisks indicate site of fungal inoculation.

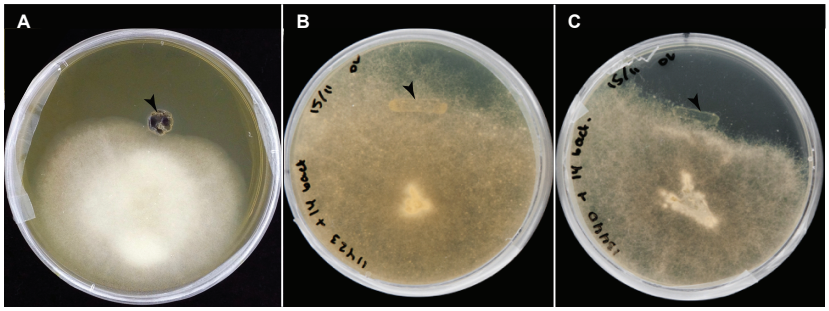

Figure S4. Endobacteria of *R. microsporus* ATCC 52813 interact antagonistically with nonhost isolates of *Mucor* and *Rhizopus*. (A) *M. circinelloides* CBS 277.49. (B) *R. oryzae* ATCC 11423. (C) *R. oryzae* ATCC 13440. Arrowheads indicates zone of bacterial inoculation.

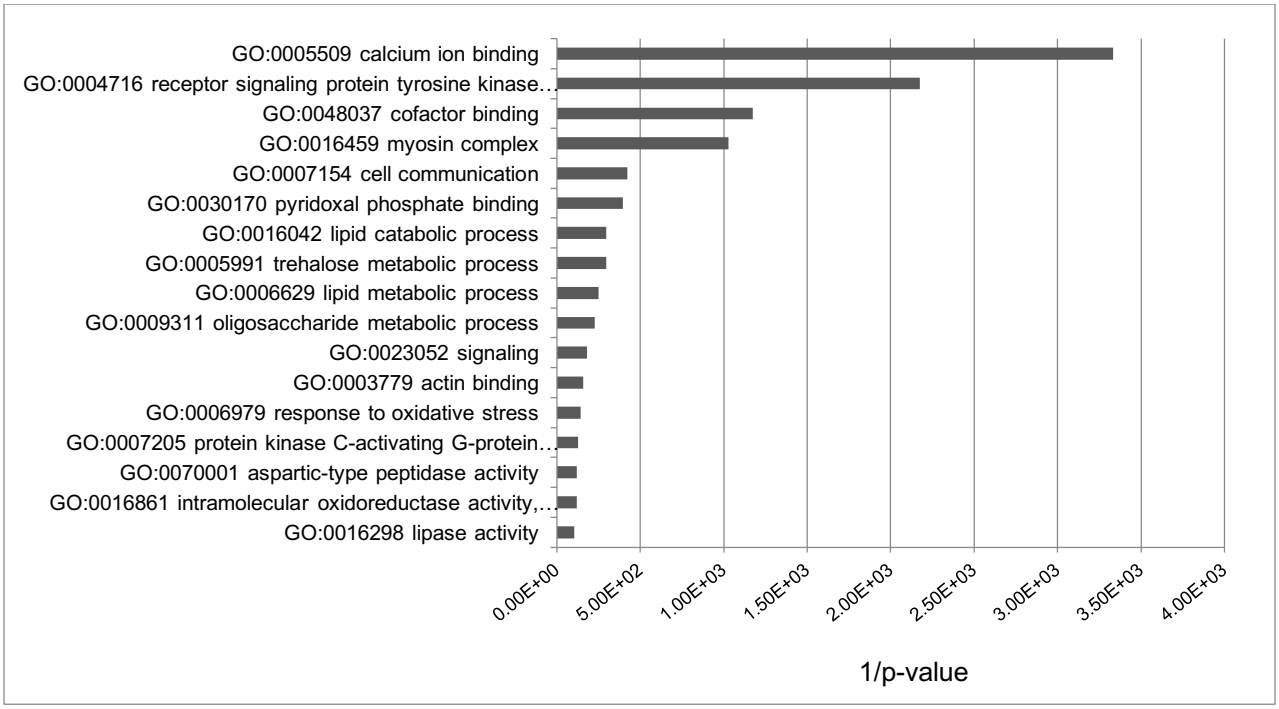

Figure S5. **GO categories enriched in the upregulated fraction of the DE host *R. microsporus* genes in response to interaction with bacterial symbionts.**

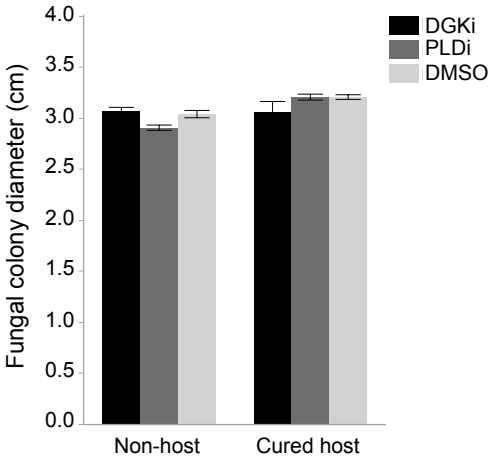

Figure S6. DGK and PLD inhibitors do not affect the growth of nonhost (ATCC 11559) and cured host (ATCC 52813) fungi. Diacylglycerol kinase inhibitors, DGKi; phospholipase D inhibitor; PLDi, dimethyl sulfoxide; DMSO, no inhibitor. Error bars represent 1 standard error of the mean.

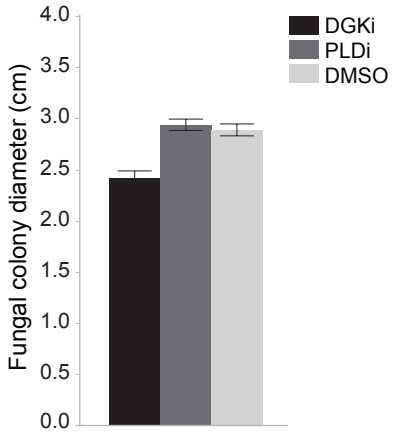

Figure S7. DGK inhibitors, but not PLD inhibitors reduced the growth of host (ATCC 52813) fungus that was not cured of its endobacteria. Diacylglycerol kinase inhibitors, DGKi; phospholipase D inhibitor; PLDi, dimethyl sulfoxide; DMSO, no inhibitor. Error bars represent 1 standard error of the mean.

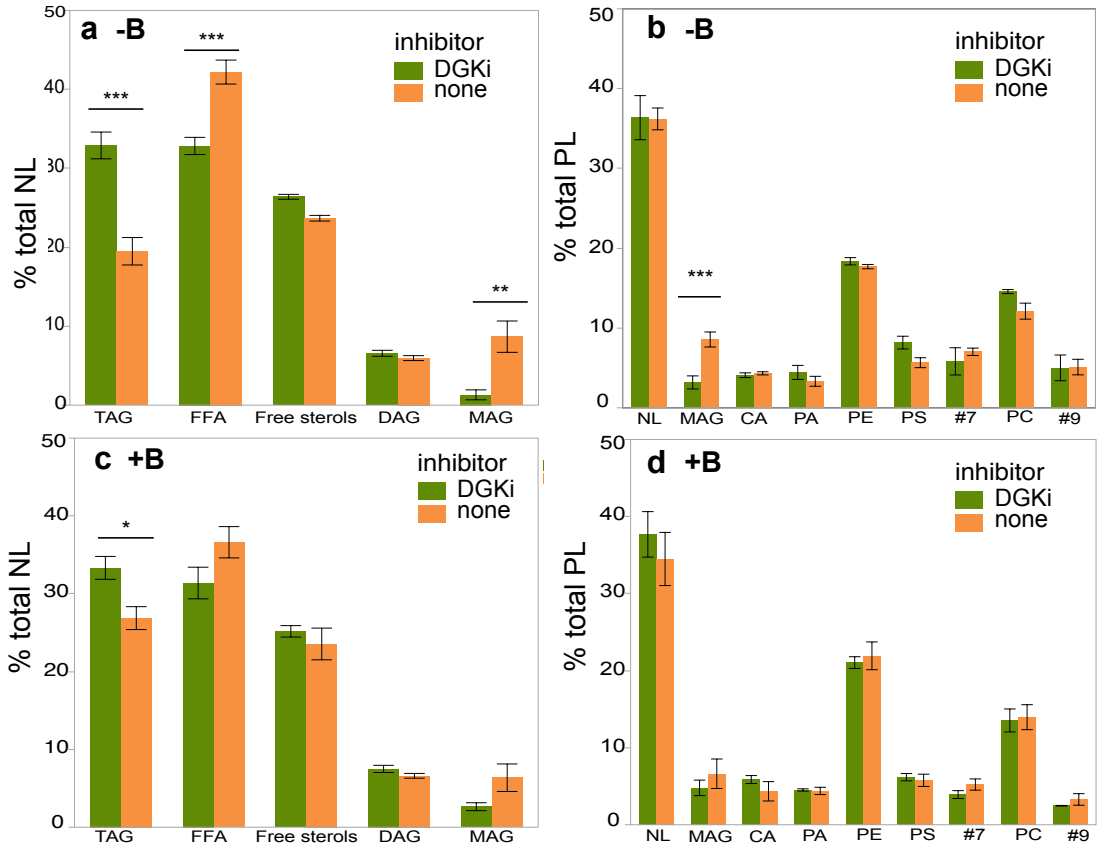

Figure S8. Effects of endobacteria on relative abundance of phospholipid (PL) and neutral lipid (NL) species in cured host *R. microsporus* ATCC 52813 grown with and without DGK inhibitor (DGKi). (a) Percent of total NLs in the presence of endobacteria (+B). **(b)** Percent of total PLs in the presence of endobacteria (+B). **(c)** Percent of total NLs in the absence of endobacteria (-B). **(d)** Percent of total PLs in the absence of endobacteria (-B). P<0.0001***, P<0.001**, P<0.01*, from post-hoc Student's t-test, corrected for multiple comparisons. FFA, free fatty acids; MAG, monoacylglycerol; DAG, 1,2- diacylglycerol; PA, phosphatidic acid; PS, phosphatidylserine, PE, phosphatidylethanolamine, PC, phosphatidylcholine, TAG, triacylglycerol; CA, cardiolipin; #7 and #9, unknown. Error bars represent 1 standard error of the mean.

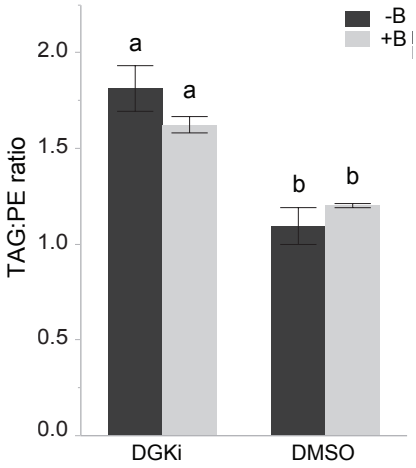

Figure S9. DGK inhibitors increase the TAG:PE ratio of host *R. microsporus*. Bar chart shows the ratio of TAG:PE in fungi grown with (+B) and without (-B) bacteria, in the presence (DGKi) and absence (DMSO) of inhibitors. Ratios not marked by the same letter are significantly different. Error bars represent 1 standard error of the mean.

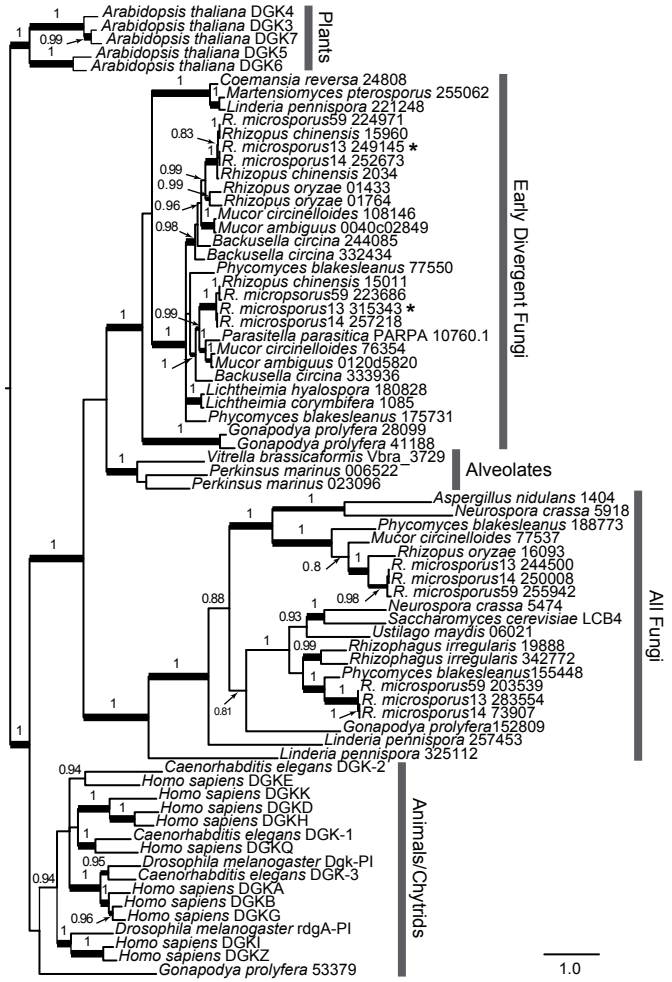

Figure S10. Phylogeny reconstruction of fungal, animal, plant and alveolate proteins with DGK domains. Bayesian posterior probability values above 0.8 are displayed above branches, branches with Maximum Likelihood bootstrap support over 70% are thickened. The tree was rooted with sequences derived from plants. *R. microsporus*13, *R. microsporus*14, *R. microsporus*59 denote *Rhizopus microsporus* isolates ATCC 52813, ATCC 52814 and ATCC 11559, respectively. Asterisks indicate the two DGK genes DE during symbiosis establishment. Strain and sequence IDs are listed in Table S5, alignment of protein sequences used for phylogeny reconstruction is provided in Text S1..

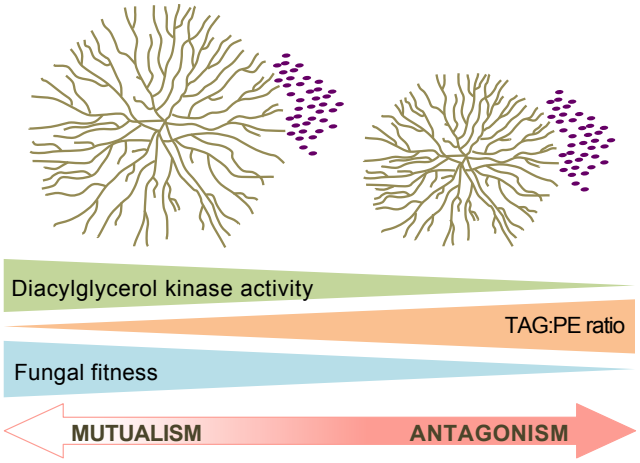

Figure S11. Manipulation of TAG:PE ratio with diacylglycerol kinase inhibitors during symbiosis establishment shifts the host-symbiont interaction into an antagonism. Fungal fitness is reduced during symbiosis establishment with bacteria, depicted by purple rods, when the activity of DGK is inhibited and the ratio of TAG:PE is increased.

CHAPTER 2

RECIPROCAL COMMUNICATION IN FUNGAL-BACTERIAL SYMBIOSES[1]

2.1 ABSTRACT

Fungal-bacterial symbioses range from antagonisms to mutualisms and remain one of the least understood inter-domain interactions despite their environmental ubiquity and medical importance. To decipher molecular dialogues between fungi and bacteria in different types of symbioses, we analyzed fungal and bacterial transcriptional responses in the mutualism between *Rhizopus microsporus* (*Rm*, host) and its *Burkholderia* endobacteria versus the antagonism between a non-host *Rm* and *Burkholderia* isolated from the host, at two time points, before and during partner physical contact. We found that bacteria and fungi sensed each other before contact and altered gene expression patterns accordingly. *Burkholderia* did not discriminate between the host and non-host and appeared equally equipped to infect both. The majority of genes responsible for the ability of *Burkholderia* endobacteria to engage *Rm* are also present in the genomes of *Burkholderia* species with other lifestyles, indicating that the capacity to interact with fungi is enabled by a pre-existing gene repertoire. Fungal responses to endobacteria were dramatically different in the host versus non-host. Gene expression patterns suggest that before contact, the non-host engaged in detoxification of an unknown metabolite produced constitutively by bacteria that did not affect the host. During physical contact, fungal cell wall chitin appeared to be broken down in favor of 1,3-beta-glucan, and reactive oxygen species (ROS) were generated in the non-host, whereas cell wall chitin synthesis was favored and ROS were quenched in the host. We speculate that specific cell wall modifications and ROS metabolism contribute to the non-host resistance to bacterial infection and the host ability to form a mutualism. Overall, our findings build a foundation for understanding the molecular factors mediating fungal-bacterial interactions.

[1] The results of this study will be submitted to *PLoS Genetics*, and is written according to their manuscript guidelines.

2.2 AUTHOR SUMMARY

Symbioses between fungi and bacteria are ubiquitous and economically important. Yet, they remain poorly explored. To build a conceptual framework for understanding of fungal-bacterial symbioses, we focused on a model symbiosis between the mold *Rhizopus microsporus* (*Rm*) and its *Burkholderia* endobacteria. In this system, some *Rm* isolates behave as hosts and form a mutualism with *Burkholderia*, whereas others (non-hosts) interact antagonistically with bacteria isolated from the host. We found that bacteria engaged a common gene repertoire in interactions with fungi, regardless of whether the outcome was mutualistic or antagonistic. Remarkably, many of these genes are present in *Burkholderia* species of diverse lifestyles, whereas others encode novel symbiosis factors. In contrast, fungal responses to bacteria differed dramatically at the gene level in a mutualism versus antagonism, with differences centered on fungal cell wall biogenesis and reactive oxygen species metabolism. Together, our study offers fundamental insights into communication patterns that differentiate fungal-bacterial mutualisms from antagonisms.

2.3 INTRODUCTION

Reciprocal communication between interacting partners is a feature central to all interspecific symbioses, antagonisms and mutualisms alike. As partners approach each other and come into contact, they exchange biochemical signals repeatedly and continuously throughout the duration of the relationship. Many molecular conversations guiding interactions between microbes and their animal and plant hosts have been deciphered, revealing that signals, receptors, and response regulatory networks are often shared between antagonisms and mutualisms (Boller & Felix, 2009). In contrast, symbioses of fungi with bacteria remain one of the least understood inter-domain relationships despite their environmental ubiquity and medical importance (Olsson *et al*., 2017). Among them, the symbiosis between *Rhizopus microsporus* (*Rm*, Mucoromycotina) and *Burkholderia* sp. endobacteria (beta-proteobacteria) is emerging as a model for the study of

mutualistic fungal-bacterial interactions (Partida-Martinez & Hertweck, 2005, Partida-Martinez *et al*., 2007, Moebius *et al*., 2014, Lastovetsky *et al*., 2016). The molecular bases governing the establishment of the *Rm-Burkholderia* symbiosis are beginning to be unraveled, with much progress made in understanding bacterial factors necessary to invade the fungus (Leone *et al*., 2010, Lackner *et al*., 2011, Moebius *et al*., 2014) and the changes that occur in the fungus to accommodate endobacteria (Lastovetsky *et al*., 2016). In particular, we have previously shown that the HOG MAPK signaling pathway and specific changes in lipid metabolism of the host are important for the mutualism establishment (Lastovetsky *et al*., 2016). We were able to make these observations because, in addition to *Rm* isolates that host endobacteria, there exist closely related but naturally bacteria-free non-host isolates that interact antagonistically with endobacteria of the host and do not become infected by them (Lastovetsky *et al*., 2016).

To build an overarching conceptual framework for understanding fungal-bacterial symbioses, we conducted global profiling of fungal and bacterial transcriptional responses in the antagonistic versus mutualistic interaction of closely related *Rm* isolates with *Burkholderia* endobacteria at two time points, before physical contact of the partners (pre-contact) and during physical contact. We dissected molecular dialogues between the partners and identified fungal and bacterial factors contributing to antagonism versus mutualism. As well as unraveling the molecular similarities between these two interactions, we aimed to understand how the non-host is able to resist infection by bacteria that are mutualists of the host. We found that in interactions with the host and non-host symbiotic bacteria engaged a common set of genes encoding known as well as novel symbiosis factors. In contrast, host and non-host responses, albeit almost entirely different at the gene level, converged on the altered expression of cell wall and reactive oxygen species (ROS) related genes, a pattern that may explain the non-host resistance to bacterial infection and the host ability to form a mutualism.

2.4 RESULTS & DISCUSSION

To identify fungal and bacterial genes involved in interactions of the non-host with endobacteria

isolated from the host (antagonism) and the host with its own endobacteria (mutualism), we analyzed their expression changes during partner co-cultivation at two time points: pre-contact and during physical contact. Fungal RNA-seq reads were mapped to genomes of *Rm* ATCC 52813 (host) and ATCC 11559 (non-host). *Burkholderia* endobacterial reads were mapped to the genome of *Burkholderia* sp. B13 (endobacteria of the host *Rm* ATCC 52813), sequenced for this study and summarized in Table S1. It should be noted that *Burkholderia* sp. B13 shares with *B. rhizoxinica* HKI454, a previously characterized symbiont of *Rm* ATCC 62417 (Partida-Martinez *et al*., 2007, Lackner *et al*., 2011), a whole-genome average nucleotide identity of 91% (Fig. S1). This value does not exceed the 95-96% similarity threshold accepted as a counterpart of a DNA-DNA hybridization value of 70% for species delineation (Richter & Rosselló-Móra, 2009). Differentially expressed (DE) fungal genes were identified by comparing expression profiles of host and non-host fungi grown alone to host and non-host fungi co-cultivated with endobacteria during the same time point. Similarly, DE endobacterial genes were identified by comparing endobacteria grown alone to endobacteria co-cultivated with either host or non-host fungi, at the same time point. False discovery rate of 0.01 was used as a cutoff for identification of DE genes.

Pre-contact Responses in Fungi. The antagonistic interaction between the non-host and endobacteria of the host was marked by changes in the fungal colony morphology, whereby the colony developed a zone of reduced growth (Lastovetsky *et al*., 2016). This pattern was more pronounced as the fungus neared the bacteria (Lastovetsky *et al*., 2016), but it was also visible during pre-contact (Fig. S2). No such growth alterations occur in the host during interaction with its endobacteria. These phenotypic patterns were consistent with the magnitude of transcriptomic responses of 145 DE genes in the non-host (122 upregulated) and 10 DE genes in the host (6 upregulated), suggesting, in turn, that both non-host and host fungi were able to sense bacterial presence pre-contact.

Detoxification. The pre-contact appearance of growth alterations in the non-host colonies suggested a reaction to an unknown bacterial compound, supported by the upregulated

expression of various non-host genes encoding transporters (Protein IDs 224825, 205631, 254867, 170380, 245627) and a detoxification enzyme, glutathione S-transferase (GST, 216648). Overexpression of transporters is a well-known feature of drug resistance in fungi (Masiá Canuto & Gutiérrez Rodero, 2002), whereas GST genes are typically overexpressed during chemical challenge and oxidative stress response (Kitagawa *et al*., 2003, Berry & Gasch, 2008). The nature of the bacterial compound that elicited the non-host response is uncertain, as we did not detect differential expression of any of the secondary metabolism gene clusters encoded in the endosymbiont genome, suggesting that the non-host reacted to a constitutively produced bacterial metabolite.

Cell wall biogenesis. While both non-host and host upregulated genes involved in cell wall synthesis and remodeling, there was no overlap between these gene sets (Table 1). Fungal cell walls are composed of a scaffold of cross-linked polysaccharides, such as glucans, chitin, chitosan, and a matrix of proteins and mannans (Osherov & Yarden, 2010). In the non-host, we detected differential expression of genes with chitin-modifying function, such as chitinases and chitin deacetylases (Table 1). Importantly, in many fungi, chitinases are tightly spatio-temporally controlled at the transcription level (Langner & Göhre, 2016). Moreover, chitin deacetylase transcription levels correlate with activity as well as chitosan content of fungal cell walls (Chakraborty *et al*., 2016). While expression of chitin-degrading chitinases was both up- and downregulated, chitin deacetylases were mostly downregulated. Chitin deacetylases produce a deacetylated form of chitin, chitosan, a structural component of *Rhizopus* cell walls (Tominaga & Tsujisaka, 1981). In addition to altered expression of genes encoding chitin-modifying enzymes, the non-host upregulated 7 genes with mannosyltransferase activity and 4 septin genes, all involved in cell wall remodeling, strengthening, and hyphal growth (Gladfelter, 2006, Osherov & Yarden, 2010). These expression patterns suggest that the non-host was reducing the amount of chitosan relative to other cell wall polysaccharides in its cell walls. Even though the host pre-contact response was more limited, some of those genes also had cell wall related function (Table 1). Specifically, in contrast to the non-host, the host appeared to initiate chitin

Table 1. Cell wall related genes DE in host and non-host fungi during pre-contact interaction with *Burkholderia* endobacteria. Log_2FC, Log_2 fold change; negative Log_2FC values denote downregulated genes; positive Log_2 FC values denote upregulated genes; FDR, false discovery rate value. *annotation obtained though CAZYmes Analysis Toolkit (Lombard *et al.*, 2014); **annotation obtained through the *myco*CLAP database (Murphy *et al.*, 2011); the remaining annotations are from JGI.

Protein ID	Log_2FC	FDR	CAZY/InterPro/PFAM	Annotation
Non-host				
178226	1.84	1.85E-04	GT15	2-alpha-mannosyltransferase*
177931	1.75	3.20E-05	GT15	2-alpha-mannosyltransferase*
177938	1.67	1.42E-04	GT15	2-alpha-mannosyltransferase*
290291	1.62	2.15E-04	GT15	2-alpha-mannosyltransferase*
210844	1.48	4.85E-05	GH16	Xylanase/beta(1,3-1,4)glucanase**
169859	1.47	4.95E-04	GT39	Mannosyltransferase activity *
118361	1.45	4.84E-04	GT39	Mannosyltransferase activity *
71975	1.37	3.58E-04	GH47	Alpha-1,2-mannosidase**
177895	1.27	2.15E-04	IPR016491	Septin
241953	1.25	1.58E-03	GT15	2-alpha-mannosyltransferase*
195250	1.20	4.63E-03	IPR016491	Septin
5395	1.17	2.15E-04	IPR016491	Septin
198617	1.08	2.57E-03	IPR016491	Septin
113619	1.07	9.37E-03	GH18	Chitinase**
288806	1.01	7.25E-03	CE4	Chitin deacetylase**
178335	-0.82	6.15E-03	CE4	Chitin deacetylase**
129845	-0.85	3.96E-03	GH18	Chitinase**
203498	-0.87	7.20E-03	CE4	Chitin deacetylase**
50892	-0.97	1.27E-03	CE4	Chitin deacetylase**
209253	-1.58	3.94E-07	CE4	Chitin deacetylase**
97566	-2.12	1.02E-03	CE4	Chitin deacetylase**
204982	-2.24	8.05E-06	GH28	Endo-polygalacturonase**
Host				
241339	1.41	4.05E-02	GT2	Chitin synthase*
245394	0.99	7.20E-03	CE4	Chitin deacetylase**
252367	0.67	3.89E-02	PF10342	Mixed-link glucanase

and chitosan synthesis through upregulation of genes encoding chitin synthase and chitin deacetylase. Overall, the non-host and host pre-contact responses to endobacteria converged on cell wall remodeling, albeit of different types, highlighting the difference between these two types of interactions. Some of the non-host responses were most likely related to the colony growth alterations. Others may reflect changes in the cell wall composition itself. Perception of an antagonistic bacterium might have prompted the non-host to alter its cell wall for protection from bacterial invasion, whereas perception of a mutualistic partner could have induced the host to initiate subtle cell wall changes to facilitate symbiont entry.

Pre-contact Responses in Bacteria. Endobacteria DE 219 genes in response to non-host (173 up- and 46 downregulated) and 123 genes (107 up- and 16 downregulated) in response to the host, suggesting that they were able to sense fungal presence and activated transcription in response to both fungi. 47 genes were commonly upregulated in response to the non-host and host.

Secretion systems and their effectors. Many of the genes commonly upregulated in response to both fungi encoded the Type III Secretion System (T3SS) machinery, candidate T3SS effector proteins, and a bacterial chitinase. T3SS is used by plant and animal pathogens to deliver protein effectors directly into the host cytoplasm for host manipulation (Costa *et al*., 2015). In the symbiosis between *Rm* and *B. rhizoxinica*, T3SS is crucial for the formation of the stable symbiotic association (Lackner *et al*., 2011). In addition to components of the T3SS machinery itself, we identified 15 candidate effectors with a T3SS signal; over half of these are proteins of unknown function (Table S2). Remarkably this occurs before physical contact with the fungi, which is needed for translocation of the effectors through the T3SS. Another set of *B. rhizoxinica* factors known to enable symbiotic colonization of the *Rhizopus* host comprises cell wall-degrading enzymes secreted through the Type II Secretion System, T2SS (Moebius *et al*., 2014). T2SS translocate various proteins across the outer membrane of gram negative bacteria into the extracellular environment (Korotkov *et al*., 2012). The genomes of *B. rhizoxinica* (Lackner *et al*.,

2011) and *Burkholderia* sp. B13 encode a number of chitin-interacting proteins, including a chitinase, chitosinase, and a chitin-binding protein. Pre-contact, bacteria upregulated in response to both non-host and host fungi the gene encoding chitinase, but not the other chitin-interacting genes or components of the T2SS machinery.

Taken together, bacterial responses to fungi pre-contact involved upregulating expression of genes with known function in symbiosis establishment, indicating that symbionts were already primed for infection (Fig. 1). Remarkably, bacteria upregulated the same symbiosis genes in response to non-host and host, suggesting that they were equally equipped to infect both fungi.

Physical Contact Responses in Fungi. In contrast to the pre-contact interaction with endobacteria, the host differentially expressed more than twice as many genes as the non-host during physical contact. In our previous work, we showed that different sets of genes were engaged in host and non-host fungi during physical contact with endobacteria, with a particular focus on activation of genes in the HOG MAPK signaling pathway, and specific changes in lipid metabolism in the host (Lastovetsky *et al*., 2016).

Cellular response to oxidative stress. Besides involvement in osmotic stress and initiation of glycerol synthesis, the HOG pathway plays roles in other stress responses, including oxidative stress (Zhao *et al*., 2007). Supporting the role of oxidative stress in the mutualistic interaction between the host and endobacteria, the 'response to oxidative stress' GO category was enriched among the upregulated host genes. In particular, we saw upregulation of genes involved in antioxidant defense, encoding catalases, GST, and a serine/threonine kinase (Table 2); the latter is a homolog to *S. cerevisiae* YAK1 (234989) overexpressed in yeast during oxidative stress (Gasch *et al*., 2000). Additionally, a gene encoding the reactive nitrogen species (RNS)-producing nitric oxide synthase was downregulated. These expression patterns indicate that reactive oxygen species (ROS) were likely neutralized by the host as opposed to being produced. In the non-host, by contrast, we detected differential expression of genes capable of generating ROS and causing oxidative damage through prooxidant activity (Table 2). Two of the

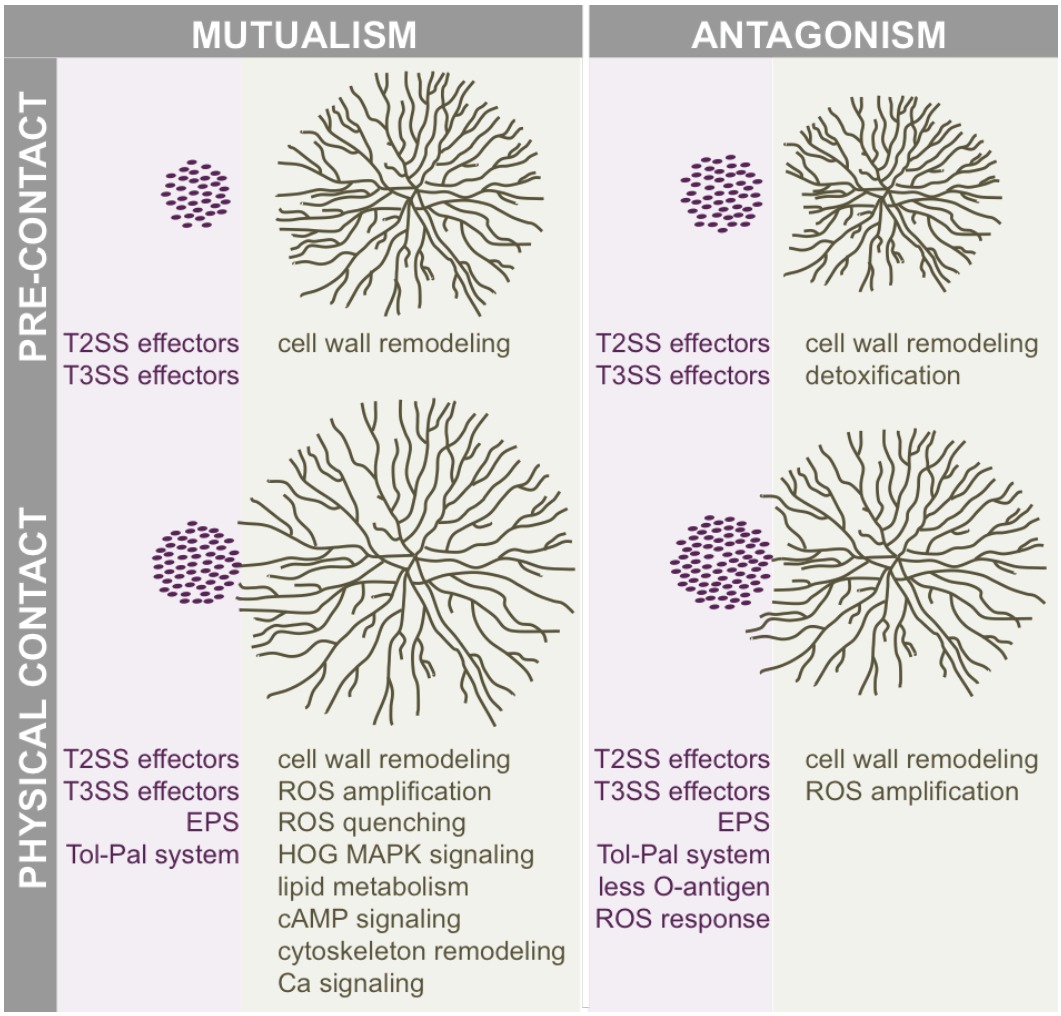

Figure 1. Molecular dialogues between bacteria and fungi in a mutualism versus antagonism before and during physical contact, inferred from changes in gene expression patterns. Bacterial cells are represented as purple ovals, fungal mycelium is depicted in green.

upregulated genes were homologs to yeast OYE2/3. In yeast, the OYE2-OYE3 complex is involved in sensitizing cells to oxidative damage and promotes ROS-mediated programmed cell death (Odat *et al*., 2007). Two laccase genes and a copper amine oxidase gene were also overexpressed, both involved in production of hydrogen peroxide (Wei *et al*., 2010, McGrath *et al*., 2011). In contrast, only a single GST gene, which could be involved in ROS detoxification, was upregulated.

In plants and animals, ROS and RNS are well known for their role in defense against microbial pathogens (Apel & Hirt, 2004, Fang, 2004). They also have a part in symbiosis establishment (Nanda *et al*., 2010). During plant-microbe interactions, production of ROS, known as the oxidative burst, exhibits a bi-phasic pattern in response to pathogens or incompatible symbionts. This bi-phasic response involves a low-amplitude first phase, followed by a higher ROS accumulation in the second phase (Apel & Hirt, 2004, Nanda *et al*., 2010). The second phase does not occur in response to compatible symbionts (Nanda *et al*., 2010). In contrast to animals and plants, little is known about fungal defense strategies involving ROS. Specifically, induction of antioxidant encoding genes in fungi challenged either by antagonistic bacteria (Gkarmiri *et al*., 2015) or by isolated microbe-associated molecular patterns (MAMPs) was interpreted as a mechanism for removal of ROS generated in response to MAMPs (Ipcho *et al*., 2016). Conversely, a disparity in ROS related transcriptional profiles between arbuscular mycorrhizal fungi (AMF) with and without mutualistic endobacteria was taken as evidence of the endosymbiont's positive impact on the ROS homeostasis in the host (Salvioli *et al*., 2016). In our dataset, host physical contact with endobacteria was accompanied by downregulation of a gene involved in RNS synthesis and upregulation of ROS-quenching antioxidant defense genes, suggesting that host interaction with endobacteria induced a transient oxidative burst, which was subsequently quenched by antioxidant defense genes, eventually leading to mutualism establishment. On the contrary, genes encoding ROS-generating enzymes were upregulated in the non-host, indicating that in response to antagonistic endobacteria the non-host mounted a more potent oxidative burst, a defense strategy analogous to the second oxidative burst phase in

Table 2. ROS response genes DE in host and non-host fungi during physical interaction with *Burkholderia* endobacteria. Log_2FC, Log_2 fold change; positive Log_2FC values denote downregulated genes; negative Log_2FC values denote upregulated genes; FDR, false discovery rate value; annotations given were generated by JGI; homology to yeast OYE2/3 genes was determined by OrthoMCL.

Protein ID	Log_2FC	FDR	IPR ID	Annotation
Host				
292375	3.99	4.43E-04	IPR002226	Catalase
237694	2.03	4.77E-13	IPR004045	Glutathione S-transferase
238090	1.49	1.00E-13	IPR002226	Catalase
287063	0.88	3.09E-03	IPR002016	Haem peroxidase, plant/fungal/bacterial
287063	0.88	3.09E-03	IPR002207	Plant ascorbate peroxidase
2966	-0.63	3.40E-03	IPR008254	Flavodoxin/nitric oxide synthase
237561	-0.78	3.30E-06	IPR002007	Haem peroxidase, animal
Non-host				
193785	4.04	5.96E-05	IPR001155	NADH:flavin oxidoreductase/NADH oxidase, yeast OYE2/3 homolog
216648	2.27	7.56E-16	IPR004046	Glutathione S-transferase, C-terminal
223952	2.00	4.44E-05	IPR001117	Multicopper oxidase, type 1
224787	1.55	2.23E-04	IPR001155	NADH:flavin oxidoreductase/NADH oxidase, yeast OYE2/3 homolog
294344	1.24	2.69E-05	IPR015798	Copper amine oxidase
15570	1.20	8.81E-03	IPR001117	Multicopper oxidase, type 1
29967	0.89	1.25E-03	IPR002007	Haem peroxidase, animal

plants responding to pathogens.

Cyclic AMP signaling. In addition to the HOG MAPK signaling cascade, genes encoding other signaling cascades were DE during the mutualistic interaction with endobacteria. Cyclic AMP (cAMP) signaling, for example, likely played a role. cAMP is a secondary messenger synthesized by adenylyl cyclases in response to activation by heterotrimeric G proteins (Park *et al*., 2010) or small GTPases of the Ras superfamily (Santangelo, 2006). cAMP directly activates cAMP-dependent kinases, which, in turn, phosphorylate their protein targets critical for fungal growth and development (Park *et al*., 2010). We detected upregulation of genes encoding two cAMP-dependent protein kinases (286008, 278678) and two small G proteins of the Ras superfamily (136105, 250648) as well as many small G protein regulators, such as guanine nucleotide exchange factors, GEFs, which activate G protein signaling, and GTPase-activating proteins, GAPs, that downregulate G protein signaling (Table S3). Many other signaling genes, largely encoding protein kinases, were also DE during the mutualistic interaction. Given an expanded repertoire and poor characterization of these signaling genes in Mucoromycotina (Corrochano *et al*., 2016) it is hard to speculate as to their function. Moreover, signaling cascades and activity of protein kinases are regulated at multiple levels in eukaryotic cells, including phosphorylation, cellular localization, translation, and transcription (Endicott *et al*., 2012). Consequently, increased levels of transcription of these genes may not be a direct reflection of their activity. However, they provide a basis for formulating hypotheses about the mechanisms underlying the mutualistic response to bacteria.

Cytoskeletal rearrangements. In the host, there were many DE genes involved in cytoskeletal rearrangements, majority of which were upregulated (Table 3), with the genes in the 'actin binding' GO category enriched significantly (Fig. S3). Several interpretations of this pattern are possible. For example, cytoskeletal rearrangements could be linked directly to cAMP signaling, as in most eukaryotes cAMP signaling is involved in regulation of mitosis, a process also tied to cytoskeletal rearrangements (Grieco *et al*., 1996). Accordingly, we identified several DE genes involved in cell cycle progression, including the cell division cycle gene cdc15 (232829) (Table

Table 3. Cytoskeleton related genes DE in the host during physical interaction with *Burkholderia* endobacteria. Log_2FC, Log_2 fold change; positive Log_2FC values denote upregulated genes; negative Log_2FC values denote downregulated genes; false discovery rate, FDR; annotations were obtained manually with PSI-BLAST against the SwissProt/UniProtKB database.

Protein ID	Log_2FC	FDR	Annotation	Organism
252161	2.65	1.07E-07	Rho-GTPase-activating protein BAG7	*Saccharomyces cerevisiae*
60967	2.56	6.19E-04	Rho1 guanine nucleotide exchange factor 2	*Schizosaccharomyces pombe*
242325	1.89	1.23E-11	Hypothetical LIM domain-containing protein	*Rhizopus microsporus*
310169	1.73	5.14E-06	Hypothetical LIM domain-containing protein	*Rhizopus microsporus*
225711	1.58	1.29E-06	Actinin-like protein	*Laccaria bicolor*
280334	1.43	1.10E-08	CAP-Gly domain containing protein	*Rhizopus delemar*
198343	1.42	3.20E-06	Myosin	*Rhizopus microsporus*
240217	1.32	9.42E-14	Regulator of cytoskeleton and endocytosis RVS167	*Candida albicans*
274088	1.21	3.24E-05	Probable Rho-type GTPase-activating protein 2	*Schizosaccharomyces pombe*
181905	1.20	8.24E-05	Myosin	*Rhizopus microsporus*
266182	1.19	5.69E-04	Kinase with actin-binding calponin homology domain	*Rhizopus delemar*
128872	1.14	4.00E-03	Hypothetical LIM domain-containing protein	*Mucor circinelloides*
226218	1.01	4.85E-03	Probable Rho-GTPase-activating protein 7	*Schizosaccharomyces pombe*
235547	1.00	4.26E-07	BZZ1	*Saccharomyces cerevisiae*
245977	0.92	4.55E-09	Fimbrin	*Rhizopus delemar*
236201	0.70	1.57E-04	Protein dip1	*Schizosaccharomyces pombe*
237596	0.69	4.25E-04	Rho-GTPase-activating protein BAG7	*Saccharomyces cerevisiae*
249809	0.67	1.42E-04	Cofilin/tropomyosin-type actin-binding domain containing protein	*Rhizopus microsporus*
291147	0.64	6.85E-03	PH domain-containing protein	*Rhizopus microsporus*
244149	0.55	8.39E-04	Myosin I	*Mucor circinelloides*
233557	-0.54	1.36E-03	Tubulin-folding cofactor D	*Schizosaccharomyces pombe*
236630	-0.63	6.23E-03	Rho guanine nucleotide exchange factor SCD1	*Schizosaccharomyces pombe*
15091	-0.81	3.17E-03	RhoGAP domain containing protein	*Rhizopus microsporus*

S4). Alternatively, cytoskeletal rearrangements could be a direct response to endosymbionts, which travel inside the host hyphae even though their genomes do not encode motility features, such as flagella (Lackner *et al*., 2011). For example, other *Burkholderia* species, such as *B. pseudomallei* and *B. mallei*, polymerize host actin for motility (Benanti *et al*., 2015). However, the endobacteria of *Rm* do not encode the *Burkholderia* intracellular motility A (BimA) protein requisite for such actin-based mobility. Instead, it is more likely that the *Rm* rearranges its cytoskeleton to accommodate endobacteria, a strategy consistent with the lack of differential expression of cytoskeleton related genes in the non-host.

Calcium ion binding. We identified 'calcium ion binding' as a GO category enriched among the host genes upregulated during interaction with endobacteria (Fig. S3). Changes in intracellular calcium ion concentrations are the basis of calcium signaling, which in turn controls many aspects of eukaryotic biology. Calcium spiking in plants is a known mediator of symbiosis establishment with microorganisms (Oldroyd, 2013). Similarly, intracellular calcium ion concentrations are affected by the presence of endobacteria in AMF (Salvioli *et al*., 2016). It is, thus, possible that *Burkholderia* also affect calcium ion concentrations in *Rm* and induce calcium signaling.

Cell wall biogenesis. As during the pre-contact interaction, cell wall related genes were involved in the physical contact and were enriched among the upregulated fraction in non-host fungi (Fig. S3). 26 genes with cell wall related function were DE in the non-host, and 8 in the host (Table 4). There was a single chitin synthase gene that was commonly DE in both fungi. Only in the host, we detected overexpression of another chitin synthase gene as well as two genes encoding activators of chitin synthesis, suggesting that the mutualistic interaction with endosymbionts was accompanied by the synthesis of chitin. In other fungi, expression of chitin synthases is known to become upregulated upon cell wall stress and correlates with increased chitin composition of cell walls upon challenge of 1,3-beta glucan synthase inhibitors (Rogg *et al*., 2012). During the antagonistic interaction, on the other hand, we detected the overexpression of a number of chitinase genes as well as chitin deacetylase genes. Their expression patterns in the non-host

Table 4. Cell wall related genes DE in host and non-host fungi during physical interaction with *Burkholderia* endobacteria. Log_2FC, Log_2 fold change; negative Log_2FC values denote downregulated genes; positive Log_2FC values denote upregulated genes; FDR, false discovery rate value. *annotations obtained though CAZYmes Analysis Toolkit (Lombard *et al.*, 2014); **annotations obtained through the *myco*CLAP database (Murphy *et al.*, 2011); the remaining annotation are from JGI.

Protein ID	Log_2FC	FDR	CAZY/InterPro	Annotation
Host				
308710	0.95	9.18E-03	CE4	Chitin deacetylase**
285170	0.69	8.08E-04	GT15	Alpha-1,2 mannosyl-transferase*
202842	1.45	1.77E-07	GT2	Chitin synthase*
211861	0.50	4.47E-03	GH9	Endoglucanase**
284826	1.05	3.90E-05	IPR006597	Extracellular protein SEL-1, homolog of SKT5 activator of chitin synthase in *Saccharomyces cerevisiae*
237437	1.02	8.69E-04	IPR006597	Extracellular protein SEL-1, homolog of SKT5 activator of chitin synthase in *Saccharomyces cerevisiae*
226625	1.76	6.06E-08	GT2	Chitin synthase
202463	-0.92	1.73E-03	GH15|CBM21	Glucoamylase**
Non-host				
177895	0.94	5.55E-04	IPR016491	Septin
195250	1.28	4.10E-03	IPR016491	Septin
54483	1.35	1.95E-03	GT48	1,3-beta-glucan synthase*
224455	1.31	2.10E-04	GT48	1,3-beta-glucan synthase*
178226	1.27	1.83E-03	GT15	Alpha-1,2 mannosyl-transferase*
177931	1.12	3.65E-03	GT15	Alpha-1,2 mannosyl-transferase*
241953	1.08	4.29E-03	GT15	Alpha-1,2 mannosyl-transferase*
97566	1.90	2.59E-03	CE4	Chitin deacetylase**
180937	1.78	7.78E-06	GH18|CBM19	Chitinase**
221684	1.70	2.61E-05	GH16	None
209732	1.65	6.41E-06	GH20	Hexosaminidase**
241802	1.65	2.30E-06	GH81	Endo-1,3-beta-glucanase**
263075	1.60	1.27E-03	GH16	Xylanase/beta(1,3-1,4) glucanase**
204754	1.52	5.01E-04	GT2	Chitin synthase*
261112	1.57	1.31E-07	CE4	Chitin deacetylase**
11846	1.55	1.19E-04	GH18	Chitinase**
81356	1.54	7.78E-06	GH47	Alpha-1,2-mannosidase**
230502	1.53	8.72E-05	GH9	Endoglucanase**
222744	1.45	2.16E-04	GH72|CBM43	Glucanosyltransferase*
198772	1.44	2.42E-04	CE4	Chitin deacetylase**
219382	1.35	4.37E-03	GH3	Beta-glucosidase**
149043	1.33	4.99E-04	GH18	Chitinase**
181330	1.32	9.27E-04	CE4	Chitin deacetylase**
212115	0.83	8.21E-03	CE4	Chitin deacetylase**
258608	-0.97	7.17E-03	GH45|CBM1	Endoglucanase**
207865	-1.41	4.69E-03	GH45|CBM1	Endoglucanase**

indicate that chitin was broken down and chitosan was made. Additionally, the non-host appeared to initiate synthesis of 1,3-beta-glucan, evident by the upregulation of 1,3-beta-glucan synthase genes, expression of which also correlates with their activity in other fungi (Park *et al*., 2014). These different cell wall modifications could be explained by the different reactions of the two fungi to chitinase, a cell wall degrading enzyme that *B. rhizoxinica* uses to gain entry into host hyphae (Moebius *et al*., 2014). The activation of chitin synthesis by the host could reflect the need to re-synthesize the chitin that endobacteria broke down during hyphal entry. It is also possible that by increasing the ratio of chitin relative to other cell wall polysaccharides, the host would facilitate bacterial entry and symbiosis establishment. On the other hand, whereas the non-host did not become infected by endobacteria, it likely still experienced cell wall stress from the bacterial chitinase, expression of which endobacteria upregulated during physical contact with both fungi. The non-host response of increasing the ratio of chitosan and 1,3-beta-glucan relative to chitin could thus be a defense strategy, as it would ensure enhanced cell wall stability in the presence of external chitinases. An analogous strategy of altering cell wall ratios of 1,3-beta-glucan to chitin is employed by filamentous fungi in response to cell wall antagonistic drugs, such as inhibitors of chitin synthase or glucan synthase (Verwer *et al*., 2012). Much like during the antagonistic interaction pre-contact, we detected the overexpression of genes encoding septins and mannosyltransferases in the non-host during physical contact with endobacteria. Septins are guanosine-5-triphosphate binding proteins functioning in cell wall stress, cytoskeleton organization, and control of hyphal growth and morphology (Khan *et al*., 2015). In mammalian cells, septins are capable of forming septin cages around intracellular bacterial pathogens (Mostowy *et al*., 2010). However, as *Burkholderia* do not enter the non-host hyphae, it is difficult to speculate about the role of septins in the *Rm-Burkholderia* antagonism.

Physical Contact Responses in Bacteria. During physical interaction with host and non-host fungi, many more bacterial genes were DE compared to the pre-contact interaction. 1119 were DE in response to the non-host and 453 genes in response to the host. There was an overlap of

253 genes that were commonly upregulated in response to both fungi and 92 were commonly downregulated. Since some of the DE bacterial genes, such as those encoding the T3SS cluster, components of the T2SS and known T2SS effectors chitinase and chitosinase, have been experimentally validated as symbiosis factors in the *Rm-Burkholderia* mutualism (Leone *et al*., 2010, Lackner *et al*., 2011, Moebius *et al*., 2014), we hypothesize that other bacterial genes DE at this stage play a similar role. They include candidate T3SS effector genes, exopolysaccharide biosynthesis genes, genes encoding the Tol-Pal system, and response to oxidative stress genes.

Secretion systems and their effectors. 64 candidate T3SS effectors were overexpressed during physical interaction with both fungi (Table S2). Over a third of these (40.6%) encoded proteins of unknown function. Four candidate effectors had DNA-binding domains with homology to transcription factors, whereas 6 were predicted transporters. Two candidate effectors contained protein-interacting domains, leucine rich repeat (LRR) and F-box-like, and showed no homology to any bacterial proteins based on BLAST, but were instead closer to eukaryotic proteins. LRR and F-box proteins are known virulence effectors in pathogenic bacteria (Rohde *et al*., 2007, Price *et al*., 2009). LRR effectors block MAPK signaling through mimicking of eukaryotic E3 ubiquitin ligases (Rohde *et al*., 2007), whereas F-box effectors mimic components of the eukaryotic protein degradation and regulation machinery (Price *et al*., 2009). Another notable candidate T3SS effector (Gene ID 2599765431), with a gene overexpressed during interaction with both fungi, displayed homology to transcription activator-like (TAL) effectors in *Xanthomonas*. TAL effectors localize to plant host nuclei, where they bind specific DNA sequences through their central repeat DNA-binding domain and activate transcription of plant genes that facilitate infection (Scholze & Boch, 2011). To date, TAL effectors have only been found in plant-pathogenic *Xanthomonas* and *Ralstonia*, with homologs recently identified in *B. rhizoxinica* HKI454 (de Lange *et al*., 2014). Importantly, *B. rhizoxinica* TAL effectors, henceforth referred to as BTALs, are capable of binding DNA with the same code as *Xanthomonas* TAL effectors (de Lange *et al*., 2014). Genomes of *Burkholderia* endobacteria of *Rm* encode between 1 and 3 BTALs, which are phylogenetically distinct from *Xanthomonas* and

Ralstonia TAL effectors (Fig. 2). The genome of *Burkholderia* sp. B13 encodes one full-length BTAL with a T3 secretion signal (2599765431), as well as a truncated BTAL with no secretion signal (2599765427). Computationally, we identified candidate targets of the full-length effector in the genomes of host and non-host *Rm* (Table S5). While none of the candidate target genes in the non-host were DE during interaction with endobacteria, two were significantly DE in the host due to bacteria: a gene encoding a hypothetical protein (238547) was upregulated and a gene encoding a zinc-finger domain containing transcription factor (193862) was downregulated. It is, thus, plausible that BTAL plays a role during the mutualistic interaction with the host by manipulating its transcription.

Lastly, as expected, we detected the upregulation of genes encoding components of the T2SS, which contributes to *B. rhizoxinica'*s ability to infect its host (Moebius *et al*., 2014). We also observed differential expression of genes encoding its known effectors, chitinase and chitosinase, which were upregulated, and the chitin-binding protein, which was downregulated. Downregulation of the gene for chitin-binding protein was unexpected, as this protein was previously shown to be upregulated during host-bacteria incubation in liquid (Moebius *et al*., 2014), but might be explained by the fact that during interaction on solid media, bacteria may not require the chitin-binding protein for attachment to fungal hyphae.

Exopolysaccharides. The upregulation of genes involved in the biosynthesis of exopolysaccharides (EPSs) during physical contact also implicated their involvement in the interaction with fungi. EPSs create a protective barrier around bacterial cells and play key roles in both pathogenesis (Vuong *et al*., 2004) and symbiosis (Jones *et al*., 2008). For example, EPS mutants of mutualistic *Sinorhizobium meliloti* and *Rhizobium leguminosarum* are impaired in their ability to initiate symbiosis with the legume host (Breedveld *et al*., 1993, Cheng & Walker, 1998). In contrast, EPS mutants of *B. rhizoxinica* appear to be able to establish symbiosis with the *Rm* host in liquid culture (Uzum *et al*., 2015). However, in our dataset, genes encoding all

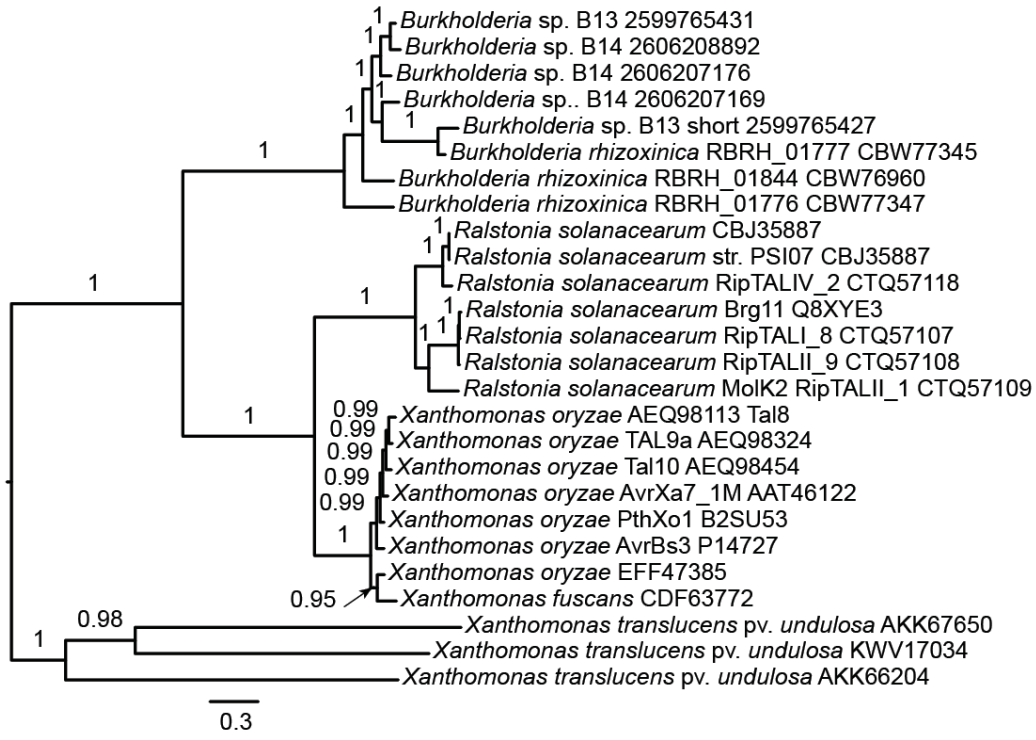

Figure 2. Bayesian phylogeny of TAL effector amino acid sequences. Posterior probabilities are shown above branches.

components of the EPS biosynthesis cluster were extremely upregulated (>30-fold) due to physical contact with both non-host and host, making it difficult to dismiss their role in interaction with fungi. It is thus possible that EPS is more important for interaction with fungi on solid media compared to liquid culture.

Outer membrane stability and lipopolysaccharide. The bacterial Tol-Pal system forms an inner-outer membrane-spanning complex that is well conserved in Gram-negative bacteria (Sturgis, 2001). It functions in maintaining outer membrane stability (Lloubès *et al*., 2001), cell division (Gerding *et al*., 2007), resistance to detergents and bile salts (Dubuisson *et al*., 2005), surface expression of the lipopolysaccharide (LPS) O-antigen (Gaspar *et al*., 2000) and virulence (Dubuisson *et al*., 2005). *Burkholderia* endobacteria encode the complete Tol-Pal system, and its genes were upregulated during physical interaction with non-host and host fungi (2599765595 – 2599765598, 2599765600). Because this system is important in maintaining the stability of the bacterial cell envelope, it could contribute to survival in the intra-host environment, where changes in osmolarity and oxidative stress are likely encountered. In addition, we saw the upregulation of a specific sigma factor gene, rpoE (2599763969), along with a gene encoding its regulator, anti-sigma E protein RseA (2599763968), which in other bacteria regulate the envelope stress response (Rowley *et al*., 2006). RpoE is required for intra-host survival of *Salmonella* Typhimurium (Rowley *et al*., 2006), where it controls transcription of genes of the Tol-Pal system as well as many others involved in outer membrane biogenesis (Skovierova *et al*., 2006). Taken together, we hypothesize that during contact with fungi, endobacteria are faced with cell envelope stress and activate envelope stress response, mediated by the specific sigma factor RpoE.

The outer membrane of Gram-negative bacteria is decorated with a LPS layer, composed of lipid A, core oligosaccharide, and O-antigen. Eukaryotic hosts are able to recognize components of bacterial LPS, which plays important roles in pathogenic and symbiotic interactions (Chu & Mazmanian, 2013). The *B. rhizoxinica* O-antigen is involved in symbiosis establishment (Leone *et al*., 2010). Specifically, deletion of the O-antigen ligase gene, *waaL*, reduced the infection

success rate and compromised intra-host proliferation of endosymbionts (Leone *et al*., 2010). The O-antigen of *B. rhizoxinica* is a homopolymer of D-galactofuranose, which is also a common component of some filamentous fungal cell walls, leading to speculations that the O-antigen could either act as a symbiosis factor recognized by the host to facilitate symbiosis establishment, or, alternatively, as a cloaking device that shields the endobacteria by mimicking of fungal cell components (Leone *et al*., 2010). Contrary to our expectations, we did not detect any differential expression of O-antigen or LPS biosynthetic genes during physical interaction with host fungi, indicating that the O-antigen is not synthesized specifically in response to the host, but rather constitutively expressed. On the other hand, we detected significant downregulation of *waaL* (2599765323) during bacterial interaction with the non-host. This pattern suggests that the O-antigen is recognized by the fungi, and either acts as a symbiosis signal during the mutualistic interaction with the host, or activates fungal defenses during the antagonistic interaction with the non-host.

Response to oxidative stress. Fungal transcriptional responses to endobacteria during physical contact revealed the likely involvement of ROS, with ROS amplification in the non-host and quenching in host. In turn, bacterial gene expression appeared to reflect a response to ROS during physical interaction with both fungi. Importantly, as bacteria are known to react to oxidative stress at the transcriptional level (Fang, 2004), this response appeared stronger during interaction with the non-host. Only a single gene encoding GST (2599764292) was upregulated in response to both fungi. Bacterial GSTs have a role in detoxification of xenobiotics and in protection from oxidative stress through their ability to conjugate a large number of substrates to glutathione (Allocati *et al*., 2009). In response to the non-host only, we observed the upregulation of a gene encoding a glutathione synthase (2599765053), an enzyme responsible for the production of glutathione, as well as the upregulation of another bacterial gene encoding antioxidant thioredoxin (2599763895). Additionally, we detected the upregulation of a gene encoding coenzyme A pyrophosphatase (2599764015), which is known to catalyze the elimination of oxidized inactive CoA, and thus prevent the inhibition of CoA-utilizing enzymes

as a result of exposure to ROS (Kang *et al*., 2003). Lastly, we saw overexpression of a gene encoding endonuclease III (2599765412) in response to non-host only. Endonuclease III is part of the base excision repair mechanism that removes damaged pyramidines (Imlay, 2013). Base excision repair becomes activated in response to damage caused by oxygen radicals and constitutes an important mechanism of oxidative stress tolerance. A number of ROS related genes were also downregulated in response to non-host, encoding a superoxide dismutase (2599764121), which produces superoxide from H2O2, a peroxidase (2599762957), which converts H2O2 to H2O, and another GST (2599765091). Overall, consistent with our inference that bacteria encounter a stronger ROS challenge during interaction with non-host fungi, we identified a larger number of ROS related genes DE by bacteria in the antagonistic interaction.

Conservation of Genes Involved in Interaction with Fungi. Little is known about the molecular underpinnings governing bacterial interaction with fungi beyond the characterized symbiosis factors of *B. rhizoxinica* (Leone *et al*., 2010, Lackner *et al*., 2011, Moebius *et al*., 2014). To learn about the conservation of genes involved in interaction with and response to fungi in *Burkholderia* endobacteria, we performed orthologous clustering of protein sequences across 20 *Burkholderia* species with different lifestyles that ranged from soil inhabitants to human pathogens (Table S6). We included 3 genomes of *Burkholderia* endosymbionts of *Rm*: *B. rhizoxinica* HKI454 (Lackner *et al*., 2011), *Burkholderia* sp. B13 and *Burkholderia* sp. B14 endobacteria of *Rm* ATCC 52813 and ATCC 52814, respectively, which were both sequenced for this study (Table S1). None of the genes encoding known *Burkholderia* endobacteria symbiosis factors (T3SS, T2SS, chitinase, chitosinase, LPS) were found exclusively in the genomes of endofungal *Burkholderia*. Moreover, majority of fungi-interacting genes identified from our transcriptional profiling (Tol-Pal, EPS, ROS response) were also not exclusive to *Burkholderia* endobacteria. This observation suggests that the ability to engage in symbioses with fungi is largely facilitated by a pre-existing gene repertoire found in *Burkholderia* of diverse lifestyles. For example, a homolog of the T2SS effector chitinase, which facilitates endobacterial

entry into host hyphae (Moebius *et al*., 2014), is also encoded in the genomes of human pathogenic *B. cenocepacia* J2315 and AU105, *B. mallei* ATCC 23344, *B. pseudomallei* BPC006 as well as a soil saprotroph *B. thailandensis* E264. Analogously, homologs of genes in the *B. rhizoxinica* T3SS cluster, which is required for successful symbiosis establishment (Lackner *et al*., 2011), are encoded in over half of the examined *Burkholderia* genomes. Conversely, 35 of the genes commonly upregulated during physical interaction with host and non-host fungi were exclusively encoded in genomes of endofungal *Burkholderia* (Table S7). Almost half of these genes were candidate T3SS effectors and included BTAL, as well as the candidate LRR- and F-box-domain effectors identified in this study. T3SS effector repertoire of pathogenic bacteria is known to shape their host range and can be extremely variable even among closely related strains (Baltrus *et al*., 2011). It is thus possible that the T3SS effector repertoire of *Burkholderia* endobacteria evolved for exclusive interaction with fungi.

2.5 CONCLUSION

Using transcriptional profiling, we deciphered molecular dialogues between fungi and bacteria in a mutualism and antagonism at two time points: pre-contact and contact (Fig. 1). Pre-contact, the antagonistic interaction involved the apparent detoxification of an unknown bacterial compound by the non-host, whereas the mutualistic interaction elicited a weak response from the host. Remarkably, pre-contact transcriptomic changes indicated that bacteria did not discriminate between host and non-host fungi, and appeared to be equally equipped to infect both. Commonalities in the fungal responses during contact centered around expression of genes involved in cell wall modification and ROS metabolism. These patterns pointed to specific alterations to the fungal cell wall and to an increase in ROS production during the antagonistic interaction, which, we speculate, contributed to non-host's ability to resist bacterial invasion. In addition to the involvement of fungal genes encoding the HOG MAPK signaling pathway and lipid metabolism described previously (Lastovetsky *et al*., 2016), the mutualistic interaction was marked by transcriptional upregulation of genes in the cAMP signaling pathway and cytoskeletal

rearrangements, thus revealing a set of fungal genes formerly unknown for their role in symbiosis establishment. During physical contact with fungi, in addition to factors specific to the *Rm-Burkholderia* symbiosis, endobacteria engaged a common set of factors used to interact with other eukaryotic hosts. Overall, these findings build a conceptual framework for understanding the molecular factors mediating fungal-bacterial interactions.

2.6 MATERIALS & METHODS

Strains, culture conditions, removal and extraction of *Burkholderia* endobacteria. *Rhizopus microsporus* (*Rm*) strains ATCC 52813 and ATCC 11559 were cultivated on potato dextrose agar (PDA) at 30oC. *Rm* ATCC 52813 was cured of its endobacteria as previously described (Partida-Martinez & Hertweck, 2005). Endobacteria were extracted from 3-day old host mycelium ground in 800 µL of Luria-Bertani (LB) broth using a plastic mortar and centrifuged at 4000×g for 2 min. The supernatant was passed twice through a 2 µm Whatman filter, plated onto LB agar plates supplemented with 1% glycerol, and incubated at 30oC.

***Burkholderia* sp. B13 and *Burkholderia* sp. B14 genome sequencing, assembly and annotation**. The draft genomes of *Burkholderia* sp. B13 and *Burkholderia* sp. B14 were generated at the US Department of Energy Joint Genome Institute (DOE JGI) using the Pacific Biosciences (PacBio) sequencing technology (Korlach *et al*., 2010). A Pacbio SMRTbellTM library was constructed and sequenced on the PacBio RS platform, which generated 144,221 filtered subreads totaling 586.4 Mbp for *Burkholderia* sp. B13 and 121,007 filtered subreads totaling 455.8 Mbp for *Burkholderia* sp. B14. All general aspects of library construction and sequencing performed at the JGI can be found at http://www.jgi.doe.gov. The raw reads were assembled using HGAP v. 2.2.0.p1 (Chin *et al*., 2013). The final draft assembly contained 2 contigs in 2 scaffolds, totaling 3.6 Mbp in size for *Burkholderia* sp. B13 and 3 contigs in 3 scaffolds, totaling 3.7 Mbp in size for *Burkholderia* sp. B14. The input read coverage was 98.4X (*Burkholderia* sp. B13) and 72.2 (*Burkholderia* sp. B14). Genes were identified using Prodigal (Hyatt *et al*., 2010), followed by a round of manual curation using GenePRIMP (Pati *et al*.,

2010) for finished genomes and draft genomes in fewer than 10 scaffolds. The predicted CDSs were translated and used to search the National Center for Biotechnology Information (NCBI) nonredundant database, UniProt, TIGRFam, Pfam, KEGG, COG, and InterPro databases. The tRNAScan-SE tool (Lowe & Eddy, 1997) was used to find tRNA genes, whereas ribosomal RNA genes were identified by searches against models of the ribosomal RNA genes built from SILVA (Pruesse *et al*., 2007). Additional gene prediction analysis and manual functional annotation was performed within the Integrated Microbial Genomes (IMG) platform (Markowitz *et al*., 2012).

RNA-seq experiment and data analysis. We examined five different conditions at two different time points: (1) cured host *Rm* (ATCC 52813) cultured alone, (2) cured ATCC 52813 cultured with *Burkholderia* sp. B13, (3) non-host *Rm* (ATCC 11559) cultured alone, (4) ATCC 11559 cultured with *Burkholderia* sp. B13, (5) *Burkholderia* sp. B13 cultured alone. The two time points corresponded to interaction at a distance (pre-contact) and interaction during physical contact. During pre-contact interaction, which occurred 50 hrs post inoculation of ATCC 52813 and 56 hrs post inoculation of ATCC 11559 due to naturally different growth rates, fungi have not yet physically contacted the site of bacterial inoculation. During physical interaction, at 67 hrs post inoculation of ATCC 52813 and 93 hrs post inoculation of ATCC 11559, fungi have just come into contact with the site of bacterial inoculation. For each condition, bacteria were inoculated on an LB+1% glycerol agar plug on one side of a half-strength PDA plate and a ~0.5 cm2 mat of fungal mycelium placed ~2 cm away. Plates were incubated at 30oC. Fungal mycelium was harvested from the interaction zone and all bacterial cells were scraped off the agar. Each condition had three biological replicates, each consisting of three culture plates pooled prior to RNA extraction. Total RNA was extracted with the Ambion ToTALLY Total RNA Isolation Kit (Life Technologies) and rRNA was removed with RiboZero Magnetic Gold Kit (Epicentre). RNA sequencing libraries were prepared using the NEBNext® mRNA Library Prep Reagent Set for Illumina® and sequenced at the Cornell University Biotechnology Resource Center using the Illumina Hi-Seq 100 bp paired-end platform. Illumina data were

quality controlled using the FASTX-Toolkit (Gordon & Hannon, 2010) and the reads were mapped onto either ATCC 52813 or ATCC 11559 genomes using TopHat (Trapnell *et al*., 2012). Transcript abundances were quantified with CuffDiff (Trapnell *et al*., 2012) and differential gene expression analysis was performed with EdgeR (Robinson *et al*., 2010). The false discovery rate (FDR) value of 0.01 was used as a cutoff for the identification of differentially expressed genes.

GO category functional enrichment analysis. GO annotation for all the genes from the ATCC 11559 genome were obtained from JGI Mycocosm (Grigoriev *et al*., 2014) and imported into Blast2GO (Conesa *et al*., 2005). Functional enrichment analysis was performed using a Fisher's Exact Test with a *P* value cutoff of 0.01 on all the up-regulated genes in response to interaction with bacteria.

Manual annotation of cytoskeleton related genes. The DE cytoskeleton related genes were manually annotated based on KOG annotations in the 'cytoskeleton' class as well as based on involvement in cytoskeleton-related function. For example, Rho GTPase-activating proteins (IPR000198) are known to control actin cytoskeletal formation. This list of genes was further validated and annotated using the PSI-BLAST program against SwissProt/Uniprot databases according to homology to known cytoskeleton-related genes (Table S7).

T3SS effector identification and in silico prediction of TAL binding sites. Effective T3 v. 2.0.1 (Jehl *et al*., 2011), through http://effectivedb.org/, accessed on October 7 2015, was used to scan the amino acid sequences of all differentially expressed genes in *Burkholderia* endobacteria during interaction with host and non-host fungi. Cutoff score of 0.9999 was used to classify 'secreted' protein. Binding sites in the host and non-host fungal genomes of the TAL effector were predicted with the TALE-NT (Doyle *et al*., 2012) prediction model under the following parameters: options_used: search reverse complement, upstream_base = T , cutoff = 3.00, rvd_sequence = YD_ND_NI_ND_NN_NI_NG_NG_NN_ND_NN_NN_NS_NG_NG_NN_NN_NI_N*. Prediction was made on the entire nucleotide scaffolds assembly of *Rm* ATCC 52813 and ATCC 11559, and the nearest gene to the predicted binding site used as the potential target.

Phylogenetic analyses of TAL effector amino acid sequences. Sequence alignment was performed with MUSCLE (Edgar, 2004) and adjusted manually. Bayesian phylogeny was reconstructed under the amino acid substitution model mixed+I+Γ to identify substitution models that best fit the data, using MrBayes 3.2.5 (Ronquist *et al*., 2012) with 25% burn-in, and the average standard deviation of split frequencies used as a convergence diagnostic.

Identification of orthologs in the genomes of *Burkholderia*. We collected amino acid sequences for all protein coding genes from *Burkholderia* genomes listed in Table S10 and conducted an All-vs-All BLASTp (Altschul *et al*., 1990) search with parameters: E-value cutoff = 1×10-3 and maximum matches = 500. OrthoMCL (Doerks *et al*., 2002) was used to identify orthologs with parameters: mode = 3, pi_cutoff = 0, pv_cutoff = 1×10-3, and inflation = 0.

2.7 ACKNOWLEDGEMENTS

We thank S. Mondo for help with RNA-seq data analysis, A. Bogdanove for conversations on BTAL, and J. Tiedje for permission to analyze unpublished genomes of *B. ambifaria* AMMD, *B. cenocepacia* AU1054, *B. phytofirmans* PsJN T, *B. vietnamiensis* G4, and *B. xenovorans* LB400. This work was supported by the National Science Foundation grant IOS-1261004 to TEP. Genomes of *Burkholderia* sp. B13 and *Burkholderia* sp. B14 were sequenced within the framework of the US DOE JGI Community Sequencing Project Proposal ID 1450. The work conducted by the US DOE JGI, a DOE Office of Science User Facility, was supported by the Office of Science of the US DOE under Contract No. DE-AC02-05CH11231.

2.8 REFERENCES

Allocati N, Federici L, Masulli M & Di Ilio C (2009) Glutathione transferases in bacteria. *FEBS J* **276**: 58-75.

Altschul SF, Gish W, Miller W, Myers EW & Lipman DJ (1990) Basic local alignment search tool. *J Mol Biol* **215**: 403-410.

Apel K & Hirt H (2004) Reactive oxygen species: Metabolism, oxidative stress, and signal transduction. *Annu Rev Plant Biol* **55**: 373-399.

Baltrus DA, Nishimura MT, Romanchuk A, Chang JH, Mukhtar MS, Cherkis K, Roach J, Grant SR, Jones CD & Dangl JL (2011) Dynamic evolution of pathogenicity revealed by sequencing and comparative genomics of 19 *Pseudomonas syringae* isolates. *PLoS Pathog* **7**: e1002132.

Benanti EL, Nguyen CM & Welch MD (2015) Virulent *Burkholderia* species mimic host actin polymerases to drive actin-based motility. *Cell* **161**: 348-360.

Berry DB & Gasch AP (2008) Stress-activated genomic expression changes serve a preparative role for impending stress in yeast. *Mol Biol Cell* **19**: 4580-4587.

Boller T & Felix G (2009) A renaissance of elicitors: perception of microbe-associated molecular patterns and danger signals by pattern-recognition receptors. *Annu Rev Plant Biol* **60**: 379-406.

Breedveld MW, Cremers HC, Batley M, Posthumus MA, Zevenhuizen LP, Wijffelman CA & Zehnder AJ (1993) Polysaccharide synthesis in relation to nodulation behavior of *Rhizobium leguminosarum*. *J Bacteriol* **175**: 750-757.

Chakraborty W, Sarkar S, Chakravorty S, Bhattacharya S, Bhattacharya D & Gachhui R (2016) Expression of a chitin deacetylase gene, up-regulated in *Cryptococcus laurentii* strain RY1, under nitrogen limitation. *J Basic Microb* **56**: 576-579.

Cheng HP & Walker GC (1998) Succinoglycan is required for initiation and elongation of infection threads during nodulation of alfalfa by *Rhizobium meliloti*. *J Bacteriol* **180**: 5183-5191.

Chin CS, Alexander DH, Marks P*, et al.* (2013) Nonhybrid, finished microbial genome assemblies from long-read SMRT sequencing data. *Nat Methods* **10**: 563-569.
Chu HT & Mazmanian SK (2013) Innate immune recognition of the microbiota promotes host-microbial symbiosis. *Nat Immunol* **14**: 668-675.

Conesa A, Gotz S, Garcia-Gomez JM, Terol J, Talon M & Robles M (2005) Blast2GO: a universal tool for annotation, visualization and analysis in functional genomics research. *Bioinformatics* **21**: 3674-3676.

Corrochano LM, Kuo A, Marcet-Houben M*, et al.* (2016) Expansion of signal transduction pathways in fungi by extensive genome duplication. *Curr Biol* **26**: 1577-1584.

Costa TR, Felisberto-Rodrigues C, Meir A, Prevost MS, Redzej A, Trokter M & Waksman G (2015) Secretion systems in Gram-negative bacteria: structural and mechanistic insights. *Nat Rev Microbiol* **13**: 343-359.

de Lange O, Wolf C, Dietze J, Elsaesser J, Morbitzer R & Lahaye T (2014) Programmable DNA-binding proteins from *Burkholderia* provide a fresh perspective on the TALE-like repeat domain. *Nucleic Acids Res* **42**: 7436-7449.

Doerks T, Copley RR, Schultz J, Ponting CP & Bork P (2002) Systematic identification of novel protein domain families associated with nuclear functions. *Genome Res* **12**: 47-56.

Doyle EL, Booher NJ, Standage DS, Voytas DF, Brendel VP, VanDyk JK & Bogdanove AJ (2012) TAL Effector-Nucleotide Targeter (TALE-NT) 2.0: tools for TAL effector design and target prediction. *Nucleic Acids Res* **40**: W117-W122.

Dubuisson JF, Vianney A, Hugouvieux-Cotte-Pattat N & Lazzaroni JC (2005) Tol-Pal proteins are critical cell envelope components of *Erwinia chrysanthemi* affecting cell morphology and virulence. *Microbiology* **151**: 3337-3347.

Edgar RC (2004) MUSCLE: multiple sequence alignment with high accuracy and high throughput. *Nucleic Acids Res* **32**: 1792-1797.

Endicott JA, Noble ME & Johnson LN (2012) The structural basis for control of eukaryotic protein kinases. *Annu Rev Biochem* **81**: 587-613.

Fang FC (2004) Antimicrobial reactive oxygen and nitrogen species: concepts and controversies. *Nat Rev Microbiol* **2**: 820-832.

Gasch AP, Spellman PT, Kao CM, Carmel-Harel O, Eisen MB, Storz G, Botstein D & Brown PO (2000) Genomic expression programs in the response of yeast cells to environmental changes. *Mol Biol Cell* **11**: 4241-4257.

Gaspar JA, Thomas JA, Marolda CL & Valvano MA (2000) Surface expression of O-specific lipopolysaccharide in *Escherichia coli* requires the function of the TolA protein. *Mol Microbiol* **38**: 262-275.

Gerding MA, Ogata Y, Pecora ND, Niki H & de Boer PA (2007) The trans-envelope Tol-Pal complex is part of the cell division machinery and required for proper outer-membrane invagination during cell constriction in *E. coli*. *Mol Microbiol* **63**: 1008-1025.

Gkarmiri K, Finlay RD, Alström S, Thomas E, Cubeta MA & Högberg N (2015) Transcriptomic changes in the plant pathogenic fungus *Rhizoctonia solani* AG-3 in response to the antagonistic bacteria *Serratia proteamaculans* and *Serratia plymuthica*. *BMC Genomics* **16**: 630.

Gladfelter AS (2006) Control of filamentous fungal cell shape by septins and formins. *Nat Rev Microbiol* **4**: 223-229.

Gordon A & Hannon GJ (2010) FASTX-Toolkit. http://hannonlabcshledu/fastx_toolkit.

Grieco D, Porcellini A, Avvedimento EV & Gottesman ME (1996) Requirement for cAMP-PKA pathway activation by M phase-promoting factor in the transition from mitosis to interphase. *Science* **271**: 1718-1723.

Grigoriev IV, Nikitin R, Haridas S*, et al.* (2014) MycoCosm portal: gearing up for 1000 fungal genomes. *Nucleic Acids Res* **42**: D699-D704.

Hyatt D, Chen GL, Locascio PF, Land ML, Larimer FW & Hauser LJ (2010) Prodigal: prokaryotic gene recognition and translation initiation site identification. *BMC Bioinformatics* **11**: 119.

Imlay JA (2013) The molecular mechanisms and physiological consequences of oxidative stress: lessons from a model bacterium. *Nat Rev Microbiol* **11**: 443-454.

Ipcho S, Sundelin T, Erbs G, Kistler HC, Newman MA & Olsson S (2016) Fungal innate immunity induced by bacterial microbe-associated molecular patterns (MAMPs). *G3* **6**: 1585-1595.

Jehl MA, Arnold R & Rattei T (2011) Effective—a database of predicted secreted bacterial proteins. *Nucleic Acids Res* **39**: D591-D595.

Jones KM, Sharopova N, Lohar DP, Zhang JQ, VandenBosch KA & Walker GC (2008) Differential response of the plant *Medicago truncatula* to its symbiont *Sinorhizobium meliloti* or an exopolysaccharide-deficient mutant. *P Natl Acad Sci USA* **105**: 704-709.

Kang LW, Gabelli SB, Bianchet MA, Xu WL, Bessman MJ & Amzel LM (2003) Structure of a coenzyme A pyrophosphatase from *Deinococcus radiodurans*: a member of the Nudix family. *J Bacteriol* **185**: 4110-4118.

Khan A, McQuilken M & Gladfelter AS (2015) Septins and generation of asymmetries in fungal cells. *Annu Rev Microbiol* **69**: 487-503.

Kitagawa E, Momose Y & Iwahashi H (2003) Correlation of the structures of agricultural fungicides to gene expression in *Saccharomyces cerevisiae* upon exposure to toxic doses. *Environ Sci Technol* **37**: 2788-2793.

Korlach J, Bjornson KP, Chaudhuri BP, Cicero RL, Flusberg BA, Gray JJ, Holden D, Saxena R, Wegener J & Turner SW (2010) Real-time DNA sequencing from single polymerase molecules. *Method Enzymol* **472**: 431-455.

Korotkov KV, Sandkvist M & Hol WG (2012) The type II secretion system: biogenesis, molecular architecture and mechanism. *Nat Rev Microbiol* **10**: 336-351.

Lackner G, Moebius N & Hertweck C (2011) Endofungal bacterium controls its host by an *hrp* type III secretion system. *ISME J* **5**: 252-261.

Lackner G, Moebius N, Partida-Martinez L & Hertweck C (2011) Complete genome sequence of *Burkholderia rhizoxinica*, an endosymbiont of *Rhizopus microsporus*. *J Bacteriol* **193**: 783-784.

Lackner G, Moebius N, Partida-Martinez LP, Boland S & Hertweck C (2011) Evolution of an endofungal lifestyle: Deductions from the *Burkholderia rhizoxinica* genome. *BMC Genomics* **12**: 210.

Langner T & Göhre V (2016) Fungal chitinases: function, regulation, and potential roles in plant/pathogen interactions. *Curr Genet* **62**: 243-254.

Lastovetsky OA, Gaspar ML, Mondo SJ, LaButti KM, Sandor L, Grigoriev IV, Henry SA & Pawlowska TE (2016) Lipid metabolic changes in an early divergent fungus govern the establishment of a mutualistic symbiosis with endobacteria. *P Natl Acad Sci USA* **113**: 15102-15107.

Leone MR, Lackner G, Silipo A, Lanzetta R, Molinaro A & Hertweck C (2010) An unusual galactofuranose lipopolysaccharide that ensures the intracellular survival of toxin-producing bacteria in their fungal host. *Angew Chem* **49**: 7476-7480.

Lloubès R, Cascales E, Walburger A, Bouveret E, Lazdunski C, Bernadac A & Journet L (2001) The Tol-Pal proteins of the *Escherichia coli* cell envelope: an energized system required for outer membrane integrity? *Res Microbiol* **152**: 523-529.

Lowe TM & Eddy SR (1997) tRNAscan-SE: A program for improved detection of transfer RNA genes in genomic sequence. *Nucleic Acids Res* **25**: 955-964.

Markowitz VM, Chen IMA, Palaniappan K*, et al.* (2012) IMG: the integrated microbial genomes database and comparative analysis system. *Nucleic Acids Res* **40**: D115-D122.

Masiá Canuto M & Gutiérrez Rodero F (2002) Antifungal drug resistance to azoles and polyenes. *Lancet Infect Dis* **2**: 550-563.

McGrath AP, Mithieux SM, Collyer CA, Bakhuis JG, van den Berg M, Sein A, Heinz A, Schmelzer C, Weiss AS & Guss JM (2011) Structure and activity of *Aspergillus nidulans* copper amine oxidase. *Biochemistry* **50**: 5718-5730.

Moebius N, Üzüm Z, Dijksterhuis J, Lackner G & Hertweck C (2014) Active invasion of bacteria into living fungal cells. *eLife* **3**: e03007.

Mostowy S, Bonazzi M, Hamon MA*, et al.* (2010) Entrapment of intracytosolic bacteria by septin cage-like structures. *Cell Host Microbe* **8**: 433-444.

Nanda AK, Andrio E, Marino D, Pauly N & Dunand C (2010) Reactive oxygen species during plant-microorganism early interactions. *J Integr Plant Biol* **52**: 195-204.

Odat O, Matta S, Khalil H, Kampranis SC, Pfau R, Tsichlis PN & Makris AM (2007) Old yellow enzymes, highly homologous FMN oxidoreductases with modulating roles in oxidative stress and programmed cell death in yeast. *J Biol Chem* **282**: 36010-36023.

Oldroyd GED (2013) Speak, friend, and enter: signalling systems that promote beneficial symbiotic associations in plants. *Nat Rev Microbiol* **11**: 252-263.

Olsson S, Bonfante P & Pawlowska TE (2017) Ecology and evolution of fungal-bacterial interactions. *The Fungal Community: its Organization and Role in the Ecosystem,*(Dighton J & White JF, eds.), p.^pp. 563-583. Taylor & Francis, In Press.

Osherov N & Yarden O (2010) The cell wall of filamentous fungi. *Cellular and Molecular Biology of Filamentous Fungi,*(Borkovich KA & Ebbole DJ, eds.), p.^pp. 224-237. ASM Press, Washington, DC.

Park BC, Park YH, Yi S, Choi YK, Kang EH & Park HM (2014) Transcriptional regulation of *fksA*, a beta-1,3-glucan synthase gene, by the APSES protein StuA during *Aspergillus nidulans* development. *J Microbiol* **52**: 940-947.

Park G, Jones CA & Borkovich KA (2010) Signal transduction pathways. *Cellular and Molecular Biology of Filamentous Fungi,*(Borkovich KA & Ebbole DJ, eds.), p.^pp. 50-59. ASM Press, Washington, DC.

Partida-Martinez LP & Hertweck C (2005) Pathogenic fungus harbours endosymbiotic bacteria for toxin production. *Nature* **437**: 884-888.

Partida-Martinez LP, Monajembashi S, Greulich KO & Hertweck C (2007) Endosymbiont-dependent host reproduction maintains bacterial-fungal mutualism. *Curr Biol* **17**: 773-777.

Partida-Martinez LP, Groth I, Schmitt I, Richter W, Roth M & Hertweck C (2007) *Burkholderia rhizoxinica* sp. nov. and *Burkholderia endofungorum* sp. nov., bacterial endosymbionts of the plant-pathogenic fungus *Rhizopus microsporus*. *Int J Syst Evol Microbiol* **57**: 2583-2590.

Pati A, Ivanova NN, Mikhailova N, Ovchinnikova G, Hooper SD, Lykidis A & Kyrpides NC (2010) GenePRIMP: a gene prediction improvement pipeline for prokaryotic genomes. *Nat Methods* **7**: 455-457.

Price CT, Al-Khodor S, Al-Quadan T, Santic M, Habyarimana F, Kalia A & Kwaik YA (2009) Molecular mimicry by an F-box effector of *Legionella pneumophila* hijacks a conserved polyubiquitination machinery within macrophages and protozoa. *PLoS Pathog* **5**: e1000704.

Pruesse E, Quast C, Knittel K, Fuchs BM, Ludwig W, Peplies J & Glöckner FO (2007) SILVA: a comprehensive online resource for quality checked and aligned ribosomal RNA sequence data compatible with ARB. *Nucleic Acids Res* **35**: 7188-7196.

Richter M & Rosselló-Móra R (2009) Shifting the genomic gold standard for the prokaryotic species definition. *P Natl Acad Sci USA* **106**: 19126-19131.

Robinson MD, McCarthy DJ & Smyth GK (2010) edgeR: a Bioconductor package for differential expression analysis of digital gene expression data. *Bioinformatics* **26**: 139-140.

Rogg LE, Fortwendel JR, Juvvadi PR & Steinbach WJ (2012) Regulation of expression, activity and localization of fungal chitin synthases. *Med Mycol* **50**: 2-17.

Rohde JR, Breitkreutz A, Chenal A, Sansonetti PJ & Parsot C (2007) Type III secretion effectors of the IpaH family are E3 ubiquitin ligases. *Cell Host Microbe* **1**: 77-83.

Ronquist F, Teslenko M, van der Mark P, Ayres DL, Darling A, Höhna S, Larget B, Liu L, Suchard MA & Huelsenbeck JP (2012) MrBayes 3.2: efficient Bayesian phylogenetic inference and model choice across a large model space. *Syst Biol* **61**: 539-542.

Rowley G, Spector M, Kormanec J & Roberts M (2006) Pushing the envelope: extracytoplasmic stress responses in bacterial pathogens. *Nat Rev Microbiol* **4**: 383-394.

Salvioli A, Ghignone S, Novero M, Navazio L, Venice F, Bagnaresi P & Bonfante P (2016) Symbiosis with an endobacterium increases the fitness of a mycorrhizal fungus, raising its bioenergetic potential. *ISME J* **10**: 130-144.

Santangelo GM (2006) Glucose signaling in *Saccharomyces cerevisiae*. *Microbiol Mol Biol R* **70**: 253-282.

Scholze H & Boch J (2011) TAL effectors are remote controls for gene activation. *Curr Opin Microbiol* **14**: 47-53.

Skovierova H, Rowley G, Rezuchova B, Homerova D, Lewis C, Roberts M & Kormanec J (2006) Identification of the sigmaE regulon of *Salmonella enterica* serovar Typhimurium. *Microbiology* **152**: 1347-1359.

Sturgis JN (2001) Organisation and evolution of the *tol-pal* gene cluster. *J Mol Microb Biotech* **3**: 113-122.

Tominaga Y & Tsujisaka Y (1981) Investigation of the structure of *Rhizopus* cell wall with lytic enzymes. *Agr Biol Chem* **45**: 1569-1575.

Trapnell C, Roberts A, Goff L, Pertea G, Kim D, Kelley DR, Pimentel H, Salzberg SL, Rinn JL & Pachter L (2012) Differential gene and transcript expression analysis of RNA-seq experiments with TopHat and Cufflinks. *Nat Protoc* **7**: 562-578.

Uzum Z, Silipo A, Lackner G, De Felice A, Molinaro A & Hertweck C (2015) Structure, genetics and function of an exopolysaccharide produced by a bacterium living within fungal hyphae. *ChemBioChem* **16**: 387-392.

Verwer PE, van Duijn ML, Tavakol M, Bakker-Woudenberg IA & van de Sande WW (2012) Reshuffling of *Aspergillus fumigatus* cell wall components chitin and beta-glucan under the influence of caspofungin or nikkomycin Z alone or in combination. *Antimicrob Agents Ch* **56**: 1595-1598.

Vuong C, Kocianova S, Voyich JM, Yao Y, Fischer ER, DeLeo FR & Otto M (2004) A crucial role for exopolysaccharide modification in bacterial biofilm formation, immune evasion, and virulence. *J Biol Chem* **279**: 54881-54886.

Wei D, Houtman CJ, Kapich AN, Hunt CG, Cullen D & Hammel KE (2010) Laccase and its role in production of extracellular reactive oxygen species during wood decay by the brown rot basidiomycete *Postia placenta*. *Appl Environ Microb* **76**: 2091-2097.

Zhao X, Mehrabi R & Xu JR (2007) Mitogen-activated protein kinase pathways and fungal pathogenesis. *Eukaryot Cell* **6**: 1701-1714.

2.9 SUPPORTING INFORMATION

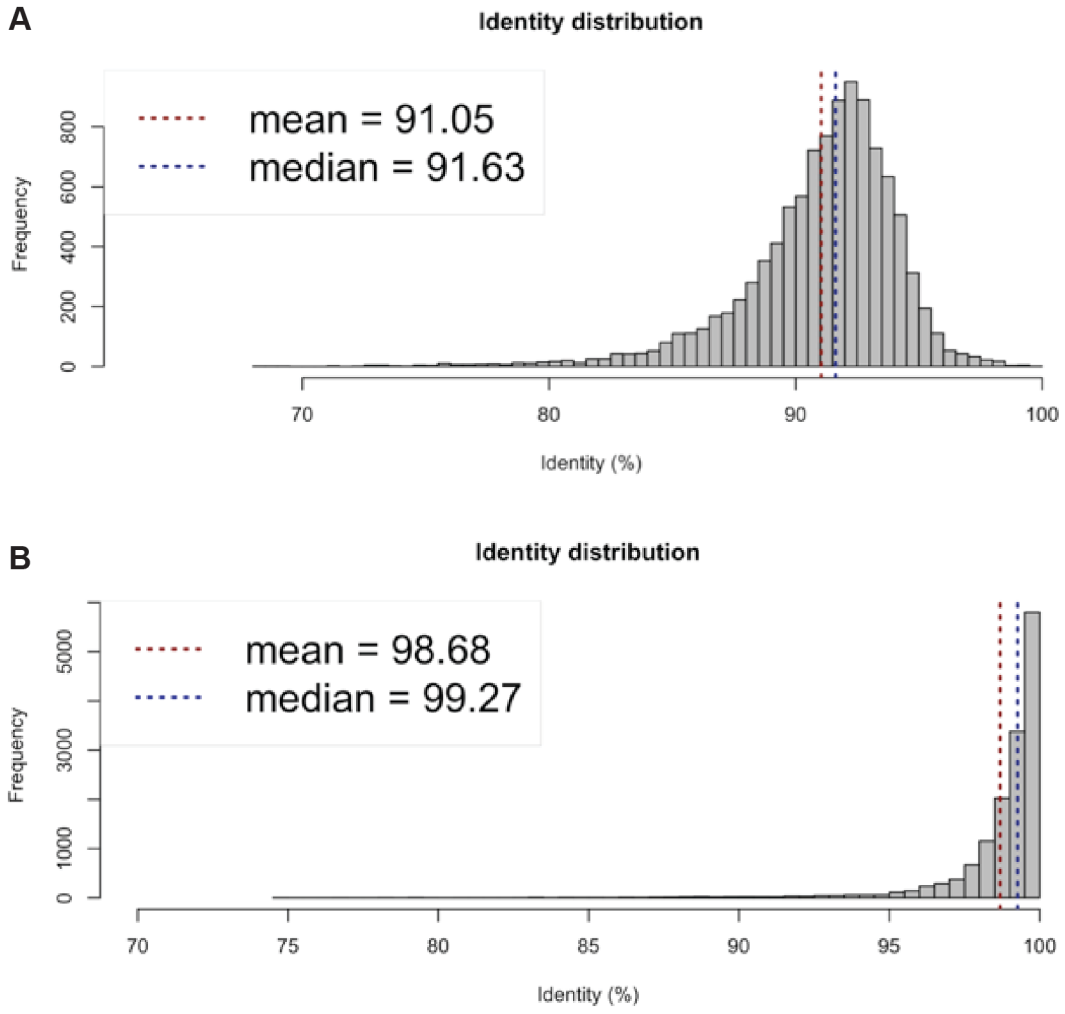

Figure S1. Average nucleotide identity (ANI) calculated for the genomes of *Burkholderia* endobacteria. (**A**) *Burkholderia* sp. B13 and *B. rhizoxinica* HKI454. (**B**) *Burkholderia* sp. B13 and *Burkholderia* sp. B14. The tool (http://enve-omics.ce.gatech.edu/ani/index) splits the genomes into 1000 bp fragments and compares nucleotide identity between them. Histogram shows frequency distribution of genome fragments sorted by percent nucleotide identity between the two genomes.

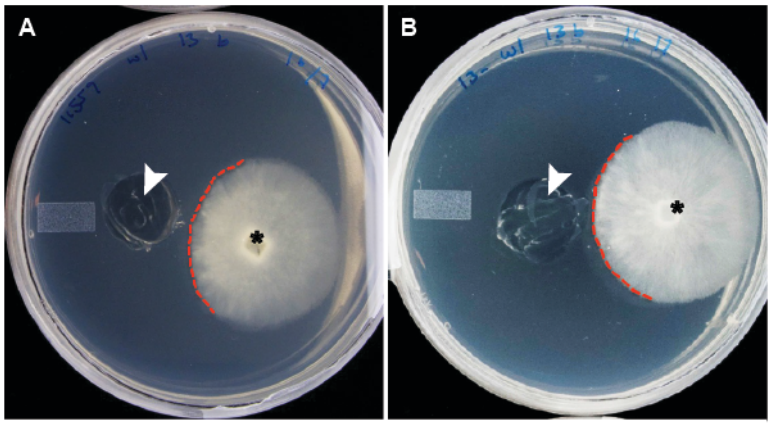

Figure S2. Co-cultivation of *Rm* ATCC 11559 (non-host) and *Rm* ATCC 52813 (host) with *Burkholderia* enodbacteria. (**A**) Non-host co-cultivated with endobacteria of the host displays growth alteration before fungal colony contacts endobacteria. (**B**) Host co-cultivated with endobacteria does not alter its growth. Arrowheads indicate site of bacterial inoculation, asterisks indicate site of fungal inoculation, red dashed line shows the outline of fungal colony in proximity to endobacteria.

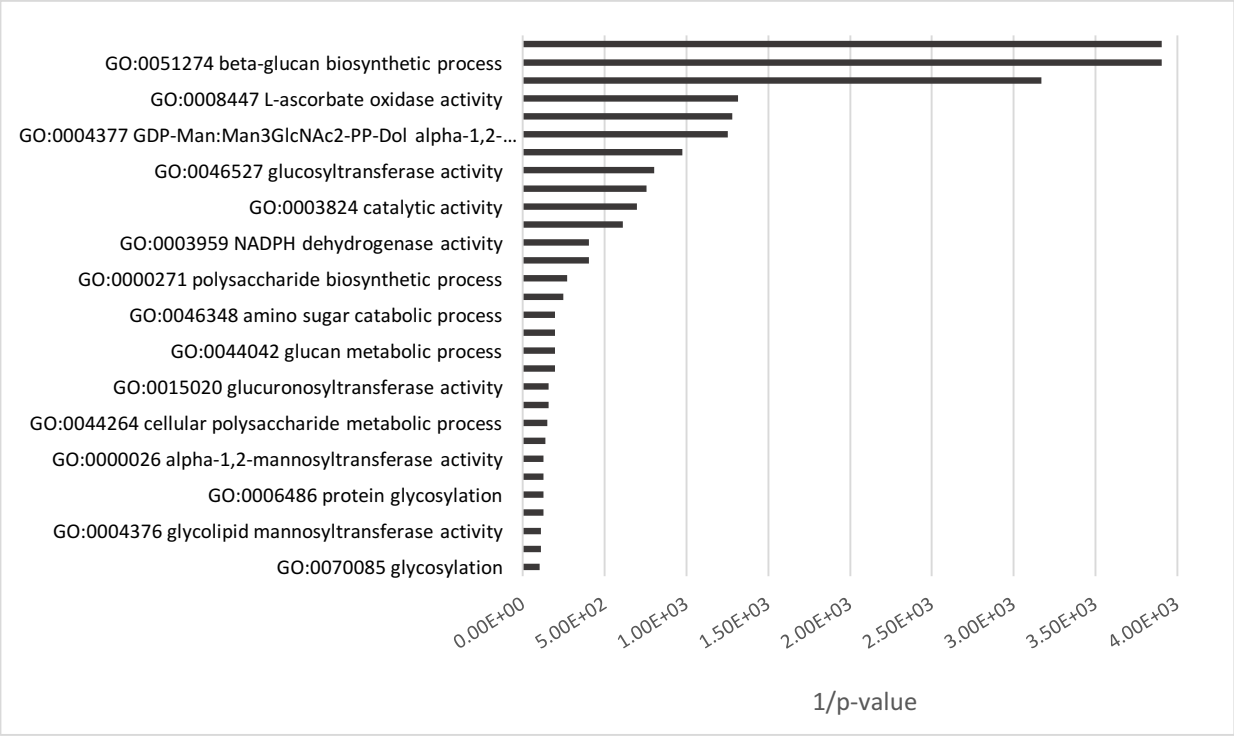

Figure S3. GO categories enriched in the upregulated fraction of the DE non-host genes in response to physical interaction with bacterial symbionts.

Table S1. Genome statistics for *Burkholderia* sp. B13 and *Burkholderia* sp. B14 as well as previously sequenced *Burkholderia rhizoxinica* HKI 454 included for comparison.

	Burkholderia sp. B13	*Burkholderia* sp. B14	*B. rhizoxinica* HKI454
DNA, total number of bases	3579262	3653645	3750138
DNA coding number of bases	87.50%	87.08%	88.73%
DNA G+C number of bases	60.59%	60.56%	60.71%
DNA scaffolds	2	3	3
Genes total number	3292	3465	3938
Protein coding genes	3219	3394	3870
Pseudo Genes	404	417	NA
RNA genes	73	71	68
rRNA genes	9	9	9
5S rRNA	3	3	3
16S rRNA	3	3	3
23S rRNA	3	3	3
tRNA genes	47	47	59
Other RNA genes	17	15	NA

Table S2. Candidate T3SS effectors upregulated during pre-contact and physical contact with host and non-host fungi. ND, not detected.

Protein ID	Effective T3 Score	Eukaryotic-like domain	Annotation IMG
Pre-contact			
2599762763	1	ND	Hypothetical protein
2599763016	1	ND	Hypothetical protein
2599763274	1	PF11937 14	Protein of unknown function (DUF3455)
2599763295	1	ND	Hypothetical protein
2599763359	1	ND	Hypothetical protein
2599763360	1	ND	Hypothetical protein
2599763806	1	ND	Hypothetical protein
2599764438	1	ND	Response regulator containing CheY-like receiver, AAA-type ATPase, and DNA-binding domains
2599764562	1	ND	Hypothetical protein
2599764578	1	ND	Hypothetical protein
2599765017	1	ND	Prevent-host-death family protein
2599765640	1	ND	Transglycosylase SLT domain
2599765794	1	PF00483 4 PF01050 6	Mannose-1-phosphate guanylyltransferase/mannose-6-phosphate isomerase
2599765018	0.99955	ND	Putative toxin-antitoxin system toxin component, PIN family
2599765428	0.99955	ND	Hypothetical protein
Physical contact			
2599762710	1	ND	Hypothetical protein
2599762745	1	ND	Hypothetical protein
2599762753	1	ND	Hypothetical protein
2599762755	1	PF00106 6	Dehydrogenases with different specificities (related to short-chain alcohol dehydrogenases)
2599762763	1	ND	Hypothetical protein
2599763016	1	ND	Hypothetical protein
2599763051	1	ND	Hypothetical protein
2599763258	1	ND	Hypothetical protein
2599763274	1	PF11937 14	Protein of unknown function (DUF3455)
2599763292	1	ND	Hypothetical protein
2599763295	1	ND	Hypothetical protein
2599763314	1	ND	Hypothetical protein
2599763359	1	ND	Hypothetical protein
2599763360	1	ND	Hypothetical protein
2599763566	1	ND	Multidrug resistance efflux pump
2599763623	1	PF13516 134	Leucine Rich repeat
2599763806	1	ND	Hypothetical protein
2599763826	1	PF04632 6	Predicted membrane protein -- fusaric acid resistance protein

2599763864	1	PF00355 6 PF00848 13	Phenylpropionate dioxygenase and related ring-hydroxylating dioxygenases, large terminal subunit
2599763909	1	PF00528 8	Phosphate ABC transporter membrane protein 2, PhoT family (TC 3.A.1.7.1)
2599763968	1	ND	Anti sigma-E protein, RseA
2599764195	1	PF00180 5	Isocitrate dehydrogenase (NADP) (EC 1.1.1.42)
2599764211	1	PF01649 12	SSU ribosomal protein S20P
2599764253	1	PF01025 4	Molecular chaperone GrpE (heat shock protein)
2599764438	1	ND	Response regulator containing CheY-like receiver, AAA-type ATPase, and DNA-binding domains
2599764562	1	ND	Hypothetical protein
2599764578	1	ND	Hypothetical protein
2599764584	1	ND	Phenylacetate-CoA oxygenase, PaaG subunit
2599764628	1	PF00106 6	Dehydrogenases with different specificities (related to short-chain alcohol dehydrogenases)
2599764718	1	ND	Hypothetical protein
2599765017	1	ND	Prevent-host-death family protein -- antitoxin Phd_YefM, type II toxin-antitoxin
2599765167	1	ND	Glutamate dehydrogenase/leucine dehydrogenase
2599765172	1	ND	Hypothetical protein
2599765375	1	ND	Hypothetical protein
2599765537	1	PF03972 14	MmgE/PrpD family -- PrpD is required for propionate catabolism, catalysing the third step of the 2-methylcitric acid cycle
2599765541	1	PF00392 5 PF07702 4	Transcriptional regulators, GntR family
2599765547	1	PF00285 6	Citrate synthase (EC 2.3.3.1)
2599765640	1	ND	Transglycosylase SLT domain
2599765719	1	ND	Hypothetical protein
2599765780	1	PF12937 10000	F-box-like
2599765789	1	ND	O-antigen ligase like membrane protein
2599765794	1	PF00483 4 PF01050 6	Mannose-1-phosphate guanylyltransferase/mannose-6-phosphate isomerase
2599765796	1	ND	Hypothetical protein
2599763567	0.99997	PF07690 6	Drug resistance transporter, EmrB/QacA subfamily
2599765433	0.99996	ND	Superfamily II DNA and RNA helicases
2599765247	0.99994	PF02629 4 PF00549 4	Succinyl-CoA synthetase (ADP-forming) alpha subunit (EC 6.2.1.5)
2599765431	0.99989	ND	*Xanthomonas* avirulence protein, Avr/PthA -- BTAL
2599765782	0.99965	ND	Hypothetical protein
2599765798	0.99963	PF12695 5	Predicted hydrolases or acyltransferases (alpha/beta hydrolase superfamily)
2599762759	0.99961	PF13193 4 PF00501 4	Acyl-coenzyme A synthetases/AMP-(fatty) acid ligases
2599765018	0.99955	ND	Putative toxin-antitoxin system toxin component, PIN family
2599765428	0.99955	ND	Hypothetical protein
2599763257	0.99891	ND	Domain of unknown function (DUF1839)

2599765536	0.99877	PF00330 5 PF00694 4	Aconitase (EC 4.2.1.3)
2599763943	0.99742	PF00005 6 PF00664 6	ABC-type multidrug transport system, ATPase and permease components
2599762742	0.99738	ND	Hypothetical protein
2599764591	0.99373	PF13302 6	Acetyltransferases, including N-acetylases of ribosomal proteins
2599765023	0.98969	ND	Protein of unknown function (DUF3567)
2599765571	0.98923	PF01557 8	2-keto-4-pentenoate hydratase
2599763910	0.97968	PF00528 8	Phosphate ABC transporter membrane protein 1, PhoT family (TC 3.A.1.7.1)
2599764559	0.9766	PF00164 10	SSU ribosomal protein S12P
2599762848	0.95747	ND	Response regulators consisting of a CheY-like receiver domain and a winged-helix DNA-binding domain
2599763775	0.95559	PF02839 8	Carbohydrate binding domain/Glycosyl hydrolase family 46 -- chitosinase
2599765574	0.95514	ND	4-hydroxy-2-oxovalerate aldolase

Table S3. Signaling genes DE in the host fungus during physical interaction with endobacteria. Log_2FC, Log_2 fold change; positive Log_2FC values denote upregulated genes, negative Log_2FC values denote downregulated genes; FDR, false discovery rate.

Protein ID	Log_2FC	FDR	IPR ID	IPR domain	KOG ID	KOG annotation	KOG class	GO ID	GO category
315343	3.78	2.47E-05	IPR001206	Diacylglycerol kinase	KOG1169	Diacylglycerol kinase	Lipid transport and metabolism	GO:0007205	protein kinase C activation
252161	2.65	1.07E-07	IPR000198	RhoGAP	KOG2710	Rho GTPase-activating protein	Signal transduction mechanisms	GO:0007165	signal transduction
60967	2.56	6.10E-04	IPR000219	Dbl homology (DH) domain	KOG4305	RhoGEF GTPase	Signal transduction mechanisms	GO:0035023	regulation of Rho protein signal transduction
249145	2.06	1.19E-09	IPR001206	Diacylglycerol kinase	KOG1169	Diacylglycerol kinase	Lipid transport and metabolism	GO:0007205	activation of protein kinase C activity
136105	2.00	2.07E-08	IPR001806	Ras GTPase	KOG0393	Ras-related small GTPase, Rho type	General function prediction only	GO:0007264	small GTPase mediated signal transduction
264384	1.97	2.88E-13	none	no domains	KOG2058	Ypt/Rab GTPase activating protein	Intracellular trafficking, secretion, and vesicular transport	GO:0004308	exo-alpha-sialidase activity
185441	1.81	1.24E-06	IPR017442	Serine/threonine protein kinase-related	KOG0612	Rho-associated, coiled-coil containing protein kinase	Signal transduction mechanisms	GO:0006468	protein amino acid phosphorylation
271786	1.72	2.78E-04	IPR000219	Dbl homology (DH) domain	KOG4424	Predicted Rho/Rac guanine nucleotide exchange factor/faciogenital dysplasia protein 3	Signal transduction mechanisms	GO:0035023	regulation of Rho protein signal transduction
201417	1.41	4.72E-13	IPR001789 IPR003661 IPR013655 IPR013655 IPR001610	Signal transduction response regulator, receiver region; Signal transduction histidine kinase, subgroup 1, dimerisation and phosphoacceptor region; PAS fold-3.ATP-binding region, ATPase-like, PAC motif	KOG0519	Sensory transduction histidine kinase	Signal transduction mechanisms	GO:0007165	signal transduction

286008	1.22	3.15E-04	IPR002373	cAMP/cGMP-dependent protein kinase	KOG1113	cAMP-dependent protein kinase types I and II, regulatory subunit	Signal transduction mechanisms	GO:0006468	protein amino acid phosphorylation
274088	1.21	3.24E-05	IPR000198	RhoGAP	KOG4270	GTPase-activator protein	Signal transduction mechanisms	GO:0007165	signal transduction
266182	1.19	5.69E-04	IPR000719 IPR003096 IPR001715	Protein kinase, core, SM22/calponin, Calponin-like actin-binding	KOG0198	MEKK and related serine/threonine protein kinases	Signal transduction mechanisms	GO:0006468	protein amino acid phosphorylation
234989	1.16	1.06E-04	IPR017442	Serine/threonine protein kinase-related	KOG0667	Dual-specificity tyrosine-phosphorylation regulated kinase	General function prediction only	GO:0006468	protein amino acid phosphorylation
226218	1.01	4.85E-03	IPR001060 IPR000198	Cdc15/Fes/CIP4, RhoGAP	KOG1450	Predicted Rho GTPase-activating protein	Signal transduction mechanisms	GO:0007165	signal transduction
300418	1.00	3.11E-05	IPR000719 IPR008352	Protein kinase, core, MAP kinase, p38	KOG0660	Mitogen-activated protein kinase	Signal transduction mechanisms	GO:0006468	protein amino acid phosphorylation
235547	1.00	4.26E-07	IPR002219 IPR001452 IPR001060	Protein kinase C, phorbol ester/diacylglycerol binding, Src homology-3, Cdc15/Fes/CIP4	KOG3565	Cdc42-interacting protein CIP4	Cytoskeleton	GO:0007242	intracellular signaling cascade
278678	0.90	3.20E-03	IPR017442	Serine/threonine protein kinase-related	KOG0616	cAMP-dependent protein kinase catalytic subunit (PKA)	Signal transduction mechanisms	GO:0006468	protein amino acid phosphorylation
233858	0.85	1.89E-03	IPR001164	Arf GTPase activating protein	KOG0702	Predicted GTPase-activating protein	Signal transduction mechanisms	GO:0008060	ARF GTPase activator activity
277000	0.84	5.10E-03	IPR001849 IPR001164	Pleckstrin-like, Arf GTPase activating protein	KOG0521	Putative GTPase activating proteins (GAPs)	Signal transduction mechanisms	GO:0008060	ARF GTPase activator activity
202982	0.82	6.04E-04	IPR002498	Phosphatidylinositol-4-phosphate 5-kinase, core	KOG0229	Phosphatidylinositol-4-phosphate 5-kinase	Signal transduction mechanisms	GO:0046488	phosphatidylinositol metabolic process
270618	0.74	1.99E-03	IPR013079 IPR003094 IPR013078	Bifunctional 6-phosphofructo-2-kinase/fructose-2,6-bisphosphate 2-phosphatase, Fructose-2,6-	KOG0234	Fructose-6-phosphate 2-kinase/fructose-2,6-biphosphatase	Carbohydrate transport and metabolism	GO:0006003	fructose 2,6-bisphosphate metabolic process

				bisphosphatase, Phosphoglycerate mutase					
286014	0.72	4.26E-03	IPR000719 IPR008352	Protein kinase, core, MAP kinase, p38	KOG0660	Mitogen-activated protein kinase	Signal transduction mechanisms	GO:0006468	protein amino acid phosphorylation
236201	0.70	1.57E-04	IPR001199	Cytochrome b5	KOG4035	Coeffector of mDia Rho GTPase, regulates actin polymerization and cell adhesion turnover	Cytoskeleton	GO:0046914	transition metal ion binding
237596	0.69	4.25E-04	IPR000198	RhoGAP	KOG4270	GTPase-activator protein	Signal transduction mechanisms	GO:0007165	signal transduction
234830	0.66	9.11E-03	IPR002073 IPR011006	3'5'-cyclic nucleotide phosphodiesteras e, CheY-like	KOG3689	Cyclic nucleotide phosphodiesterase	Signal transduction mechanisms	GO:0007165	signal transduction
268827	0.65	2.36E-03	IPR003109	GoLoco				GO:0007165	signal transduction
250648	0.63	9.71E-03	IPR001806 IPR017441	Ras GTPase, Protein kinase ATP binding, conserved site	KOG4423	GTP-binding protein-like, RAS superfamily	Signal transduction mechanisms	GO:0007264	small GTPase mediated signal transduction
244189	0.50	5.10E-03	IPR002014 IPR000306 IPR003903	VHS, Zinc finger, FYVE-type, Ubiquitin interacting motif	KOG1818	Membrane trafficking and cell signaling protein HRS, contains VHS and FYVE domains	Signal transduction mechanisms	GO:0006886	intracellular protein transport
197380	-0.55	4.85E-04	IPR005946	Phosphoribosyl pyrophosphokinas e					
233491	-0.57	4.69E-04	IPR001048 IPR000706 IPR000534	Aspartate/glutama te/uridylate kinase, N-acetyl-gamma-glutamyl-phosphate reductase, Semialdehyde dehydrogenase, NAD-binding	KOG2436	Acetylglutamate kinase/acetylglutamate synthase	Amino acid transport and metabolism	GO:0006520	amino acid metabolic process
284787	-0.61	1.06E-03	IPR002290	Serine/threonine protein kinase	KOG3741	Poly(A) ribonuclease subunit	RNA processing and modification	GO:0006468	protein amino acid phosphorylation
236630	-0.63	6.23E-03	IPR001849 IPR000219 IPR000270	Pleckstrin-like, Dbl homology (DH) domain,	KOG3519	Invasion-inducing protein TIAM1/CDC24 and related RhoGEF	Signal transduction mechanisms	GO:0005089	Rho guanyl-nucleotide exchange factor activity

			IPR001331	Octicosapeptide/Phox/Bem1p, Guanine-nucleotide dissociation stimulator, CDC24, conserved site		GTPases			
284927	-0.69	8.96E-04	IPR016034	Phosphatidylinositol-4-phosphate 5-kinase, core, subgroup	KOG0229	Phosphatidylinositol-4-phosphate 5-kinase	Signal transduction mechanisms	GO:0046488	phosphatidylinositol metabolic process
200320	-0.76	6.26E-03	IPR000195	RabGAP/TBC	KOG2058	Ypt/Rab GTPase activating protein	Intracellular trafficking, secretion, and vesicular transport	GO:0005097	Rab GTPase activator activity
235463	-0.76	4.66E-03	IPR001895 IPR000651	Guanine-nucleotide dissociation stimulator CDC25, Guanine nucleotide exchange factor for Ras-like GTPases, N-terminal	KOG3417	Ras1 guanine nucleotide exchange factor	Signal transduction mechanisms	GO:0005085	guanyl-nucleotide exchange factor activity
15091	-0.81	3.17E-03	IPR008936	Rho GTPase activation protein				GO:0007165	signal transduction
88449	-0.81	1.17E-04	IPR000719	Protein kinase, core				GO:0004672	protein kinase activity
199697	-0.83	1.64E-04	IPR001048	Aspartate/glutamate/uridylate kinase	KOG0456	Aspartate kinase	Amino acid transport and metabolism	GO:0008652	amino acid biosynthetic process
313597	-0.83	9.83E-06	IPR000403 IPR016024	Phosphatidylinositol 3- and 4-kinase, catalytic, Armadillo-type fold	KOG0903	Phosphatidylinositol 4-kinase, involved in intracellular trafficking and secretion	Signal transduction mechanisms	GO:0016773	phosphotransferase activity, alcohol group as acceptor
222087	-1.27	7.48E-19	IPR017442	Serine/threonine protein kinase-related	KOG0590	Checkpoint kinase and related serine/threonine protein kinases	Cell cycle control, cell division, chromosome partitioning	GO:0006468	protein amino acid phosphorylation

Table S4. Cell cycle related genes DE in the host during physical interaction with *Burkholderia* endobacteria.
Log_2FC, Log_2 fold change; positive Log_2FC values denote upregulated genes, negative Log_2FC values denote downregulated genes; false discovery rate, FDR.

Protein ID	Log_2FC	FDR	Interpro ID	Domain	KOG ID	KOG definition	KOG Class
232829	1.69	1.08E-07	IPR001060 IPR001452	Cdc15/Fes/CIP4, Src homology-3	KOG2398	Predicted proline-serine-threonine phosphatase-interacting protein (PSTPIP)	Cell cycle control, cell division, chromosome partitioning
286595	1.16	1.59E-11	IPR007632	Protein of unknown function DUF590	KOG2513	Protein required for meiotic chromosome segregation	Cell cycle control, cell division, chromosome partitioning
312571	1.00	6.81E-03	IPR001452 IPR001060	Src homology-3, Cdc15/Fes/CIP4	KOG2398	Predicted proline-serine-threonine phosphatase-interacting protein (PSTPIP)	Cell cycle control, cell division, chromosome partitioning
294963	0.77	1.95E-05	IPR007087 IPR015880	Zinc finger, C2H2-type, Zinc finger, C2H2-like	KOG4124	Putative transcriptional repressor regulating G2/M transition	Cell cycle control, cell division, chromosome partitioning
232886	0.73	3.06E-06	IPR001005 IPR009057	SANT, DNA-binding	KOG2043	Signaling protein SWIFT and related BRCT domain proteins	Cell cycle control, cell division, chromosome partitioning
232349	0.72	1.71E-03	IPR005045	Protein of unknown function DUF284	KOG2952	Cell cycle control protein	Signal transduction mechanisms
215598	-0.81	0.0016	IPR011025 IPR001019 IPR002975	G protein alpha subunit, helical insertion, Guanine nucleotide binding protein (G-protein), alpha subunit, Fungal G-protein, alpha subunit	KOG0082	G-protein alpha subunit (small G protein superfamily)	Cell cycle control, cell division, chromosome partitioning
222087	-1.27	7.48E-19	IPR000719 IPR017442	Protein kinase, core Serine/threonine protein kinase-related	KOG0590	Checkpoint kinase and related serine/threonine protein kinases	Cell cycle control, cell division, chromosome partitioning

Table S5. Predicted targets of the *Burkholderia* sp. B13 full length BTAL protein in genomes of host and non-host fungi. Protein ID of the fungal gene located closest to the predicted BTAL binding site is given along with its expression level during physical interaction with endobacteria. NDE, not differentially expressed; NE, not expressed; ↑, significantly upregulated; ↓, significantly downregulated.

Assembly Scaffold	Strand	Start Position	Protein ID of closest gene	Annotation	Expression due to bacteria
Host					
scaffold_14	Plus	309394	205587	Predicted DNA damage inducible protein	NDE
scaffold_10	Plus	869779	238547	Hypothetical protein	↑
scaffold_33	Minus	117411	274454	Fungal specific transcription factor	NDE
scaffold_13	Minus	356653	259025	Hypothetical protein	NE
scaffold_14	Minus	503726	37976	Polycomb-like PHD Zn-finger protein	NDE
scaffold_2	Minus	1943403	193862	CCCH-type Zn-finger protein	↓
scaffold_3	Plus	1678568	212753	Vacuolar protein sorting-associated protein	NDE
scaffold_5	Plus	869168	200524	Ca^{2+} sensor (EF-Hand superfamily)	NDE
scaffold_20	Plus	329116	267366	Cl^- channel CLC-3 and related proteins (CLC superfamily)	NDE
scaffold_11	Plus	476332	314198	Hypothetical protein	NDE
Non-host					
scaffold_49	Plus	89137	226198	Predicted DNA damage inducible protein	NDE
scaffold_443	Plus	1961	No genes in this region		
scaffold_243	Plus	10818	267898	Hypothetical protein	NDE
scaffold_99	Plus	38470	244065	Cl^- channel CLC-3 and related proteins (CLC superfamily)	NDE
scaffold_521	Minus	273	152420	Hypothetical protein	NDE
scaffold_8	Minus	177476	247443	Hypothetical protein	NDE
scaffold_128	Minus	10928	201848	Membrane trafficking and cell signaling protein HRS, contains VHS and FYVE domains	NDE
scaffold_313	Plus	7146	239576	Thyroid hormone receptor-associated protein complex, subunit TRAP230	NDE
scaffold_164	Minus	11193	273727	Hypothetical protein	NE
scaffold_44	Plus	5584	226003	Monocarboxylate transporter	NDE
scaffold_195	Plus	21175	245593	GATA-4/5/6 transcription factors	NDE

Table S6. *Burkholderia* species and strains used in the OrthoMCL clustering analysis.

Organism	Source	Citation
B. rhizoxinica HKI 454	*Rm* ATCC 62417	(1)
Burkholderia sp. B13	*Rm* ATCC 52813	This study
Burkholderia sp. B14	*Rm* ATCC 52814	This study
B. ambifaria AMMD [LMG 19182]	Plant rhizosphere	JGI Genome Portal
B. cenocepacia AU1054	Blood of cystic fibrosis patient	JGI Genome Portal
B. cenocepacia J2315	Cystic fibrosis patient	(2)
Burkholderia sp. GG4	Ginger rhizosphere	(3)
B. dolosa AUO158	Causal agent of necrotizing pneumonia	(4)
B. glumae BGR1	Diseased rice pinacle	(5)
B. gladioli BSR3	Diseased rice sheath	(6)
B. mallei ATCC 23344	Agent of glanders	(7)
B. mallei NCTC 10247	Agent of glanders and pneumonia	(8)
B. multivorans ATCC 17616	Soil	(9)
B. phenoliruptrix BR3459a (CLA1)	Nitrogen-fixing symbiont of *Mimosa flocculosa*	(10)
B. phymatum STM815	Root nodule of *Machaerium lunatum*	(11)
B. phytofirmans PsJN T	Endophyte of onion roots	JGI Genome Portal
B. pseudomallei BPC006	Melioidosis patient	(12)
B. thailandensis E264	Non-pathogenic saprophyte	(13)
B. vietnamiensis G4	Wastewater treatment facility	JGI Genome Portal
B. xenovorans LB400 (formerly *B. fungorum*)	Landfill	JGI Genome Portal

References

1. Lackner G, Moebius N, Partida-Martinez L, & Hertweck C (2011) Complete genome sequence of *Burkholderia rhizoxinica*, an endosymbiont of *Rhizopus microsporus*. *J. Bacteriol.* 193(3):783-784.
2. Holden MT*, et al.* (2009) The genome of *Burkholderia cenocepacia* J2315, an epidemic pathogen of cystic fibrosis patients. *J. Bacteriol.* 191(1):261-277.
3. Hong KW, Koh CL, Sam CK, Yin WF, & Chan KG (2012) Complete genome sequence of *Burkholderia* sp. Strain GG4, a betaproteobacterium that reduces 3-oxo-N-acylhomoserine lactones and produces different N-acylhomoserine lactones. *J. Bacteriol.* 194(22):6317.
4. Johnson SL*, et al.* (2015) Complete genome sequences for 59 *Burkholderia* isolates, both pathogenic and near neighbor. *Genome Announc.* 3(2):e00159-00115.
5. Lim J*, et al.* (2009) Complete genome sequence of *Burkholderia glumae* BGR1. *J. Bacteriol.* 191(11):3758-3759.
6. Seo YS*, et al.* (2011) Complete genome sequence of *Burkholderia gladioli* BSR3. *J. Bacteriol.* 193(12):3149.
7. Nierman WC*, et al.* (2004) Structural flexibility in the *Burkholderia mallei* genome. *P. Natl. Acad. Sci. USA* 101(39):14246-14251.
8. Daligault HE*, et al.* (2014) Whole-genome assemblies of 56 *Burkholderia* species. *Genome Announc.* 2(6):e01106-01114.
9. Nishiyama E, Ohtsubo Y, Nagata Y, & Tsuda M (2010) Identification of *Burkholderia multivorans* ATCC 17616 genes induced in soil environment by in vivo expression technology. *Environ. Microbiol.* 12(9):2539-2558.
10. de Oliveira Cunha C*, et al.* (2012) Complete genome sequence of *Burkholderia phenoliruptrix* BR3459a (CLA1), a heat-tolerant, nitrogen-fixing symbiont of *Mimosa flocculosa*. *J. Bacteriol.* 194(23):6675-6676.
11. Moulin L*, et al.* (2014) Complete Genome sequence of *Burkholderia phymatum* STM815(T), a broad host range and efficient nitrogen-fixing symbiont of *Mimosa* species. *Stand. Genomic Sci.* 9(3):763-774.
12. Fang Y*, et al.* (2012) First genome sequence of a *Burkholderia pseudomallei* isolate in China, strain BPC006, obtained from a melioidosis patient in Hainan. *J. Bacteriol.* 194(23):6604-6605.
13. Kim HS*, et al.* (2005) Bacterial genome adaptation to niches: divergence of the potential virulence genes in three *Burkholderia* species of different survival strategies. *BMC Genomics* 6:174.

Table S7. *Burkholdria* sp. B13 genes encoded exclusively in genomes of *Burkholderia* endobacteria and upregulated during physical contact with host and non-host fungi. Annotations provided by JGI IMG. T3SS signals are predicted by Effective T3 V2.0 model.

Protein ID	Annotation	T3SS signal
2599762710	Hypothetical protein	Yes
2599762721	Hypothetical protein	Absent
2599762734	Acetyltransferase (GNAT) family	Absent
2599762742	Hypothetical protein	Yes
2599762754	Glycosyl hydrolase catalytic core	Absent
2599762763	Hypothetical protein	Yes
2599762840	Acyl carrier protein	Absent
2599762841	Acyl-CoA dehydrogenases	Absent
2599762848	Response regulators consisting of a CheY-like receiver domain and a winged-helix DNA-binding domain	Yes
2599762998	Glycine zipper	Absent
2599763016	Hypothetical protein	Yes
2599763051	Hypothetical protein	Yes
2599763251	Methionyl-tRNA formyltransferase	Absent
2599763268	Bacterial type III secretion protein (HrpB1_HrpK)	Absent
2599763281	Bacterial type III secretion protein (HrpB2)	Absent
2599763289	Hypothetical protein	Absent
2599763292	Hypothetical protein	Yes
2599763295	Hypothetical protein	Yes
2599763360	Hypothetical protein	Yes
2599763422	Hypothetical protein	Absent
2599763623	Leucine Rich repeat	Yes
2599763727	Conserved hypothetical phage tail region protein	Absent
2599764053	Hypothetical protein	Absent
2599764576	Hypothetical protein	Absent
2599764986	Hypothetical protein	Absent
2599765016	Hypothetical protein	Absent
2599765415	Hypothetical protein	Absent
2599765428	Hypothetical protein	Yes
2599765431	*Xanthomonas* avirulence protein, Avr/PthA	Yes
2599765635	Hypothetical protein	Absent
2599765640	Transglycosylase SLT domain	Yes
2599765719	Hypothetical protein	Yes
2599765780	F-box-like	Yes
2599765789	O-antigen ligase like membrane protein	Yes
2599765858	Transposase domain (DUF772)/Transposase DDE domain	Absent

CHAPTER 3

BACTERIAL ENDOSYMBIONTS INFLUENCE SEXUAL REPRODUCTION OF THEIR FUNGAL HOST[2]

3.1 ABSTRACT

Bacterial symbionts can have a great impact on the biology of their eukaryotic hosts. In the symbiosis between the fungus *Rhizopus microsporus* and *Burkholderia* sp. endobacteria, the symbionts have gained control over fungal asexual reproduction, whereby their removal results in compete loss of fungal sporulation. In this study I built upon existing data to explore the impact of endobacteria on fungal sexual reproduction. I discovered that, unlike bacterial control over asexual reproduction, control over sexuality is incomplete and formation of sexual propagules was either eliminated or diminished in matings between bacteria-free host (partial mating). Consistent with incomplete control, transmission of endosymbionts through sexual propagules was much lower than through asexual sporangiospores. I confirmed that, analogously to when mating is entirely abolished, partial mating was marked by significant downregulation of *ras2,* a small GTPase central to reproductive development in fungi. Moreover, I discovered that the secondary messenger cyclic AMP decreases mating in *R. microsporus* and that these negative effects are buffered by the presence of *Burkholderia* endobacteria.

3.2 INTRODUCTION

Members of early divergent fungi (Mucoromycotina, Mortierellamycotina, Glomeromycotina)

[2] Results from this study are included in a manuscript entitled "Bacterial endosymbionts interact with host sexuality and reveal reproductive genes of early divergent fungi" and submitted to *Nature Communications*

are unique among fungi in their ability to form highly coevolved associations with heritable bacterial endosymbionts (Bianciotto *et al.*, 1996, Partida-Martinez & Hertweck, 2005, Sato *et al.*, 2010). The impact of endobacteria on fungal biology, however, is poorly understood due to difficulty in cultivation and manipulation of one or both of the interacting partners (Olsson S., 2017). In this respect the symbiosis between the fungus *Rhizopus microsporus* (Mucoromycotina) and *Burkholderia* endobacteria (beta-proteobacteria) is a useful model due to ease of manipulation of both partners under laboratory conditions. *R. microsporus* is a saprotrophic fungus responsible for food spoilage, pathogenesis of plants (Noda *et al.*, 1980) and immune-compromised humans (Ibrahim *et al.*, 2011). Like other Mucorales, fungi in the genus *Rhizopus* are broadly utilized in industry for food fermentation, production of extracellular enzymes, organic acids and pharmaceuticals (Couto & Sanromán, 2006, Petrič *et al.*, 2010), as well as being a promising source of microbial oils for biodiesel production (Vorapreeda *et al.*, 2012). *Burkholderia* endobacteria reside directly in the fungal cytoplasm, and aid in the production of a toxin, rhizoxin, which facilitates *R. microsporus* pathogenesis of rice (Partida-Martinez & Hertweck, 2005). *Burkholderia* endobacteria have evolved full control over host asexual reproduction and are vertically transmitted in fungal sporangiospores (Partida-Martinez *et al.*, 2007). In contrast, interaction of the endobacteria with the sexual phase of the fungal life cycle is unknown. In Mucoromycotina, sexual reproduction involves the union of gametangia, leading to the formation of a zygospore inside a thick-walled zygosporangium (Blakeslee, 1904). In heterothallic species, such as *R. microsporus*, two compatible strains, sex (+) and sex (–), are required for mating to be successful.

Previous work by Mondo (Mondo, 2013) investigated the impact of endobacteria on fungal sexual reproduction by mating endobacteria-containing (B+) or cured (B–) isolates of *R. microsporus*. He found that elimination of endobacteria lead to complete loss of sexual reproduction and leveraged this into identifying fungal genes involved in mating. Specifically, abolishment of mating due to loss of endobacteria lead to significant downregulation of expression of fungal *ras2*, which encodes a small GTPase protein. Importantly, *ras2* was also

downregulated during vegetative growth in the absence of endobacteria, indicating that endobacteria control *ras2* expression.

Building upon the work of Mondo, I discovered that endobacterial control over fungal mating is, in fact, incomplete, and that elimination of endobacteria still allows for partial mating to occur. I confirmed that, analogously to when mating is entirely abolished partial mating was also marked by significant downregulation of *ras2*, verifying endobacterial control over its expression. Moreover, I showed that only ~40% of zygospores formed between B(+) mates inherited endobacteria, in contrast to 100% of sporangiospores harboring endobacteria. The low transmission rate of endobacteria in sexual zygospores is consistent with their incomplete control over this reproductive mode and indicates a relaxed evolutionary pressure for gaining full control. Lastly, I discovered that cAMP plays a role in *R. microsporus* mating interactions, and that increasing levels of exogenous cAMP inhibits zygospores formation. Interestingly, when endobacteria are present, this inhibition is less severe, indicating that endobacteria buffer the negative effects of cAMP on mating. Overall, this work contributed to our understanding of fungal-bacterial endosymbioses and uncovered novel aspects of sexual reproduction in an understudied group of early divergent fungi, the Mucoromycotina.

3.3 RESULTS

Loss of endobacteria reduced production of zygospores during *R. microsporus* mating.

Previous work by Mondo (Mondo, 2013) showed that mating between different compatible pairs of *R. microsporus* was completely abolished in the absence of endobacteria (Fig. 1A-B, E-F). During attempts to repeat this experiment, I discovered that there were cases when mating between cured (B-) isolates still occurred, but resulted in a significant reduction in zygospore formation, compared to (B+) isolates (P=0.0027) (Fig. 1C-D, G-H, Fig. 2). This partial loss of mating occurred irrespective of which isolates were used in mating, and instead seemed to depend on individual curing events. Importantly, isolates that exhibited partial loss of mating

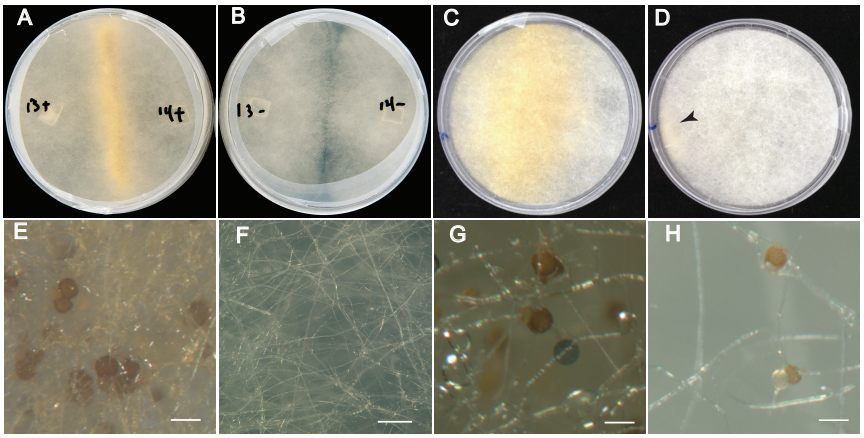

Figure 1. Impact of *Burkholderia* endobacteria on sexual reproduction of the *Rhizopus* host. Interactions between sex-compatible *Rhizopus* isolates: (A) successful mating between ATCC 52813 (13+) and ATCC 52814 (14+) harboring endobacteria, (B) complete loss of mating between ATCC 52813 (13–) and ATCC 52814 (14–) cured of endobacteria, (C) successful mating between ATCC 52813 and ATCC 52811 harboring endobacteria, (D) partial mating between ATCC 52813 and ATCC 52811 cured of endobacteria, with zygospores formed in the area indicated by an arrow, (E) and (G) accumulation of zygospores in the zone of interaction between endobacteria-harboring mates; scale bar 100 μm, (F) no sexual structures in the zone of interaction between mates cured of endobacteria that show complete loss of mating; scale bar 500 μm, (H) rare zygospores produced during an interaction between compatible mates cured of their endobacteria that results in partial mating; scale bar 100 μm.

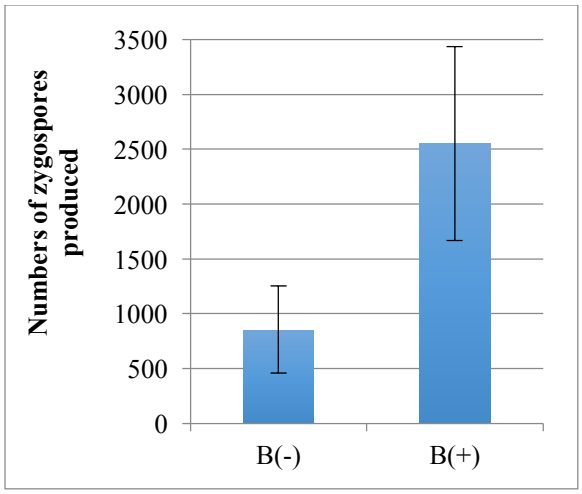

Figure 2. Removal of endobacteria from *R. microsporus* results in partial loss of mating. Bar graphs show numbers of zygospore produced during mating of cured (B-) or uncured (B+) isolates of *R. microsporus* ATCC 52813 and ATCC 52814. Error bars indicate 1 SD from mean of 6 biological replicates. The difference between numbers of zygospore was evaluated by a Student's t-test and was statistically significant (P=0.0027)

were still unable to reproduce asexually, confirming that loss of endobacteria completely abolishes fungal asexual reproduction.

Inheritance of endobacteria in *R. microsporus* zygospores. Endobacteria are faithfully transmitted in 100% of sporangiospores of *R. microsporus* (Partida-Martinez *et al*., 2007). To assess the rate of *Burkholderia* transmission during host sexual reproduction, we mated *Rm* isolates ATCC52813 and ATCC52814, which harbored endobacteria in their mycelium, and surveyed zygospores for bacterial presence by PCR targeting their 23S rRNA gene. We detected *Burkholderia* in 40% (± 6% SEM) of zygospores, suggesting that the rate of symbiont transmission through the sexual pathway is substantially lower than through the asexual pathway.

Endobacteria control expression of fungal *ras2*. Transcriptional profiling conducted by Mondo (Mondo, 2013) on B(+) and B(-) isolates of *R. microsporus* revealed significant downregulation in the absence of endobacteria of an ortholog of *ras2*, which encodes a small GTPase protein. Downregulation was evident in comparisons between B(+) and B(-) isolates grown vegetatively, and in comparisons of (B+) mating cultures to B(-) cultures which were unable to mate. This indicated that endobacteria control expression of fungal *ras2*, and that *ras2* is involved in mating.

In order to learn, whether partial loss of mating was also marked by downregulation of *ras2*, I conducted qPCR of B(+) and B(-) isolates of *R. microsporus* ATCC 52813 and ATCC 52811 during mating. I compared *ras2* expression between: (i) B(-) cultures exhibiting complete loss of mating, (ii) B(-) cultures exhibiting partial loss of mating, and (iii) B(+) successfully mating cultures. I found that *ras2* expression was significantly lower during interaction between B(-) isolates compared to B(+) ($P<0.001$ from post-hoc Student's t-test) (Fig. 3). Remarkably, the level of *ras2* expression did not differ between interactions exhibiting complete loss of mating versus partial loss of mating, a pattern consistent with incomplete control of mating by the endobacteria. Together these results corroborated findings that endobacteria control *ras2*

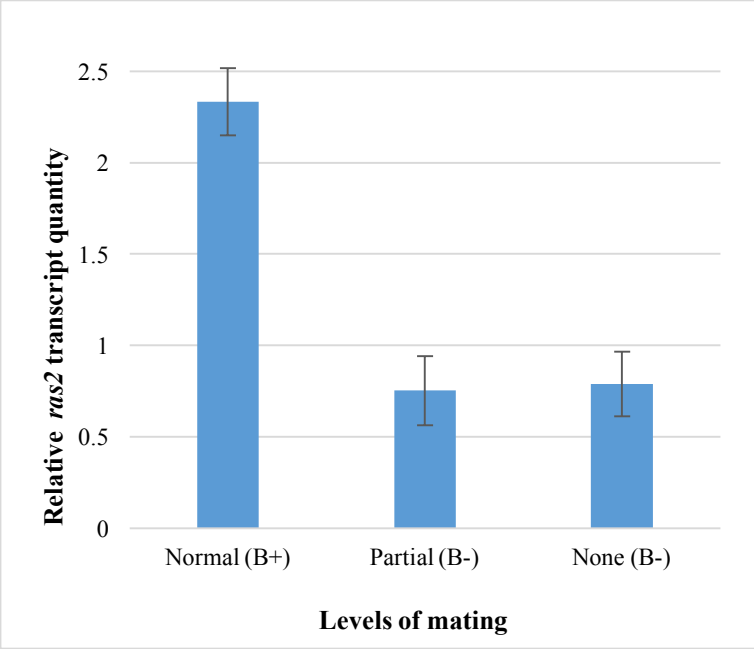

Figure 3. Expression levels of the *ras2* gene during mating between *R. microsporus* ATCC 52813 and ATCC 52811 exhibiting either normal mating levels, partial levels of mating, or complete loss of mating (none). B(+), endobacteria present; B(–), endobacteria absent; error bars represent 1 standard deviation from the mean.

expression. Furthermore, this indicates that being in control of *ras2* expression alone is not enough to gain full control over fungal sexual reproduction. By the same token, whereas *ras2* is clearly involved in *R. microsporus* mating, its role in mating is likely not solely regulated at the level of transcription.

Effects of cAMP on *R. microsporus* mating. Ras proteins serve as major signal transducers in eukaryotic cells and are known to regulate many processes in filamentous fungi including germination and growth, conidiation, stress response and mating (Fortwendel, 2015). In some fungi, such as *Ustilago maydis,* Ras2 interacts with the cyclic adenosine monophosphate (cAMP) signaling pathways and controls morphogenesis (Lee & Kronstad, 2002). cAMP is a secondary messenger that, in coordination with the pheromone MAP kinase cascade, regulates sexual development in many fungi, albeit often with contrasting effects (D'Souza & Heitman, 2001). Consequently, I explored the impact of exogenous cAMP on *R. microsporus* mating by exposing B(+) and (B-) mates to 0 mM, 1 mM, and 2 mM of di-butyryl cAMP. I found that increased concentrations of cAMP significantly reduced the rate of zygospore formation in the interactions between the B(-) mates that were capable of partial mating, whereas the decrease in zygospores formation in interactions between B(+) mates was not statistically significant (Fig. 4). These results suggest that: (1) elevated levels of cAMP interfere with mating in *R. microsporus*, and (2) endosymbiont presence buffers the negative effects of high cAMP levels on sexual reproduction.

3.4 DISCUSSION

Rhizopus microsporus is highly dependent for survival on the *Burkholderia* endobacteria. Although the fungus can grow vegetatively in the absence of endosymbionts, it is unable to reproduce asexually (Partida-Martinez & Hertweck, 2005) and its ability to reproduce sexually is severely restricted. The *Burkholderia* endosymbionts are, therefore, important to the host's

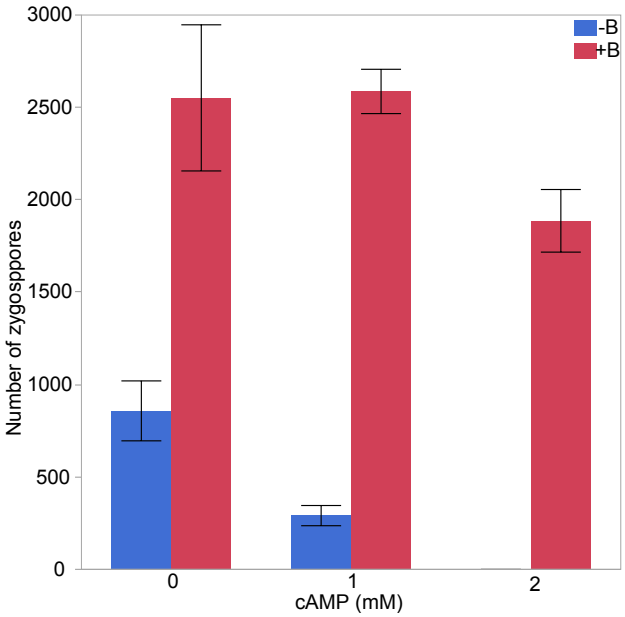

Figure 4. Increased levels of exogenous cAMP reduce the rate of zygospore production in B(-) but not B(+) mating isolates. (-B) mating between cured isolates, (+B) mating between uncured isolates. Error bars represent 1 SE from the mean.

survival because they have hijacked an indispensable component of the host's developmental machinery. In particular, together with Mondo, we have shown that these endosymbionts strongly impact expression of *ras2*, encoding a G-protein responsible for controlling the reproductive development in Dikarya (Kana-uchi *et al.*, 1997, Lee & Kronstad, 2002).

Sexual and asexual forms of reproduction play distinct roles in the life history of fungi. In Mucorales, asexual spores are produced continuously throughout colony growth under favorable environmental conditions, and are capable of rapid germination (Alexopoulos *et al.*, 1996). Aerial dissemination of these spores facilitates colonization of new habitats. Sexual reproduction, on the other hand, typically occurs at the end of the growing season or when colony growth is restricted by harsh environmental conditions (Aanen & Hoekstra, 2007), and, in heterothallic taxa, requires the presence of a compatible strain of the opposite mating type (Alexopoulos *et al.*, 1996). Sexually produced zygospores are dormant survival structures capable of withstanding harsh environmental conditions (Kirk *et al.*, 2001). For the vertically transmitted bacterial endosymbionts, it is advantageous to gain control over both kinds of fungal reproduction to facilitate their own propagation and survival under variable environmental conditions. In this way, when growth conditions are favorable, dissemination through asexual spores would facilitate colonization of new habitats. With growth conditions worsening, transmission through sexual zygospores becomes more important, allowing long-term survival for both partners and preserving the bacterial-fungal symbiosis.

In this study, I showed that unlike the endosymbiont control over fungal asexual reproduction, their control over sexual reproduction is incomplete. Incomplete control is evidenced by partial loss in ability to form zygospores when endobacteria are removed, as well as low vertical transmission rate of endobacteria in sexual zygospores compared to asexual sporangiospores. The differential endobacterial control over fungal sexual and asexual reproductive modes could be explained by the environmental conditions in which the *Rhizopus-Burkholderia* symbiosis might have evolved. If, for example, the *R. microsporus* environment was stable or if there was an imbalance of mating type frequencies, endosymbionts could gain stronger control over

asexual reproduction, which is expected to be the dominant reproduction mode under those conditions. Gaining control over sexual reproduction in such environments would be under weaker selective pressure, and might explain incomplete endobacterial control over sexual reproduction. In reality, little is known about the ecology of *R. microsporus* and other Mucorales (Richardson, 2009) and additional work is needed to confirm this hypothesis.

Consistent with Mondo's findings that Ras2 is involved in mating of *R. microsporus* and that its expression is controlled by the endobacteria, I found that *ras2* is downregulated in mating interactions between B(-) isolates, compared to B(+), regardless of whether zygospores are produced. Ras2 is therefore clearly involved in mating of *R. microsporu*s (Mondo, 2013). However, fungal ability to form small numbers of zygospores under reduced levels of *ras2* expression indicates that Ras2 activity is not exclusively controlled at the level of transcription, but likely at multiple levels including GTP activation and localization (Fortwendel, 2015).

Given the role of Ras2 in mediation of the cAMP signaling cascade (Gold *et al.*, 1994), it was plausible that cAMP plays a role in mating interactions of *R. microsporus*. Indeed, we found that application of increasing levels of exogenous cAMP significantly reduced the rate of zygospores production, indicating that cAMP acts as a negative regulator of mating in these fungi. This is consistent with what has been shown in other fungi, for example, in *Mucor mucedo* (Jones & Bu'Lock, 1977) and *Schizosaccharomyces pombe* (Mochizuki & Yamamoto, 1992), sexual reproduction is inhibited by elevated levels of cAMP. Interestingly, this pattern is not universal among fungi and cAMP can trigger mating in *Ustilago maydis* (Gold *et al.*, 1994). Importantly, the negative effects of cAMP on the rate of zygospores production in *R. microsporus* were buffered by the presence of bacteria, whereby increasing cAMP levels did not significantly reduce mating in B(+) isolates.

Altogether, these findings provide new insights into how sexual reproduction is controlled in *R. microsporus* and the role that bacterial endosymbionts play in the biology of their fungal host.

3.5 MATERIALS & METHODS

Strains, culture conditions, and removal of endobacteria. *R. microsporus* was cultivated on half-strength (1/2) potato dextrose agar (PDA, Sigma). Plates were sealed with Parafilm® M (Pechiney Plastic Packaging Company, Chicago, Il), unless otherwise noted. Fungi were cured of the *Burkholderia* endobacteria as described in Partida-Martinez & Hertweck (2005). Absence of endosymbionts was confirmed by PCR using *Burkholderia*-specific primers (Mondo *et al.*, 2012).

Extraction, cultivation, and reintroduction of endobacteria. Young fungal mycelium (1-2 days old) containing endosymbionts was finely chopped in 500 µL Luria-Bertani (LB) broth, and pressed gently to ensure that cellular contents were released into the broth. The broth was then filtered twice through a 2 µm filter to remove fungal debris. Filtrate was added to LB plates containing 1% v/v glycerol and incubated at 30°C. For reinfection of fungal hosts with endobacteria, a plug of agar was removed from 1/2 PDA using the upper end of a P-1000 pipette tip and replaced with a plug of LB agar. Bacterial inoculum was then placed on the LB agar plug, and a plug containing cured fungus was positioned nearby on the plate.

Fungal mating interactions. *R. microsporus* compatible mates ATCC 52813 (mating type +) and ATCC 52814 (mating type –) as well as ATCC 52813 (+) and ATCC 52811 (–) were examined for the success of mating with (B+) or without (B–) endobacteria present. 1/2 PDA, contained in 100 mm × 15 mm petri plates, was used for all mating experiments. Compatible mates were placed at the edges of the plate, allowing fungi to grow towards each other and develop an interaction zone in the center of the plate. Fungal cultures were incubated in the dark at 30°C. Each interaction was examined in 6-10 replicates.

Detection of endobacteria in *Rhizopus* zygospores. Mating interactions between *R. microsporus* ATCC 52813 and ATCC 52814 were set up on PDA (Sigma), zygospores were analyzed after 7 days incubation in the dark at 30°C. A tuft of mycelium containing zygospores was removed from the mating zone and placed into 10% w/v chloramine-T (Sigma) for 20 min to

kill hyphae. The tuft was subsequently transferred into sterile water and shaken slowly for 5 min. Two additional water transfers were performed in the same way with shaking, last shaking was done for 20 min to ensure removal of all traces of chloroamine-T. Mycelial tuft was then transferred onto a sterile 1.5% water agar petri plate and zygospores were dissected out from the surrounding hyphae using sterile forceps, taking care to remove all attached hyphae. A total of 80 zygospores from 2 separate mating plates were transferred into 0.2 mL PCR tubes (1 per tube), crushed with sterile forceps and subjected to whole-genome amplification using the Illustra Genomiphi Kit (GE) following manufacturer's instructions. 1 µl from the last water wash was used as a negative control during whole genome amplification and subsequent PCR, a total of 16 such negative controls were performed. PCR was performed on the 1/20 diluted whole-genome amplified products using LR1 and NDL22 (van Tuinen *et al.*, 1998) as well as *Burkholderia*-specific primers (Mondo *et al.*, 2012) to detect presence of fungal and bacterial DNA in zygospores.

Exogenous cAMP application during mating. Interactions between B(+) and B(-) compatible mates *R. microsporus* ATCC 52813 and ATCC 52811 were examined on 1/2 PDA amended with 0 mM, 1 mM, 2 mM di-butyryl cAMP (Enzo Life Sciences). 10 plates were mated per condition, and incubated in the dark at 30°C for 10 days, after which zygospores were counted.

3.6 REFERENCES

Aanen DK & Hoekstra RF (2007) Why Sex Is Good: On Fungi and Beyond. *Sex in Fungi: Molecular Determination and Evolutionary Implications* 527-534.

Alexopoulos CJ, Mims CW, Blackwell M, Alexopoulos CJ, Mims CW & Blackwell M (1996) *Introductory mycology, Fourth edition*. John Wiley and Sons, Inc., 605 Third Avenue, New York, New York 10158-0012, USA; John Wiley and Sons Ltd., Baffin Lane, Chichester PO 19 1UD, England.

Bianciotto V, Bandi C, Minerdi D, Sironi M, Tichy HV & Bonfante P (1996) An obligately endosymbiotic mycorrhizal fungus itself harbors obligately intracellular bacteria. *Appl Environ Microb* **62**: 3005-3010.

Blakeslee AF (1904) Sexual reproduction in the Mucorineae. *Proceedings of the American Academy of Arts and Sciences* **40**: 205-319.

Couto SR & Sanromán MÁ (2006) Application of solid-state fermentation to food industry—A review. *Journal of Food Engineering* **76**: 291-302.

D'Souza CA & Heitman J (2001) Conserved cAMP signaling cascades regulate fungal development and virulence. *FEMS Microbiology Reviews* **25**: 349-364.

Fortwendel JR (2015) Orchestration of Morphogenesis in Filamentous Fungi: Conserved Roles for Ras Signaling Networks. *Fungal Biol Rev* **29**: 54-62.

Gold S, Duncan G, Barrett K & Kronstad J (1994) cAMP regulates morphogenesis in the fungal pathogen *Ustilago maydis*. *Genes & Development* **8**: 2805-2816.

Ibrahim AS, Edwards JEJ, Filler SG & Spellberg B (2011) Mucormycosis and entomophthoramycosis (zygomycosis). *Essentials of Clinical Mycology,*(Kauffman CA, Pappas PG, Sobel JD & Dismukes WE, eds.), p.^pp. 265-280. Springer, New York.

Jones BE & Bu'Lock JD (1977) The effect of $N^6,O^{2'}$-dibutyryl adenosine-3',5'-cyclic monophosphate on morphogenesis in Mucorales. *Journal of General Microbiology* **103**: 29-36.

Kana-uchi A, Yamashiro CT, Tanabe S & Murayama T (1997) A *ras* homologue of *Neurospora crassa* regulates morphology. *Molecular & General Genetics* **254**: 427-432.

Kirk PM, Cannon PF, David JC & Stalpers JA (2001) *Ainsworth and Bisby's dictionary of the fungi: 9th edition*. CABI Publishing, Wallingford, UK.

Lee N & Kronstad JW (2002) *ras2* controls morphogenesis, pheromone response, and pathogenicity in the fungal pathogen *Ustilago maydis*. *Eukaryot Cell* **1**: 954-966.

Lee N & Kronstad JW (2002) ras2 Controls morphogenesis, pheromone response, and pathogenicity in the fungal pathogen Ustilago maydis. *Eukaryotic cell* **1**: 954-966.

Mochizuki N & Yamamoto M (1992) Reduction in the intracellular cAMP level triggers initiation of sexual development in fission yeast. *Molecular & General Genetics* **233**: 17-24.

Mondo SJ (2013) Evolutionary Stability of Fungal-Bacterial Endosymbioses. PhD Dissertation Thesis, Cornell University, Ithaca, NY.

Mondo SJ, Toomer KH, Morton JB, Lekberg Y & Pawlowska TE (2012) Evolutionary stability in a 400-million-year-old heritable facultative mutualism. *Evolution* **66**: 2564-2576.

Noda T, Hashiba T & Sato Z (1980) The structural changes in young swollen roots of rice seedlings infected with *Rhizopus chinensis* Saito. *Annals of the Phytopathological Society of Japan* **46**: 40-45.

Olsson S. BP, Pawlowska T.E. (2017) Ecology and evolution of fungal-bacterial interactions *The Fungal Community: its Organization and Role in the Ecosystem,*p.^pp. 563-583. Taylor & Francis, In Press.

Partida-Martinez LP & Hertweck C (2005) Pathogenic fungus harbours endosymbiotic bacteria for toxin production. *Nature* **437**: 884-888.

Partida-Martinez LP, Monajembashi S, Greulich KO & Hertweck C (2007) Endosymbiont-dependent host reproduction maintains bacterial-fungal mutualism. *Curr Biol* **17**: 773-777.
Petrič Š, Hakki T, Bernhardt R, Žigon D & Črešnar B (2010) Discovery of a steroid 11α-hydroxylase from Rhizopus oryzae and its biotechnological application. *Journal of Biotechnology* **150**: 428-437.

Richardson M (2009) The ecology of the Zygomycetes and its impact on environmental exposure. *Clin Microbiol Infect* **15 Suppl 5**: 2-9.

Sato Y, Narisawa K, Tsuruta K, Umezu M, Nishizawa T, Tanaka K, Yamaguchi K, Komatsuzaki M & Ohta H (2010) Detection of Betaproteobacteria inside the Mycelium of the Fungus Mortierella elongata. *Microbes and Environments* **25**: 321-324.

van Tuinen D, Jacquot E, Zhao B, Gollotte A & Gianinazzi-Pearson V (1998) Characterization of root colonization profiles by a microcosm community of arbuscular mycorrhizal fungi using 25S rDNA-targeted nested PCR. *Molecular ecology* **7**: 879-887.

Vorapreeda T, Thammarongtham C, Cheevadhanarak S & Laoteng K (2012) Alternative routes of acetyl-CoA synthesis identified by comparative genomic analysis: involvement in the lipid production of oleaginous yeast and fungi. *Microbiology* **158**: 217-228.

CHAPTER 4

DISTRIBUTION AND POPULATION STRUCTURE OF ENODBACTERIA IN A NATURAL POPULATION OF ARBUSCULAR MYCORRHIZAL FUNGI[3]

4.1 ABSTRACT

Arbuscular mycorrhizal fungi (AMF, Mucoromycota, Glomeromycotina) form symbioses with the majority of terrestrial plants and provide their hosts with mineral nutrients in exchange for photosynthetic carbon. While AMF have long been known to harbor vertically transmitted endosymbiotic bacteria (EB) '*Candidatus* Glomeribacter gigasporarum' (*Ca*Gg, beta-proteobacteria) and '*Candidatus* Moeniiplasma glomeromycotorum' (*Ca*Mg, Mollicutes), the interactions between AMF and their EB have not been studied in nature. We examined diversity and distribution of EB associated with AMF in dunes at Cape Cod National Seashore. *Ca*Gg is a nonessential mutualist of AMF, whereas the lifestyle of *Ca*Mg is unknown. Of nearly 500 AMF isolates examined, 2% harbored *Ca*Gg and 88% *Ca*Mg. *Ca*Gg was only found in the Gigasporaceae, whereas *Ca*Mg was present across all families of dune AMF. Distribution of both EB across AMF was affected significantly by soil calcium levels, which likely relates to the effect of calcium on the host plant. Distance from the beach, AMF genotype, soil pH, and *A. breveligulata* dominance impacted incidence of *Ca*Mg but not of *Ca*Gg. *Ca*Mg populations associated with individual AMF isolates displayed high levels of genetic diversity but no evidence of gene flow across different AMF hosts, suggesting that host physical proximity is not sufficient to facilitate horizontal transmission of *Ca*Mg. Lastly, Cape Cod AMF harbor a novel clade of *Ca*Gg as well as previously unreported group of EB that are closely related to *Burkholderia* endosymbionts of other Mucoromycota fungi.

[3] The results of this study will be submitted to *ISME J*, and is written according to their manuscript guidelines.

4.2 INTRODUCTION

Arbuscular mycorrhizal fungi, AMF (Mucoromycota, Glomeromycotina) form mutualistic associations with roots of majority of terrestrial plants (Smith & Read, 2008). They provision plants with mineral nutrients, such as phosphorus and nitrogen, in exchange for photosynthesis-derived carbon (Smith & Read, 2008). Consequently, AMF play important roles in functioning of terrestrial ecosystems and global nutrient cycling, and are of rising interest in sustainable agriculture as alternatives to non-renewable mineral fertilizers (Gianinazzi *et al.*, 2010, Weber, 2014).

For decades, AMF were known to harbor morphologically diverse endosymbiotic bacteria (EB) in their hyphae and spores (Mosse, 1970). '*Candidatus* Glomeribacter gigasporarum' (*Ca*Gg, beta-proteobacteria) is the most extensively studied EB of AMF (Bianciotto *et al.*, 2003). *Ca*Gg resides in fungus-derived vesicles inside hyphae and spores of AMF in the family Gigasporaceae. AMF spores that harbor *Ca*Gg produce longer pre-symbiotic hyphae than those that are *Ca*Gg-free (Lumini *et al.*, 2007), a phenomenon attributed to the ability of *Ca*Gg to prime the energy metabolism of the fungus (Salvioli *et al.*, 2016). Despite the ancient origin of the *Ca*Gg-Gigasporaceae association, *Ca*Gg remains nonessential to its AMF host, and the symbiosis does not appear to be in transition towards a reciprocally obligate state (Mondo *et al.*, 2012), as is expected in facultative associations where endosymbionts are vertically transmitted within host populations (Yamamura, 1993). *Ca*Gg is nutritionally dependent on its host (Ghignone *et al.*, 2012), and therefore exerts a carbon cost. Stability of the *Ca*Gg-Gigasporaceae association in its current non-reciprocally obligate form was thus hypothesized to be the result of shifting environmental conditions, whereby only certain environments, likely requiring extensive presymbiotic hyphal proliferation to contact the plant host, would favor *Ca*Gg in AMF (Mondo *et al.*, 2012). However, the exact conditions that favor *Ca*Gg incidence is AMF are unknown due to lack of ecological studies.

In addition to *Ca*Gg, AMF harbor another EB of unknown lifestyle, recently identified as a member of the *Mollicutes* class, '*Candidatus* Moeniiplasma glomeromycotorum' (*Ca*Mg)

(Naumann *et al.*, 2010, Naito *et al.*, 2017). Importantly, *Ca*Gg and *Ca*Mg can co-exist and form an intracellular 'microbiome' of AMF (Desiro *et al.*, 2014). Like *Ca*Gg, *Ca*Mg is vertically transmitted in fungal spores (Naito, 2014). However in contrast to *Ca*Gg, which has only been found in the family Gigasporaceae, *Ca*Mg is widely distributed among phylogenetically distinct AMF lineages (Naumann *et al.*, 2010, Desiro *et al.*, 2014, Toomer *et al.*, 2015). Populations of *Ca*Mg in AMF isolates/spores/operational individuals exhibit unexpected genetic diversity, and can harbor a collection of *Ca*Mg genotypes (Desiro *et al.*, 2014, Naito, 2014, Toomer *et al.*, 2015). Based on genomic and molecular evolution analyses, this genetic diversity is thought to be the result of recombination and symbiont horizontal transmission (Naito *et al.*, 2015, Toomer *et al.*, 2015).

Our knowledge of the biology of AMF-associated EB, their population structure, and distribution across hosts comes exclusively from analyses of culture collection-derived isolates, and nothing is known about these EB in natural populations of AMF. In the present study, we set out to analyze the natural distribution of *Ca*Gg and *Ca*Mg in AMF in the North Atlantic dune environment with a particular focus on: (**1**) understanding incidence of EB in AMF in nature, (**2**) identifying environmental factors that favor the association between AMF and EB, and (**3**) assessing diversity of *Ca*Gg and *Ca*Mg. The North Atlantic dune ecosystem is perfectly suited for addressing these questions. To link incidence of EB with specific AMF genotypes and to quantify their occurrence within AMF, we chose to work with AMF spores instead of plant roots. The sandy dune soils permit easy isolation of AMF spores directly from field samples without the need for enrichment in pot cultures (Koske & Halvorson, 1981). Moreover, the North Atlantic dune ecosystem is dominated by a single plant species, American beachgrass (*Ammophila breveligulata*), which reduces the impact of plant community structure on AMF. Lastly, steep environmental gradients that extend from the ocean inland, allow for analyses of environmental impacts on AMF and their associated EB at conveniently small spatial scales.

We found that *Ca*Gg and *Ca*Mg differed in their distribution patterns across dune AMF. *Ca*Gg was found in 2% of AMF isolates, whereas *Ca*Mg was detected in 88% of all surveyed spores.

*Ca*Gg was associated exclusively with *Gigaspora,* whereas *Ca*Mg was found in all genera of dune AMF. Soil calcium levels significantly affected distribution of both *Ca*Gg and *Ca*Mg, with the decrease in soil calcium levels amplifying the probability of EB incidence in AMF. In addition, distribution of *Ca*Mg was affected by distance from the beach, AMF genotype, and *A. breveligulata* dominance. As in previous studies, high levels of diversity were apparent within *Ca*Mg populations associated with individual AMF isolates. The lack of evidence of gene flow between *Ca*Mg from different AMF hosts suggested that host physical proximity is not sufficient for horizontal transmission of *Ca*Mg. Cape Cod genotypes of *Ca*Gg were distinct from those reported before. Additionally, in *Gigaspora* and *Acaulospora,* we discovered EB previously not known to associate with Glomeromycotina. These *Burkholderia*-related endobacteria (BRE) are closely related to EB of other Mucoromycota fungi.

4.3 RESULTS

We collected soil samples from the rhizosphere of *A. breveligulata* in the grassland dunes of the Province Lands area at Cape Cod National Seashore in early November 2013 (Fig. S1). Samples were collected every 10 m along four 100 m long transects extending from the coastal bluff (henceforth referred to as 'beach') inland, in the direction perpendicular to the ocean (Fig. S1). This sampling scheme was designed to capture the environmental gradients that occur in the sand dune ecosystem. Typically, salinity and environmental disturbances, such as wind and substrate mobility decrease inland from the ocean, whereas biotic pressures increase (Hesp & Martínez, 2007). As a consequence, AMF collected closer to the ocean were expected to be exposed to higher abiotic pressure and disturbances, whereas those collected further away form the ocean were likely to experience less disturbance and lower abiotic pressure. Spores of AMF were isolated from each sample and genotyped by PCR followed by sequencing of the 28S rRNA gene (van Tuinen *et al.*, 1998). Each spore was surveyed for incidence of *Ca*Gg and *Ca*Mg using *Burkholderia*- and *Ca*Mg-specific PCR primers (Naumann *et al.*, 2010, Mondo *et al.*, 2012). To assess the influence of environmental factors on EB distribution, we measured along each

transect distance from the beach, soil pH, salinity, plant density, and the level of dominance of *A. breviligulata* over other plant species.

Environmental parameters varied along the distance from beach. The pH of soil ranged from 5.5 to 7.5, with the average of 6.21. These values are consistent with what has been previously reported by the National Park Service (Smith, 2006). Soil pH did not depend on distance from the beach. Soil salinity, measured as soluble salts (conductivity, mmhos/cm) declined with increasing distance from the beach (P=0.03, r^2=0.37), as did the sodium (P=0.01, r^2=0.45) and calcium (P=0.001, r^2=0.65) ion concentrations. These patterns were largely expected, because the dune environment is typically characterized by decreasing levels of soil salinity with increasing distance from the shore due to decreased exposure to sea spray (Hesp & Martínez, 2007).

Plant density was measured in two ways: (1) total number of plants in a 70 cm radius from the sampling point, and (2) average nearest neighbor distance (NND, distance to nearest plant from the sampling point). Total plant number was inversely proportional to average NND, *i.e.* as the number of plants at a sampling point increased, distance between them decreased (P<0.001, R^2=0.75, Fig. 1a). Because total number of plants and average distance between them were so tightly correlated, we focused on total plant number as the measure of plant density. We found that plant density decreased slightly with increasing distance from the beach (P<0.001, R^2=0.04, Fig. 1b), and that dominance of *A. breviligulata* also declined with increasing distance from the beach (P<0.001, R^2=0.1, Fig. 1c). Moreover, plant density showed a weak positive correlation with soil calcium levels (P= 0.046, r^2=0.05).

Collectively, these patterns reflect gradients in abiotic and biotic conditions expected to occur in the sand dune environment with the increasing distance from the beach.

Characterization of the AMF community. Based on the sequence of the 28S rRNA gene, we identified 23 AMF operational taxonomic units (OTUs) in a total of 499 isolates/spores that

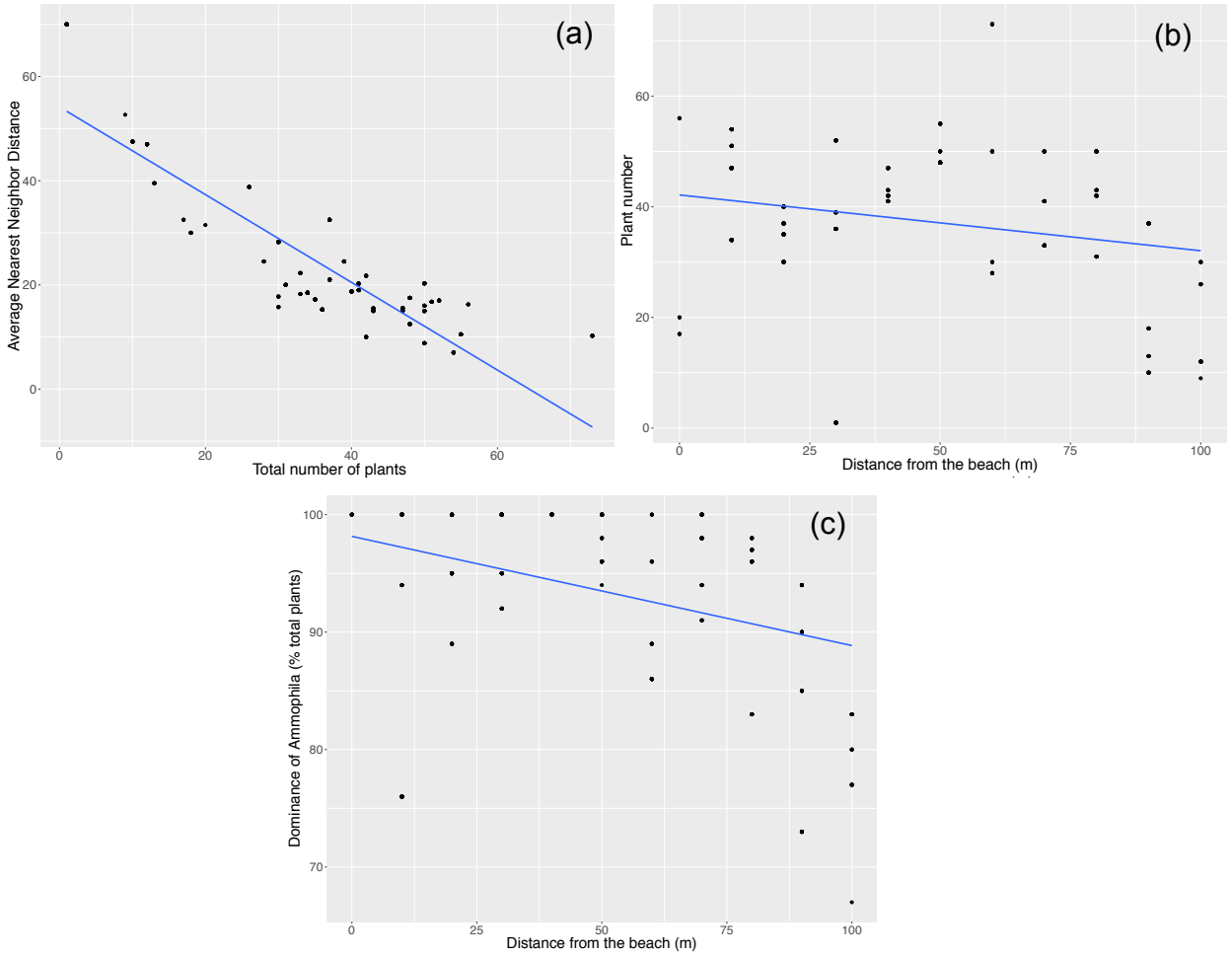

Figure 1. Vegetation characteristics at the Cape Cod National Seashore study site. (A) Relationship between Average NND and total number of plants in a 70 cm radius from the sampling point. (B) Relationship between plant number and distance from the beach. (C) Relationship between dominance of *A. breviligulata* and distance from the beach. Line represents linear regression analysis.

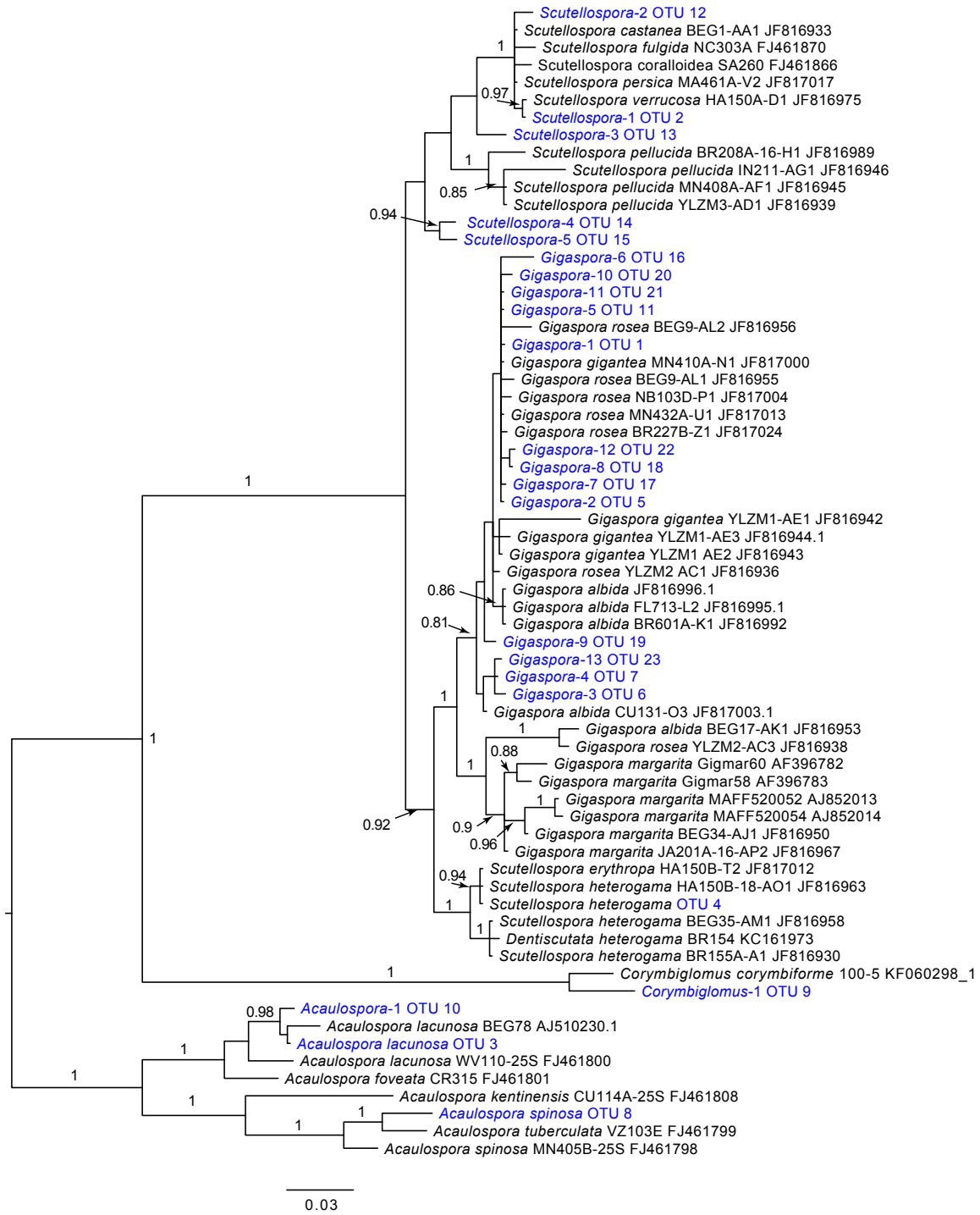

Figure 2. AMF phylogeny based on the 28S rRNA gene sequence. Taxa in bold are representatives of Cape Cod OTUs grouped at 95% sequence similarity; the remaining are reference taxa. Numbers above branches are Bayesian posterior probability values, values above 0.8 are displayed.

could be genotyped, and represented ~48% of all spores sampled. These OTUs belonged to 4 genera: *Gigaspora, Scutellospora, Acaulospora* and *Corymbiglomus*, with the majority of the recovered spores representing the genus *Gigaspora,* and clustering with *Gigaspora albida, Gi. gigantea*, and *Gi. rosea* (Fig. 2, Table S1). Overall, the AMF community was dominated by a few very abundant OTUs (OTU1 to OTU5), and the remainder of the diversity was made up of rare OTUs that were recovered only once (Fig. S2). At the edge of the vegetation line (0 m away from the beach), AMF spores were sparse, and the ones that were isolated oftentimes failed to yield PCR amplicons of an AMF 28S rRNA gene sequence. As a result, there was a low number of AMF sequences obtained at 0 m away from the beach. *Gigaspora* dominated the AMF community at all sampling points except at 0 and 70 m that were dominated by *Acaulospora*. In general, *Gigaspora* spores were more abundant at distances closer to the beach, and *Scutellospora* spores increased in abundance after 20 m (Fig. 3).

Influence of environmental factors on EB incidence in AMF. We surveyed all AMF spores for incidence of the two types of EB known to inhabit Glomeromycotina, *Ca*Gg and *Ca*Mg. Abundance of *Ca*Gg in AMF spores was very low, with only 2% of all spores harboring it. *Ca*Mg, on the other hand, was very abundant and found in 88% of all spores. Consistent with previous reports (Bianciotto *et al.*, 2003, Mondo *et al.*, 2012), *Ca*Gg was only detected in AMF spores belonging to the family Gigasporaceae, whereas *Ca*Mg was also found in representatives of *Acaulospora* and *Corymbiglomus*. Remarkably, all spores that harbored *Ca*Gg also harbored CaMg, which was not always the case in AMF surveyed from culture collections (Desiro *et al.*, 2014).

To assess the effects of environmental parameters on the distribution of *Ca*Gg and *Ca*Mg, we used generalized linear mixed models with the four sampling transects as replicates. We performed these analyses separately across all AMF OTUs, and then within individual AMF OTUs, focusing on distance from the beach, soil parameters, plant density and *A. breviligulata* dominance.

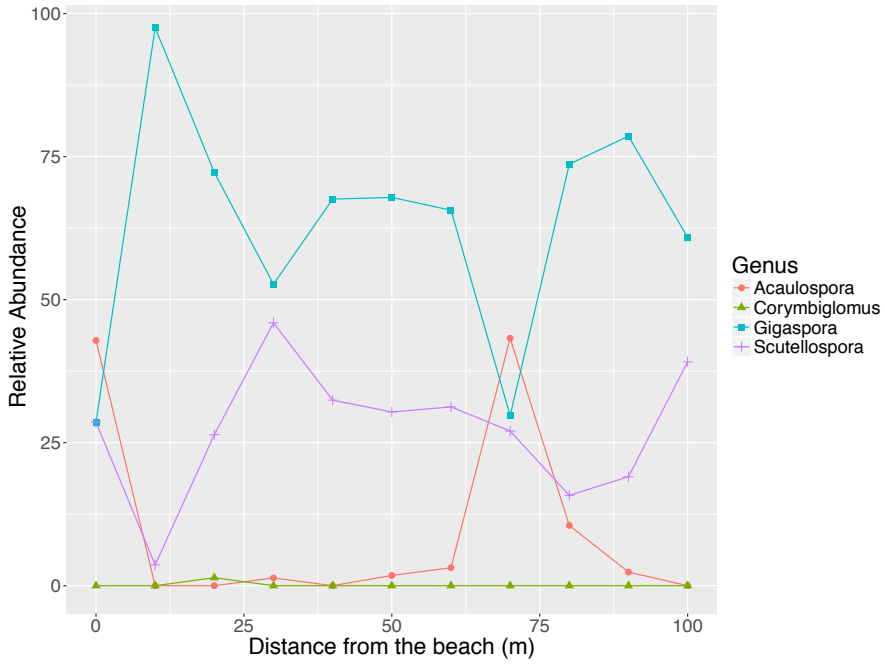

Figure 3. Relative abundance of the four AMF genera recovered from Cape Cod dunes at varying distances form the beach.

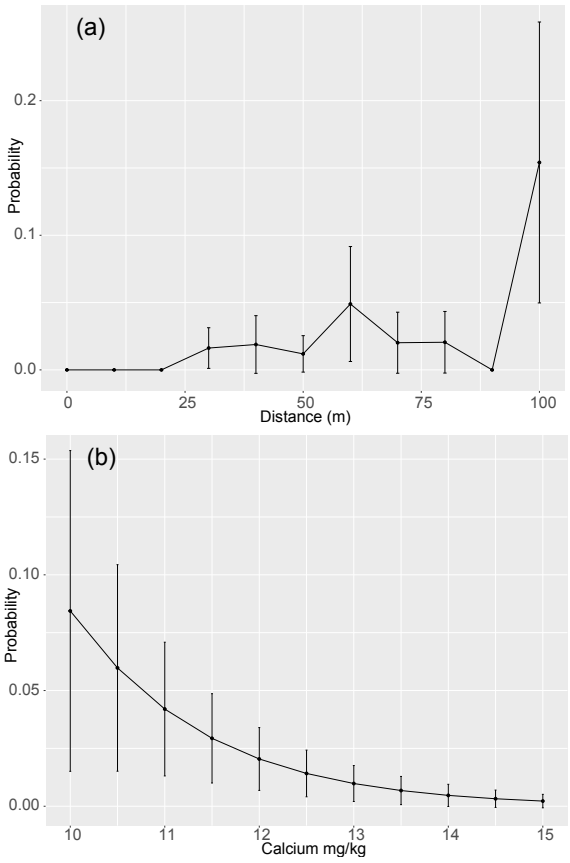

Figure 4. Distribution of *Ca*Gg at Cape Cod dunes. (A) Probability of *Ca*Gg incidence across all AMF at different distances from the beach. (B) Probability of harboring *Ca*Gg by AMF OTU1 (*Gigaspora*-1) at different soil calcium levels. Error bars represent 1 SEM.

Distance from the beach explained some of the variation in the distribution of *Ca*Gg in AMF (*P*=0.045, Fig. 4a). However, comparison of the probabilities of finding *Ca*Gg at various distances did not reveal any significant difference among them. In particular, the probability of harboring *Ca*Gg by AMF increased at 100 m from the beach, although that increase was not statistically significant. No other environmental parameters affected *Ca*Gg distribution across all AMF spores. However, when we looked at *Ca*Gg distribution in *Gigaspora-1*, where it was mostly found, its incidence was significantly affected by soil calcium levels (*P*<0.04), increasing under lower calcium ion concentrations (Fig. 4b).

When analyzed across all AMF isolates, distance from the beach had a significant effect on *Ca*Mg distribution (*P*<0.001). Specifically, *Ca*Mg was more likely to be found at distances of 10 to 50 m and 80 to 100 m from the beach, and its incidence at 0 m and 60 to 70 m was less likely (Fig. 5a). In addition, *Ca*Mg incidence was negatively affected by *A. breviligulata* dominance (*P*=0.015), *i.e. Ca*Mg was more likely to be found in spores isolated from samples with fewer *A. breviligulata* tillers relative to other plant species (Fig. 5c). Lastly, *Ca*Mg was negatively affected by soil calcium ion concentrations(*P*<0.01), whereby its incidence was more likely under lower soil calcium levels (Fig. 5b).

*Ca*Mg distribution varied significantly among the different AMF OTUs. *Ca*Mg was abundant in spores of *Gigaspora*-1, *Scutellospora*-1, and *S. heterogama* (>83%), and found in less than half of spores of *A. lacunosa* (Fig. S3). This difference, however, was only apparent closer to the beach and disappeared further away form the beach becoming no longer statistically significant at 90 m (Table S2). Because incidence of *Ca*Mg varied between the AMF OTUs, we modeled the effect of environmental parameters on *Ca*Mg incidence in the 3 most abundant AMF OTUs: *Gigaspora-1* (OTU1), *Scutellospora-1* (OTU2), *Acaulospora lacunosa* (OTU3). The remaining AMF OTUs were recovered in such low abundance that it was not possible to perform these analyses. We found that in *Gigaspora-1*, *Ca*Mg distribution was significantly affected by distance from the beach (*P*<0.001, Fig. 6a), calcium ion concentrations (*P*<0.01, Fig. 6b) and pH

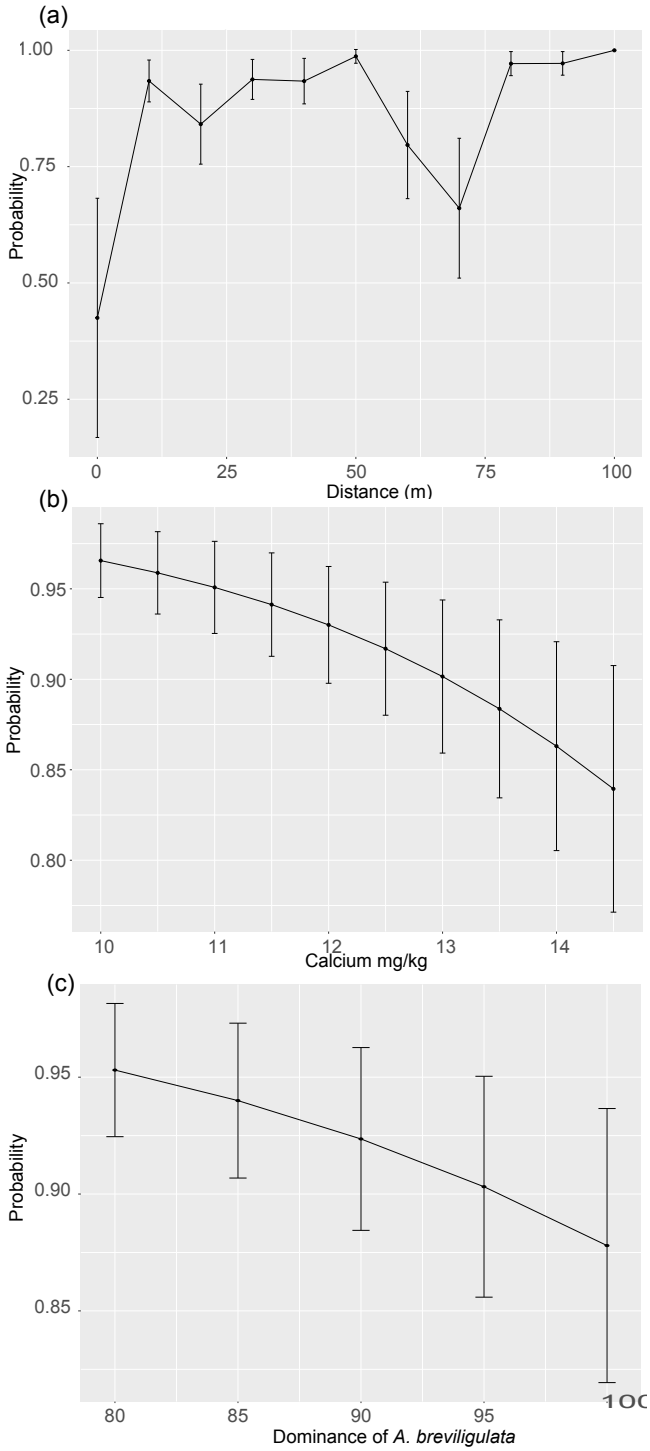

Figure 5. Probability of harboring *Ca*Mg by all AMF at different distances from the beach (A), and different soil calcium levels (B) and at different levels of *A. breviligulata* dominance (C). Error bars represent 1 SE of the mean.

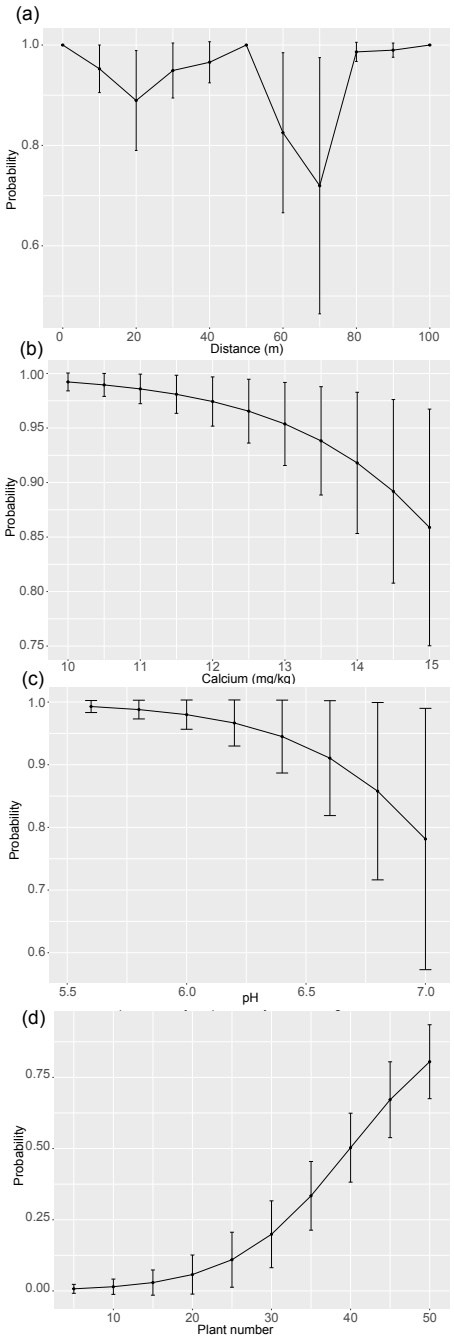

Figure 6. Distribution of *Ca*Mg in individual AMF. (A) Probability of OTU1 (*Gigaspora*-1) harboring *Ca*Mg at different distances from the beach (B) Probability of OTU1 (*Gigaspora*-1) harboring *Ca*Mg at different soil calcium concentrations. (C) Probability of OTU1 (*Gigaspora*-1) harboring *Ca*Mg at different soil pH values. (D) Probability of OTU3 (*A. lacunosa*) harboring *Ca*Mg at different plant density. Error bars represent 1 SE of the mean.

of the soil (P<0.02, Fig. 6c). In *Scutellospora-1*, none of the environmental variables affected *Ca*Mg, whereas *Ca*Mg incidence in *A. lacunosa*, correlated with plant density (P=0.02, Fig. 6d).

Analysis of *Ca*Gg diversity at Cape Cod reveals previously uncharacterized EB in AMF. To date, our knowledge of *Ca*Gg and *Ca*Mg population structure comes from analyses of culture collection isolates of AMF (Mondo *et al*., 2012, Desiro *et al*., 2014, Naito *et al*., 2015, Toomer *et al*., 2015, Mondo *et al*., 2016), and little is known about these EB in nature. Using 23S rRNA gene sequences PCR amplified with *Burkholderia*-specific primers, we reconstructed a phylogeny of *Ca*Gg detected by our structured sampling, and discovered a new clade of *Ca*Gg in Cape Cod AMF that was distinct from EB in culture collection isolates. Our *Ca*Gg sequences grouped together with other sequences previously recovered at Cape Cod in 2010 (Mondo & Pawlowska unpublished) (Fig. 7). Interestingly, they shared 99.9% identity with each other, regardless of the sampling year, indicating a temporally stable population.
During our effort to detect *Ca*Gg in dune AMF using *Burkholderia*-specific primers, we discovered novel Burkholderiaceae sequences in AMF spores. These sequences were repeatedly recovered from *Gigaspora* and *A. lacunosa* spores, and grouped into two different clades, away from the *Ca*Gg clade (Fig. 7). One clade of these *Burkholderia*-related endobacteria (BRE) clustered with EB of other Mucoromycota fungi, *Rhizopus microsporus* and *Mortierella elongata*. Endosymbionts of *R. microsporus* (*B. rhizoxinica*, *Burkholderia* sp. B13 and B14) are known to form a sister group to *Ca*Gg. However, they have not been previously reported outside of *R. microsporus*. The remaining sequences grouped with free-living *Burkholderia*. Based on these data, we propose that AMF can harbor a third kind of endosymbiont, BRE, distinct from *Ca*Gg and *Ca*Mg. However, additional molecular and microscopy studies are needed to confirm this.

***Ca*Mg diversity in Cape Cod AMF.** *Ca*Mg is known to exhibit high genetic diversity in culture

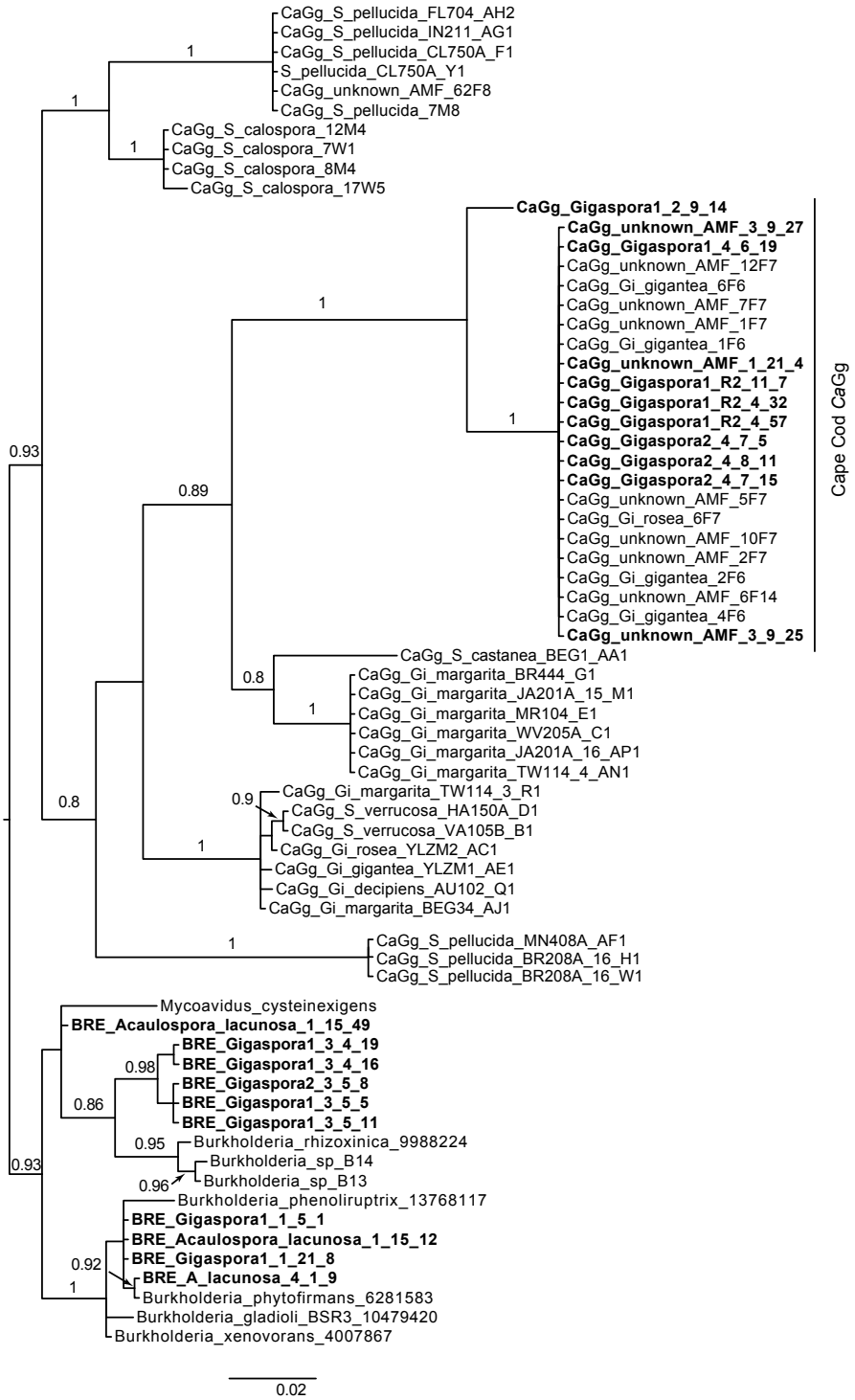

Figure 7. Relationships between *Ca*Gg, BRE of *Rhizopus microsporus* and *Mortierella elongata,* and free-living *Burkholderia*. Names highlighted in bold represent bacterial sequences obtained from spores of dune AMF in 2013. Other sequences within the Cape Cod clade were obtained from a previous sampling effort by Mondo & Pawlowska, data unpublished. Numbers after sequence names indicate, in order, sample location (transect, distance from beach) followed by spore number. Numbers above branches represent Bayesian posterior probability, values >0.8 are shown.

collection isolates of AMF with higher levels of diversity present within than among host individuals (Toomer *et al.*, 2015). To determine whether this pattern is also apparent in natural populations of *Ca*Mg from sand dunes, we analyzed *Ca*Mg population structure from two distantly related AMF genotypes identified in our samples, *Gigaspora*-1 (OTU1) and *A. lacunosa* (OTU3). Besides being distantly related phylogenetically, these AMF differed significantly in *Ca*Mg incidence, with *Gigaspora*-1 having a much higher *Ca*Mg incidence than *A. lacunosa* (Fig. S3).

To examine *Ca*Mg diversity, we assessed multiple cloned 16S rRNA gene sequences from different spores of *Gigaspora*-1 (OTU1) and *A. lacunosa* (OTU3) co-occurring within the same soil sample (Fig. 8, Fig. S4). We found that *Gigaspora-1* harbored six unique and deeply divergent *Ca*Mg genotypes, which were interspersed across the entire *Ca*Mg phylogenetic tree (Fig. 8). In *A. lacunosa*, we found two unique but deeply divergent genotypes, one of which grouped with *Ca*Mg from Glomeraceae, and another one with *Ca*Mg from Gigasporacea. We used AMOVA to analyze how *Ca*Mg diversity was partitioned and found that the "among AMF OTUs" variance component of *Ca*Mg diversity was small (Table S3). Instead, high levels of diversity were apparent within *Ca*Mg populations associated with individual AMF isolates (over 70% of variance) as well as among isolates within AMF OTUs (over 26% of variance). The latter pattern resembles partitioning of *Ca*Mg diversity within and among AMF isolates within a geographic region (Toomer *et al*., 2015).

*Ca*Mg transmission within AMF is predominantly vertical (Naumann *et al*., 2010). However, their molecular evolution patterns indicate a low level of horizontal transmission, which together with recombination contributes to their complex intra-host diversity (Toomer *et al*., 2015). The mechanism of horizontal transmission is unknown, but is expected to take place between AMF isolates co-occurring in close spatial proximity. In this way, mechanical damage to hyphae, such as from grazing by soil fauna could facilitate *Ca*Mg transfer. We did not, however, detect evidence of gene flow between *Ca*Mg associated with *Gigaspora*-1 and *A. lacunosa* co-occurring within the same sample (Fig. 8), suggesting that physical proximity between AMF

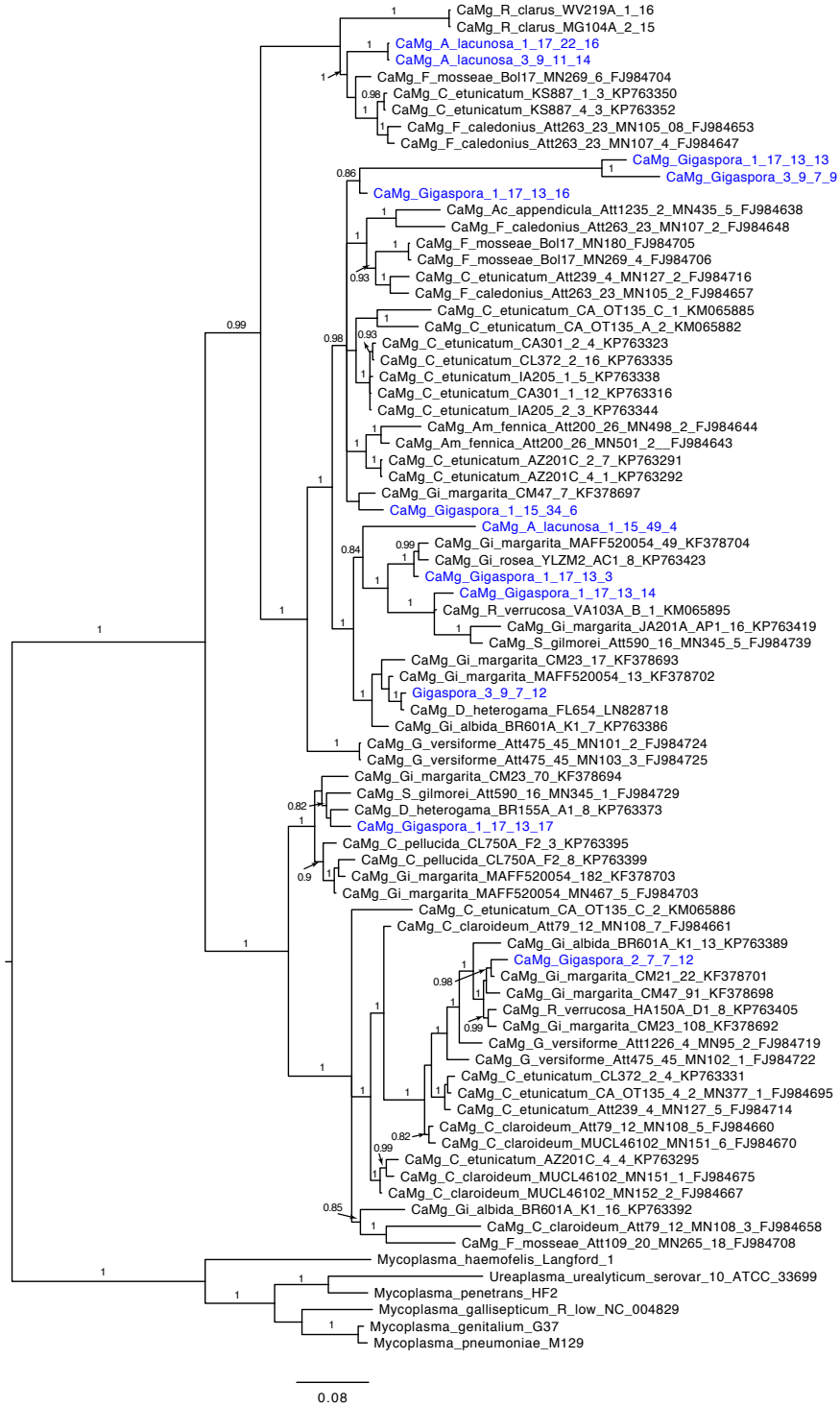

Figure 8. *Ca*Mg phylogeny based on 16S rRNA gene sequence. *Ca*Mg 16S rRNA clones were obtained from individual spores of *A. lacunosa*, OTU3 and *Gigaspora-1*, OTU1 and grouped into genotypes at 95% sequence similarity. Representative sequences from each genotype and spore were used in phylogeny reconstruction (names in blue). Numbers after sequence names indicate, in order, sample location (transect, distance from beach), spore number and clone number. Numbers above branches represent Bayesian posterior probability, values >0.8 are shown.

hosts is not the only factor required for horizontal transmission of *Ca*Mg to occur.

4.4 DISCUSSION

The dune ecosystem is characterized by steep gradients in abiotic and biotic conditions, making it a convenient study system for analyzing how different environmental conditions affect EB distribution in AMF. We confirmed the existence of such environmental gradients in our study site at Cape Cod National Seashore, noting changes in soil salinity, plant density and plant composition (dominance of *A. breviligulata*) with increased distance from the ocean. Considering that environmental conditions change as the distance from the ocean increases, it was not surprising that the distance factor had a significant effect on EB distribution in dune AMF. However, the relationship between distance and EB distribution was not linear, for example *Ca*Mg were less likely to be found between 40 and 60 m from the beach (Fig. 5a), which coincided with increased abundance of *A. lacunosa* at those sites. *A. lacunosa* had a much lower *Ca*Mg incidence compared to other AMF (Fig. S3), therefore this drop in EB incidence between 40 and 60 m was likely due to increased abundance of *A. lacunosa*.

After distance from the ocean, the plant factor was expected to affect EB distribution the most. The plant factor has a great influence on shaping the AM fungal community, and different plants preferentially associate with different AM fungi (Eom *et al*., 2000). In our study, we limited the influence of the plant factor on AMF because the dune environment is dominated by a single plant species, *A. breviligulata*. However, being obligate biotrophs, AMF are still influenced by biotic and abiotic factors that affect their plant host. For example, calcium is an essential plant nutrient and is considered available to plants in its ionic form. Soil calcium levels are known to positively correlate with plant cover (Anderson *et al*., 1984), and in our study it correlated positively with plant density. In turn, higher soil calcium levels are known to correlate with increased AMF spore abundance, whereas lower levels of calcium in plant tissues correlate with reduced AM fungal colonization (Anderson *et al*., 1984, Jarstfer *et al*., 1998). These patterns suggest that soil calcium levels may have an indirect impact on AM fungal fitness. In our study,

we discovered that probability of *Ca*Mg and *Ca*Gg incidence in AMF increased under reduced soil calcium levels (Fig. 4b & 5b). It is thus possible that the EB buffer in some way the negative effects of low calcium levels on AMF fitness. This speculation is further supported by observations that EB, including *Ca*Gg, affect calcium metabolism of their fungal host (Salvioli *et al*., 2016, Lastovetsky O. A., Submitted).

*Ca*Gg in AMF spores increases the length of the germinating hyphae (Lumini *et al*., 2007) that initially seek out and contact the plant host for symbiosis establishment. Considering *Ca*Gg carbon cost to AMF, this EB is expected to be advantageous only under environmental conditions that require extensive presymbiotic hyphal growth. Such conditions are likely to occur when chances of a germinating fungal spore to contact its plant host are lowered due to low plant density typified by larger distances between potential plant hosts. In our study site, plant density declined with increasing distance from the ocean (Fig. 1b), with larger distances recorded between individual plants. However, we detected no correlation between *Ca*Gg distribution and plant density. Consequently, plant density may not be a factor in determining *Ca*Gg incidence in AMF. However, it is important to consider that incidence of *Ca*Gg was extremely low in our study site (2%), and it is possible that we were simply unable to detect a significant correlation signal.

*Ca*Mg was extremely abundant in dune AMF, with almost 90% of spores harboring this EB. This was largely unexpected, since *Ca*Mg molecular evolution patterns indicate that it is likely a parasite of AMF (Toomer *et al*., 2015). According to evolutionary theory, vertically transmitted parasites must enhance host fitness or else be eliminated from the host population through natural selection (Lively *et al*., 2005). It therefore follows that *Ca*Mg must provide a benefit to its fungal host at least under certain conditions. Such conditions could occur when a host population, infected with a vertically transmitted parasite (*Ca*Mg), is exposed to a horizontally transmitted parasite. In this case, *Ca*Mg could provide protection for the host, acting as a conditional defensive mutualist (Lively *et al*., 2005). This could explain why heritable *Ca*Mg retains the high level of diversity within AMF, and why it remains so prevalent in natural

populations of AMF despite its energy cost to the fungus. Whereas no known horizontally transmitted parasites have been characterized in AMF to date, it is well known that they inevitably associate with soil bacteria in the mycorhizosphere environment and these bacteria can have both mutualistic and antagonistic/parasitic effects on the fungus (Johansson *et al*., 2004). Moreover, in our study we identified four AMF spores from which we recovered sequences of bacteria related to free-living *Burkholderia* as well as six spores which harbored *Burkholderia* related to symbionts of other Mucoromycota fungi (Fig. 7). Considering that we surface-decontaminated all spores, these bacteria were likely present inside the fungal spores and could be potential AMF parasites. Together, our data indicate that *Ca*Mg could serve as a conditional defensive mutualist of AMF, although further experiments are needed to address this hypothesis. Lastly, our study confirmed the existence of heterogeneous *Ca*Mg populations within Gigasporaceae AMF individuals (spores) in nature. These diversity patterns were consistent with those reported previously within and among AMF isolates within a geographic region (Toomer *et al*., 2015).

4.5 CONCLUSION

Overall, our systematic study of AMF-associated EB in a model natural system identified environmental parameters that influence their distribution. A decrease in levels of soil calcium increased the probability of harboring *Ca*Gg and *Ca*Mg EB in AMF, suggesting that they might buffer the negative effects of low calcium levels on AMF fitness. Assessment of EB diversity revealed a novel group of *Ca*Gg as well as a previously unreported group of *Burkholderia*-related EB in AMF. Moreover, diversity analysis of *Ca*Mg populations revealed similar patterns as in culture collections and confirmed the existence of heterogeneous populations in Gigasporacea AMF in nature. Collectively, we have conducted the first ecological study of AMF-associated EB, identified environmental factors affecting their incidence and assessed their diversity and population structure.

4.6 ACKNOWLEDGMENTS

We thank M. Barker and S. Mondo for help with sample collection, E. Ahn and A. Zhang for help with processing samples and generating data, S. Perry and L. Johnson for help with statistical analysis and the National Park Service for permission to collect samples Cape Cod National Seashore. This work was supported by the National Science Foundation grants IOS-1261004 and DBI-1263103 to TEP, and the Frederic N. Gabler'93 Memorial Research Endowment grant to EA.

4.7 MATERIALS & METHODS

Study site and sampling. Samples were collected in the Province Lands Area of the Cape Cod National Seashore (42°4'50.2''N 70°13'2.4''W) on 3 November 2013. *A. breviligulata* (American beach grass) was the dominant plant species at all sampling points (>60% of all plants). Four transects were laid out starting from the edge of vegetation at the seaward side (corresponding to the end of the beach) and extending 100 m inland. Samples were taken every 10 m by digging the soil around a plant nearest to each 10 m mark. All soil samples were stored at 4°C until further processing. At each sampling point, the following was recorded: (1) total number of individual plants in a 70 cm radius around the area of soil sampling, (2) distance to 4 nearest plants in the 70 cm radius around the area of soil sampling, later averaged to give average nearest neighbor distance (NND), and (3) total number of non-*A. breviligulata* plants. These parameters were used to estimate total plant density at each sampling point as well as dominance of *Ammophila breviligulata* over other plants. Transects were 10, 20 and 40 meters apart (10 m between Transect 1 and 2; 20 m between Transect 2 and 3; 40 m between transect 3 and 4).

Soil chemistry analysis. Soil samples were dried at room temperature and stored at 4 °C until further processing. Samples were analyzed at the Cornell Nutrient Analysis laboratory (tests #1060 and #1880). Details of the procedures are described in (Moebius-Clune B. N., 2016). In brief, nutrients were extracted from soil by shaking with Modified Morgan's solution and then filtered through a paper filter. The filtrate was analyzed on an inductively coupled plasma

emission spectrometer (ICP, Spectro Arcos) for the elements Al, As, B, Ba, Be, Ca, Cd, Co, Cu, Fe, Li, Mg, Na, P, Pb, S, Se, Sr, Ti, V, Zn and Cl. pH of a 2:1 suspension of water and soil was determined using a Lignin pH robot. Soluble salts were extracted in a 1:1 soil-water suspension, and the electrical conductivity of the supernatant measured with a calibrated conductivity meter Three soil samples from each transect was analyzed corresponding to distances 0, 40 and 100 m from the beach.

Spore extraction, collection and decontamination. AMF spores were extracted from soil samples as described by Daniels and Skipper (1982) with some modifications. In brief, 50 g of air-dried soil was mixed with 200 ml of water and shaken vigorously for 15 min. Soil suspensions allowed to sediment for a few seconds and poured through stacked sieves: 250 um (top), 90 um (middle), 38 um (bottom). Material in each sieve was rinsed with a jet of water catching smaller particles on the sieve below. Material collected on the 250 um sieve was transferred into a petri plate, sealed with parafilm and stored at 4^{o}C. Material collected on the 90 um and 38 um sieves was transferred separately into centrifuge tubes, to which a generous pinch of kaolin and water were added, mixed thoroughly and centrifuged for 5 min. Immediately after centrifugation the supernatant was collected from each tube on a small 38 um sieve, rinsed with a jet of water, and transferred into the filtration apparatus. Spores were collected on 0.45 mm filters. 30 ml of 2 M sucrose was then added to the sediment remaining in centrifuge tubes, stirred thoroughly with a spatula, and centrifuged for 3 min. Immediately after centrifugation, supernatant was poured through the 38 um sieve, rinsed thoroughly with a jet of water, and spores transferred into the filtration apparatus. Again, 0.45 mm nitrate cellulose filters used to collect spores. Filters were allowed to dry and were stored at 4^{o}C. Spores were collected at random following the protocol from Moebus-Clune *et al.* (2013). Spores were decontaminated individually following the protocol from Mondo *et al* (2012). In brief, spores were sequentially washed with 1 mM and 50 mM H_2O_2, then with 4% chloramine T, before final wash with nanopure water.

AMF spore identification and screening for EB. Following surface decontamination, total

DNA of individual spores was amplified using Illustra^{TM}GenomiPhi-V2 kit (GE Healthcare) and the 1/20 diluted product was used for PCR. PCR was used to amplify the fungal 23S rRNA gene from individual spores with primers described in (Mondo *et al.*, 2012) using JumpStart RedTaq DNA Polymerase Master Mix (Sigma). Spores were also screened by PCR for incidence of *Ca*Gg with *Burkholderia*-specific primers amplifying a portion of the 23S rRNA gene (Mondo *et al.*, 2012) and *Ca*Mg-specific primers amplifying a portion of the 16S rRNA gene (Naumann *et al.*, 2010) using the JumpStart RedTaq polymerase master mix (Sigma). AMF and *Ca*Gg PCR products were cycle-sequenced with the BigDye Terminator 3.1 Cycle Sequencing Kit (Applied Biosystems). Fungal sequences were grouped into operational taxonomic units (OTUs) at 95% similarity cutoff (Moebius-Clune *et al.*, 2013) using MOTHUR (Schloss *et al.*, 2009), and named based on clustering with reference AMF at this cut-off level combined and phylogenetic reconstruction.

Because of their diversity in host individuals, *Ca*Mg 16S rRNA sequences were subcloned for sequencing after PCR amplification with *Ca*Mg-specific primers (Naumann *et al.*, 2010) and Phusion High-Fidelity DNA polymerase (New England Biolabs) under conditions: 5 min initial denaturation at 98°C followed by 15 cycles of 10 sec at 98°C, 30 sec at 50°C, and 1 min at 72°C, followed by a final extension of 10 min at 72°C. Amplicons were cloned using the TOPO TA Cloning Kit for Sequencing (Invitrogen Life Technologies). Plasmid DNA from recombinant bacterial colonies was amplified using the Illustra TempliPhi 100/500 DNA Amplification Kit (GE Healthcare Life Sciences). Plasmid inserts were cycle-sequenced with the BigDye Terminator 3.1 Cycle Sequencing Kit (Applied Biosystems) using T3 and T7 primers. Cloned MRE sequences were clustered at 94% similarity level using MOTHUR (Schloss *et al.*, 2009), followed by phylogeny reconstruction of the representative sequence from each OTU.

Phylogeny reconstruction. All sequences were edited in Geneious 9.1.2 (Biomatters Ltd.) and aligned using MUSCLE(Edgar, 2004). Phylogenies were reconstructed under the GTR+I+Γ nucleotide substitution model implemented in MrBayes 3.2.5 with a 25% burn-in, while the average standard deviation of split frequencies (<0.01) was used as a convergence diagnostic.

Statistical analyses. Soil chemistry data from samples located 0, 40, and 100 m from the beach was extrapolated, separately for each transect, to the remaining samples using 3 different methods: (i) distances 0 to 20 m, 30 to 60 m and 70 to 100 m were assumed to represent blocks with the same soil chemistry parameters, (ii) liner interpolation values were computed for each missing distance from the beach based on soil chemistry parameters at distances 0, 40 and 100 m, (iii) LOESS curve was fitted to the soil chemistry parameters at distances 0, 40, 100 m versus distance relationship and values were computed for the remaining missing distances. Influence of environmental parameters on EB incidence in AMF spores was analyzed using the lsmeans and lme4 packages in R. Generalized linear mixed models with binomial distribution were used to model *Ca*Gg and *Ca*Mg incidence in AMF spores. Environmental variables (distance from the beach, plant density, dominance of *A. breviligulata*, soil salinity, and pH) were modeled as fixed effects, and transect was modeled as a random effect. All environmental variables, except distance, were included as integer variables. Distance was included as a factor variable because log odds of EB incidence did not appear to be a linear function of distance. Significance of distance was tested with a likelihood ratio test, post-hoc pairwise comparisons between distances were performed using Tukey adjustments for multiple comparisons. Influence of soil chemistry parameters (soluble salts, sodium, calcium and pH) on incidence of EB within AMF spores was modeled four independent times, using either only the data that was obtained for distances 0, 40, 100 m, or the values from the three different extrapolations described above. Influence of soil chemistry parameters on EB incidence was taken to be significant only if at least three out of the four independent methods yielded $P<0.05$. Consequently, the reported P values represent the highest P-value that was obtained from the four different methods.

AMOVA. To quantify the extent of differentiation among *Ca*Mg genotypes, we conducted hierarchical analysis of molecular variance (AMOVA) implemented in Arlequin 3.5 (Excoffier et al. 2005). We tested the null hypothesis that any variation among *Ca*Mg is due to random sampling. To estimate variance components and Φ statistics, which are F statistic analogues and

reflect the correlations of genotypic diversity at different levels of hierarchical subdivsion, we used p-distances computed from the alignment of the 16S rRNA gene haplotypes found in *Ca*Mg associated with *Gigaspora*-1 (OTU1) and *A. lacunosa* (OTU3) that co-occurred at three sampling points. The specific Φ statistics were: (i) Φ_{ST}, the correlation of the molecular diversity of random *Ca*Mg genotypes within host isolates relative to the correlation of random pairs of genotypes drawn from the entire *Ca*Mg diversity, (ii) Φ_{SC}, the correlation of random *Ca*Mg genotypes among host isolates relative to the correlation of random pairs of *Ca*Mg genotypes drawn from a AMF OTU, and (iii) Φ_{CT}, the correlation of the molecular diversity of random *Ca*Mg genotypes within AMF OTUs relative to the correlation of random pairs of genotypes drawn from the entire *Ca*Mg diversity. Statistical significance of the null hypothesis was tested by permutational analysis: 90 000 permuted matrices were generated to obtain the null distribution and to test for the significance of the variance components and the Φ statistics.

4.8 REFERENCES

Anderson RC, Liberta AE & Dickman LA (1984) Interactions of vacular plants and vesicular-arbuscular mycorrhizal fungi across a soil moisture-nutrient gradient. *Oecologia* **64**: 111-117.

Bianciotto V, Lumini E, Bonfante P & Vandamme P (2003) 'Candidatus glomeribacter gigasporarum' gen. nov., sp. nov., an endosymbiont of arbuscular mycorrhizal fungi. *International journal of systematic and evolutionary microbiology* **53**: 121-124.

Desiro A, Salvioli A, Ngonkeu EL, Mondo SJ, Epis S, Faccio A, Kaech A, Pawlowska TE & Bonfante P (2014) Detection of a novel intracellular microbiome hosted in arbuscular mycorrhizal fungi. *Isme j* **8**: 257-270.

Edgar RC (2004) MUSCLE: multiple sequence alignment with high accuracy and high throughput. *Nucleic Acids Research* **32**: 1792-1797.

Eom A-H, Hartnett DC & Wilson GW (2000) Host plant species effects on arbuscular mycorrhizal fungal communities in tallgrass prairie. *Oecologia* **122**: 435-444.

Ghignone S, Salvioli A, Anca I*, et al.* (2012) The genome of the obligate endobacterium of an AM fungus reveals an interphylum network of nutritional interactions. *ISME J* **6**: 136-145.

Gianinazzi S, Gollotte A, Binet MN, van Tuinen D, Redecker D & Wipf D (2010) Agroecology: the key role of arbuscular mycorrhizas in ecosystem services. *Mycorrhiza* **20**: 519-530.

Hesp PA & Martínez ML (2007) Disturbance Processes and Dynamics in Coastal Dunes - Johnson, Edward A. *Plant Disturbance Ecology,*(Miyanishi K, ed.) p.^pp. 215-247. Academic Press, Burlington.

Jarstfer AG, Farmer-Koppenol P & Sylvia DM (1998) Tissue magnesium and calcium affect arbuscular mycorrhiza development and fungal reproduction. *Mycorrhiza* **7**: 237-242.

Johansson JF, Paul LR & Finlay RD (2004) Microbial interactions in the mycorrhizosphere and their significance for sustainable agriculture. *FEMS microbiology ecology* **48**: 1-13.

Koske R & Halvorson W (1981) Ecological studies of vesicular-arbuscular mycorrhizae in a barrier sand dune. *Canadian Journal of Botany* **59**: 1413-1422.

Lastovetsky O. A. HM, Clum A., Pillay M., Palaniappan K., Varghese N., Mikhailova N., Stamatis D., Reddy T. B. K., Daum C., Shapiro N., Ivanova N., Kyrpides N., Woyke T., Pawlowska T. E. (Submitted) Reciprocal communication in fungal-bacterial symbioses.

Lively CM, Clay K, Wade MJ & Fuqua C (2005) Competitive co-existence of vertically and horizontally transmitted parasites. *Evolutionary Ecology Research* **7**: 1183-1190.

Lumini E, Bianciotto V, Jargeat P, Novero M, Salvioli A, Faccio A, Becard G & Bonfante P (2007) Presymbiotic growth and sporal morphology are affected in the arbuscular mycorrhizal fungus Gigaspora margarita cured of its endobacteria. *Cellular microbiology* **9**: 1716-1729.

Moebius-Clune B. N. M-CDJ, Gugino B. K., Idowu O. J., Schindelbeck R. R., Ristow A. J., van Es H. M., Thies J. E., Shayler H. A., McBride M. B., Wolfe D. W., Abawi G. S. (2016) Comprehensive Assessment of Soil Health - the Cornell Framework Manual. p.^pp. Cornell University, Geneva, NY.

Moebius-Clune DJ, Moebius-Clune BN, van Es HM & Pawlowska TE (2013) Arbuscular mycorrhizal fungi associated with a single agronomic plant host across the landscape: community differentiation along a soil textural gradient. *Soil Biology and Biochemistry* **64**: 191-199.

Mondo SJ, Toomer KH, Morton JB, Lekberg Y & Pawlowska TE (2012) Evolutionary stability in a 400-million-year-old heritable facultative mutualism. *Evolution; international journal of organic evolution* **66**: 2564-2576.

Mondo SJ, Salvioli A, Bonfante P, Morton JB & Pawlowska TE (2016) Nondegenerative Evolution in Ancient Heritable Bacterial Endosymbionts of Fungi. *Mol Biol Evol* **33**: 2216-2231.

Mosse B (1970) Honey-coloured, sessile Endogone spores: II. Changes in fine structure during spore development. *Archiv für Mikrobiologie* **74**: 129-145.

Naito M (2014) The Biology and Evolution of the Mollicutes/Mycoplasma-related Endobacteria of Arbuscular Mycorrhizal Fungi. Ph.D. Dissertation Thesis, Cornell University.

Naito M, Morton JB & Pawlowska TE (2015) Minimal genomes of mycoplasma-related endobacteria are plastic and contain host-derived genes for sustained life within Glomeromycota. *Proc Natl Acad Sci U S A* **112**: 7791-7796.

Naito M, Desiro A, Gonzalez JB, Tao G, Morton JB, Bonfante P & Pawlowska TE (2017) 'Candidatus Moeniiplasma glomeromycotorum', an endobacterium of arbuscular mycorrhizal fungi. *International journal of systematic and evolutionary microbiology*.

Naumann M, Schussler A & Bonfante P (2010) The obligate endobacteria of arbuscular mycorrhizal fungi are ancient heritable components related to the Mollicutes. *ISME J* **4**: 862-871.

Salvioli A, Ghignone S, Novero M, Navazio L, Venice F, Bagnaresi P & Bonfante P (2016) Symbiosis with an endobacterium increases the fitness of a mycorrhizal fungus, raising its bioenergetic potential. *ISME J* **10**: 130-144.

Schloss PD, Westcott SL, Ryabin T, Hall JR, Hartmann M, Hollister EB, Lesniewski RA, Oakley BB, Parks DH & Robinson CJ (2009) Introducing mothur: open-source, platform-independent, community-supported software for describing and comparing microbial communities. *Applied and environmental microbiology* **75**: 7537-7541.

Smith SE & Read DJ (2008) *Mycorrhizal Symbiosis, 3rd Edition*.
Smith SM (2006) Dune Vegetation Monitoring - 2005. p.^pp. NPS report. National Park Service, Cape Cod National Seashore, Wellflet, MA.

Toomer KH, Chen X, Naito M, Mondo SJ, den Bakker HC, VanKuren NW, Lekberg Y, Morton JB & Pawlowska TE (2015) Molecular evolution patterns reveal life history features of mycoplasma-related endobacteria associated with arbuscular mycorrhizal fungi. *Mol Ecol* **24**: 3485-3500.

van Tuinen D, Jacquot E, Zhao B, Gollotte A & Gianinazzi-Pearson V (1998) Characterization of root colonization profiles by a microcosm community of arbuscular mycorrhizal fungi using 25S rDNA-targeted nested PCR. *Mol Ecol* **7**: 879-887.

Weber OB (2014) Biofertilizers with Arbuscular Mycorrhizal Fungi in Agriculture. **41**: 45-66.
Yamamura N (1993) Vertical transmission and evolution of mutualism from parasitism. *Theoretical Population Biology* **44**: 95-109.

4.9 SUPPORTING INFORMATION

Table S1. AMF OTUs and their taxonomic affinity based on 0.05 similarity cutoff using MOTHUR together with phylogenetic analysis.

OTU identifier	OTU name
OTU1	*Gigaspora-1*
OTU2	*Scutellospora-1*
OTU3	*Acaulospora lacunosa*
OTU4	*Scutellospora heterogama*
OTU5	*Gigaspora-2*
OTU6	*Gigaspora-3*
OTU7	*Gigaspora-4*
OTU8	*Acaulospora tuberculata*
OTU9	*Corymbiglomus-1*
OTU10	*Acaulospora-1*
OTU11	*Gigaspora-5*
OTU12	*Scutellospora-2*
OTU13	*Scutellospora-3*
OTU14	*Scutellospora-4*
OTU15	*Gigaspora-5*
OTU16	*Gigaspora-6*
OTU17	*Gigaspora-7*
OTU18	*Gigaspora-8*
OTU19	*Gigaspora-9*
OTU20	*Gigaspora-10*
OTU21	*Gigaspora-11*
OTU22	*Gigaspora-12*
OTU23	*Gigaspora-13*

Table S2. Results from post-hoc comparisons of *Ca*Mg distribution in AMF OTUs 1 to 3 at different distances from the beach in meters. Tukey test *P* values are given.

Distance (m)	Contrast	Odds ratio	SE	Z ratio	P value
10	OTU1-OTU2	0.8983	0.623418	-0.154	0.9869
	OTU1-OTU3	387.5973	981.4833	2.354	**0.0488**
	OTU2-OTU3	431.4534	1116.7833	2.344	**0.05**
40	OTU1-OTU2	1.083142	0.4754343	0.182	0.9819
	OTU1-OTU3	69.088625	92.993716	3.147	**0.0047**
	OTU2-OTU3	63.785383	87.840732	3.018	**0.0072**
60	OTU1-OTU2	1.2269994	0.63777	0.394	0.9182
	OTU1-OTU3	21.8821	14.81310	4.558	**<0.0001**
	OTU2-OTU3	17.833887	13.5995542	3.778	**0.0005**
90	OTU1-OTU2	1.4793906	1.3162353	0.44	0.8987
	OTU1-OTU3	3.9004	3.8970788	1.362	0.3609
	OTU2-OTU3	2.63653	3.1638672	0.808	0.6981

Table S3. Hierarchical analysis of molecular variance in *Ca*Mg.

Source of variation	df	Variance	% variation	Φ statistics	*P*
Among AMF OTUs	1	0.0030	0.60	$\Phi_{CT} = 0.0060$	0.4
Among *Ca*Mg populations within AMF OTUs	4	0.1356	26.89	$\Phi_{SC} = 0.2705$	<0.0001
Within *Ca*Mg populations of individual AMF isolates	42	0.3655	72.51	$\Phi_{ST} = 0.2749$	<0.0001

Figure S1. Study site in the grassland dunes of the Province Lands area at Cape Cod National Seashore. (A) Aerial view of the sampling site at the time of sample collection in November 2013 taken from Google Maps. Black lines and numbers 1-4 represent location of the sampling transects. (B) Photograph of one of the transects marked by the yellow tape extending from the beach inland.

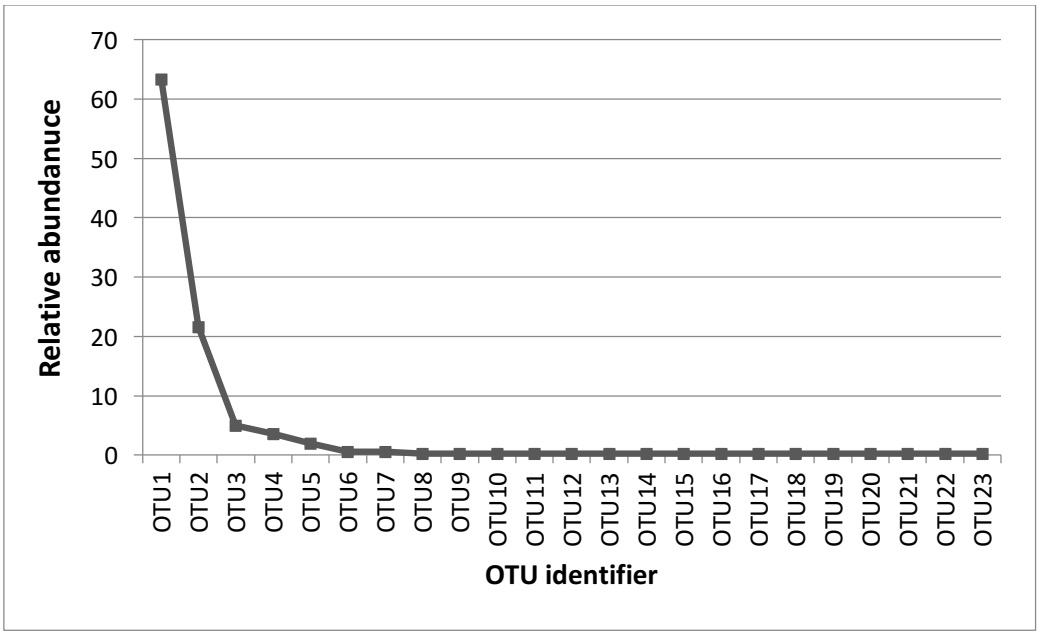

Figure S2. Relative abundance of AMF OTUs recovered from Cape Cod dunes.

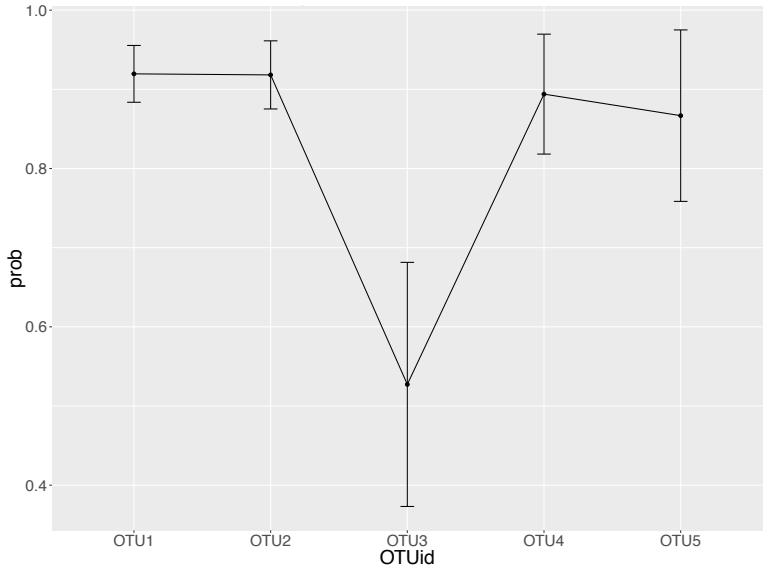

Figure S3. Probability of harboring MRE in the top 5 abundant AMF OTUs. Difference in MRE distribution in the AMF OTUs was statistically significant between OTU1 and OTU3 (P<0.0001), as well as OTU2 and OTU3 (P=0.0005). Error bars represent 1 standard error from the mean.

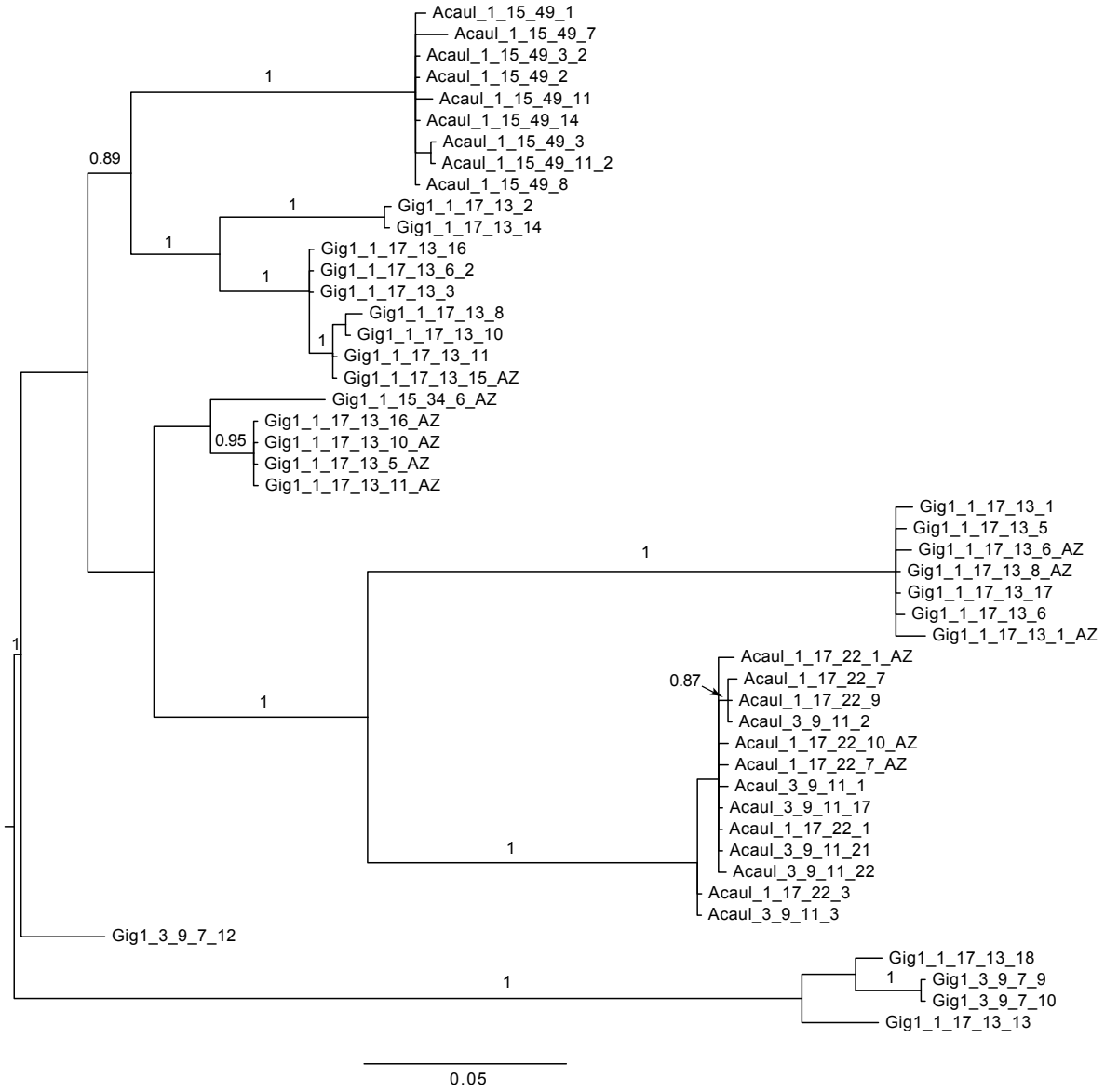

Figure S4. *Ca*Mg phylogeny of 16S rRNA gene haplotypes from AMF OTU1, *Gigaspora*-1 and OTU3, *A. lacunosa*. Acaul, *A. lacunosa*; Gig1, *Gigaspora*-1. Numbers after sequence names indicate, in order, sample location (transect, distance from beach), spore number and clone number. Numbers above branches represent Bayesian posterior probability, values >0.8 are shown. The tree was midpoint rooted.